JYU DISSERTATIONS 450

Wenya Liu

Dysconnectivity of Oscillatory Networks in Major Depression Disorder

UNIVERSITY OF JYVÄSKYLÄ
FACULTY OF INFORMATION TECHNOLOGY

JYU DISSERTATIONS 450

Wenya Liu

Dysconnectivity of Oscillatory Networks in Major Depression Disorder

Esitetään Jyväskylän yliopiston informaatioteknologian tiedekunnan suostumuksella
julkisesti tarkastettavaksi
marraskuun 3. päivänä 2021 kello 12.

Academic dissertation to be publicly discussed, by permission of
the Faculty of Information Technology of the University of Jyväskylä,
on November 3, 2021, at 12 o'clock.

JYVÄSKYLÄN YLIOPISTO
UNIVERSITY OF JYVÄSKYLÄ

JYVÄSKYLÄ 2021

Editors
Timo Männikkö
Faculty of Information Technology, University of Jyväskylä
Päivi Vuorio
Open Science Centre, University of Jyväskylä

ISBN 978-951-39-8903-3 (PDF)
URN:ISBN:978-951-39-8903-3
ISSN 2489-9003

Permanent link to this publication: http://urn.fi/URN:ISBN:978-951-39-8903-3

ABSTRACT

Liu, Wenya
Dysconnectivity of Oscillatory Networks in Major Depression Disorder
Jyväskylä: University of Jyväskylä, 2021, 70 p. (+included articles)
(JYU Dissertations
ISSN 2489-9003; 450)
ISBN 978-951-39-8903-3 (PDF)

Major depression disorder (MDD) is a prevalent psychiatric disorder globally, affecting one in six people. From the view of theoretical models, the dysconnectivity of functional networks is considered a critical cause in the cognitive and emotional dysfunctions of MDD. However, the pathophysiology of MDD remains unclear due to the non-replicability in terms of methodologies and datasets. Both of the causes of MDD and the human connectome are incredibly complex, and novel experimental paradigms and advanced methodologies are needed to explore the pathophysiological mechanisms of MDD.

In this thesis, we explored the altered oscillatory functional connectivity in MDD during music listening conditions and resting states. In the first study, we investigated the frequency-specific static functional connectivity (FC) in MDD during music listening at the sensor level. We found altered FC networks and the non-lateralized effect in the delta and beta bands, and we got the best classification performance in the beta band by the support vector machine classifier. In the second study, we proposed a comprehensive framework to identify the dysconnectivity of oscillatory networks in MDD during resting states at the cortical source level. Fully considering the incomplete consistency in the adjacency and spectral modes between the healthy group and the MDD group and the multiway structure of the constructed data, we first introduced the coupled tensor decomposition (CTD) model for EEG signals recorded during music listening. We identified three hyperconnectivity networks and three hypoconnectivity networks characterizing the dysconnectivity networks in MDD under music perception. Based on the CTD model, we also explored the hyper- and hypoconnectivity networks in MDD during resting states. In the third study, we examined the dysfunction of sensor-level networks in the alpha band. In the fourth study, we explored the source-level dysconnectivity networks characterized by spatio-temporal-spectral modes of covariation in MDD.

In conclusion, this thesis investigated potential biomarkers of oscillatory networks and provided promising references to reveal the pathoconnectomics in MDD. The proposed analysis pipeline based on the CTD model can be extended to other psychiatric disorders.

Keywords: Major depression disorder, functional connectivity, coupled tensor decomposition, dynamic functional connectivity, oscillatory networks

TIIVISTELMÄ (ABSTRACT IN FINNISH)

Liu, Wenya
Värähtelyverkkojen merkitys vakavan masennuksen häiriössä
Jyväskylä: University of Jyväskylä, 2021, 70 s. (+artikkelit)
(JYU Dissertations
ISSN 2489-9003; 450)
ISBN 978-951-39-8903-3 (PDF)

Suuri masennushäiriö (MDD, Major Depression Disorder) on yksi yleisimmistä psykiatrisista häiriöistä maailmanlaajuisesti, ja se vaikuttaa joka kuudenteen ihmiseen. Teoreettisten mallien näkökulmasta toiminnallisten verkostojen yhteyshäiriöitä pidetään kriittisenä syynä MDD:n kognitiivisiin ja emotionaalisiin toimintahäiriöihin. MDD:n patofysiologia on kuitenkin epäselvä, koska menetelmiä ja tietojoukkoja ei voida toistaa. MDD:n syyt ja ihmisen rakenne ovat monimutkaisia, ja uusia kokeellisia paradigmoja ja kehittyneitä menetelmiä tarvitaan MDD:n patofysiologisten mekanismien tutkimiseksi.

Tässä väitöskirjassa tutkitaan MDD:n muuttunutta värähtelevää toiminnallista yhteyttä (FC, Functional Connectivity) musiikin kuuntelu- ja lepotilassa. Ensimmäisessä tutkimuksessa tutkitaan taajuuskohtaista staattista toiminnallista yhteyttä MDD:ssä musiikin kuuntelun aikana anturitasolla. Löysimme muuttuneita FC-verkkoja ja ei-lateralisoidun vaikutuksen delta- ja beeta-kaistoilta, ja saimme parhaan luokittelun suorituskyvyn beeta-kaistalla tukivektorikoneiden luokittelijan avulla. Toisessa tutkimuksessa ehdotimme kattavaa kehystä MDD:n värähtelyverkkojen epäyhteyden tunnistamiseksi lepotilassa aivokuoren lähteen tasolla. Ottaen täysin huomioon terveen ryhmän ja MDD -ryhmän välisen vierekkäisyyden ja spektritilojen epätäydellisen johdonmukaisuuden ja konstruoidun datan monisuuntaisen rakenteen, esittelimme ensin kytketyn tensorin hajoamismallin (CTD, Coupled Tensor Decomposition) musiikin kuuntelun aikana tallennetuille EEG -signaaleille. Tunnistimme kolme hyperyhteysverkkoa ja kolme hypoyhteysverkkoa, jotka luonnehtivat MDD:n häiriöverkkoja musiikin havaitsemisessa. CTD-mallin perusteella tutkimme myös MDD:n hyper- ja hypoyhteysverkkoja lepotilassa. Kolmannessa tutkimuksessa tutkimme anturitason verkkojen toimintahäiriöitä alfa-kaistalla. Neljännessä tutkimuksessa tutkimme lähdetason häiriöverkkoja, joille on tunnusomaista tila-ajallinen-spektrinen kovariaatiomuoto MDD:ssä.

Yhteenvetona voidaan todeta, että tämä opinnäytetyö tutki värähtelyverkkojen mahdollisia biomarkkereita ja tarjosi lupaavia viitteitä MDD:n patokonektomian paljastamiseksi. Ehdotettu CTD -malliin perustuva analyysiputki voidaan laajentaa koskemaan myös muita psykiatrisia häiriöitä.

Avainsanat: vakava masennushäiriö, toiminnallinen liitettävyys, kytketty tensorin hajoaminen, dynaaminen toiminnallinen yhteys, värähtelevät verkot

Author

Wenya Liu
Faculty of Information Technology
University of Jyväskylä
Finland

Supervisors

Professor Tapani Ristaniemi
Faculty of Information Technology
University of Jyväskylä
Finland

Professor Fengyu Cong
School of Biomedical Engineering
Dalian University of Technology
China
Faculty of Information Technology
University of Jyväskylä
Finland

Professor Timo Hämäläinen
Faculty of Information Technology
University of Jyväskylä
Finland

Docent Zheng Chang
Faculty of Information Technology
University of Jyväskylä
Finland

Doctor Chi Zhang
School of Biomedical Engineering
Dalian University of Technology
China

Reviewers

Professor Peng Xu
School of Life Science and Technology
University of Electronic Science and Technology of China
China

Professor Li Hu
Department of Psychology
University of Chinese Academy of Sciences
China

Opponent

Professor Fabio Babiloni
Department of Molecular Medicine
University of Rome Sapienza
Italy

ACKNOWLEDGEMENTS

I appreciate the experience of four-year doctoral studies in Finland. It is a fantastic journey, which I will cherish and memorize during my whole life. I would like to express my sincere thanks to all the people who have helped me make this thesis possible.

First of all, I would like to express my sincere gratitude to my supervisor Prof. Tapani Ristaniemi. He is very supportive of attending summer school and international conferences, and he always gave me constructive suggestions on my research. When I reported on our biweekly seminars, he always encouraged me no matter I had progressed or not, and his smiles and humor released me from nervousness in public speaking. I am grateful for his timely responses whenever I need help. It is my great honor to work with him in Finland, and I will never forget his wisdom and kindness. This thesis is to memorize Prof. Tapani Ristaniemi for his great help to me.

I would like to give my deepest thanks to my supervisor Prof. Fengyu Cong. Thanks for providing me the opportunity to study in Finland when I am confused about my future at the end of my master's study and introducing me to the field of cognitive neuroscience. I benefited a lot from every discussion with him because he always pointed the key points of my research problems and gave helpful suggestions. His efficiency, rigor and passion in academic research is a great treasure that will inspire me over my whole research career. I appreciate his support on each of my decision and his care about my future plans. I am proud of being a member of our ASAP family.

I have to express my sincere appreciation to Prof. Timo Hämäläinen, who became my supervisor in the last year of my doctoral study. He is a very responsible supervisor. I appreciate every 'Good work!' he said in the emails and our monthly group meetings, which made me encouraged. Thanks for his quick responses to all my research issues even during holidays and his constructive suggestions on my manuscripts. Thanks for helping me translate the abstract and summary of my thesis into Finnish. I am so proud and lucky with your help and guidance through the last year of my Ph.D. journey.

I also want to thank my supervisors Dr. Zheng Chang and Dr. Chi Zhang. Zheng always shared his experience and gave valuable suggestions on research and daily life. Thanks for all your help and guidance. Chi helped me a lot at the beginning of my doctoral study, and I am grateful for our discussions. I also want to thank all the colleagues in the Faculty of Information Technology at the University of Jyväskylä and the ASAP members in the Dalian University of Technology.

I am very grateful to have Prof. Peng Xu from the University of Electronic Science and Technology in China and Prof. Li Hu from the University of Chinese Academy of Sciences in China as the reviewers of this dissertation. Their constructive comments and suggestions helped to improve this thesis. I would also like to express my sincere appreciation to my opponent Prof. Fabio Babiloni from

the University of Rome Sapienza in Italy.

I sincerely thank all my friends, who helped me with my research and enriched my daily life, and I appreciate all the memorable times we had. Thanks to Dr. Xiulin Wang for all his patient help in my research and daily life. Thanks to Lili Tian for her lovely company during my whole Ph.D. journey. Thanks to Dr. Jia Liu, Dr. Ye Ren, Dr. Deqing Wang, Dr. Yongjie Zhu, Dr. Rui Yan, Tiantian Yang, Biying Wang, Huashuai Xu, Dr. Guanghui Zhang, Xiaoshuang Wang, Mahini Sheikhhosseini Reza, Dongdong Zhou, Xin Zuo, Jiaqi Zheng, and Liting Song for all the help and company. Thanks to Xueqiao Li, Weiyong Xu, and Haoran Dou from the T building, I appreciate all the delicious food and relaxed time we shared. Thanks to my old friend Hongyu Liu for her encouragement and care.

I would like to thank the financial support from the China Scholarship Council, China, and the Grant from the Faculty of Information Technology, University of Jyväskylä, Finland.

Finally, I am forever thankful to my whole family. Thanks to my parents for their endless love. They always support and respect all my decisions. Thanks for giving me so much freedom and trust. Special thanks to my nephew, Ruiqi Liu, for all the joy and happiness you bring to our whole family, and thanks for all the warm moments you bring to me.

Jyväskylä, October 2021

Wenya Liu

LIST OF ACRONYMS

CTD Coupled tensor decomposition
MDD Major depression disorder
FC Functional connectivity
dFC Dynamic functional connectivity
EEG Electroencephalogram
CP Canonical polyadic
MEG Electroencephalogram
ERP Event-related potential
fHALS Fast hierarchical alternating least squares
fMRI Functional magnetic resonance imaging
HALS Hierarchical alternating least squares
ICA Independent component analysis
MEG Magnetoencephalography
NMF Nonnegative matrix factorization
NTF Nonnegative tensor factorization
PARAFAC Parallel factor analysis
PCA Principle component analysis
ICNs Intrinsic connectivity networks
DMN Default mode network
FN Frontoparietal network
CEN Central executive network
SN Salience network
DSM-5 Diagnostic and Statistical Manual of Mental Disorders V
ICD-10 International Statistical Classification of Diseases and Related Health Problems
RSNs Resting state networks
dFC Dynamic functional connectivity
ROI Region of interest
sMRI Structural magnetic resonance imaging
DTI Diffusion tensor imaging
ImC Imaginary part of coherency
PLV Phase locking value
PLI Phase lag index
WPLI Weighted phase lag index

LIST OF FIGURES

CONTENTS

LIST OF INCLUDED ARTICLES

PI Wenya Liu, Chi Zhang, Xiaoyu Wang, Jing Xu, Yi Chang, Tapani Ristaniemi, and Fengyu Cong. Functional Connectivity of Major Depression Disorder Using Ongoing EEG during Music Perception. *Clinical Neurophysiology, 131(10), 2413-2422*, https://doi.org/10.1016/j.clinph.2020.06.031, 2020.

PII Wenya Liu, Xiulin Wang, Jing Xu, Yi Chang, Timo Hämäläinen and Fengyu Cong. Identifying Oscillatory Hyperconnectivity and Hypoconnectivity Networks in Major Depression Using Coupled Tensor Decomposition. *IEEE Transactions on Neural Systems & Rehabilitation Engineering, 29, 1895-1904*, https://doi.org/10.1109/TNSRE.2021.3111564, 2021.

PIII Wenya Liu, Xiulin Wang, Fengyu Cong and Timo Hämäläinen. Alpha Band Dysconnectivity Networks in Major Depression during Resting State. *29th European Signal Processing Conference (EUSIPCO 2021), Dublin, Ireland*, Accepted, 2021.

PIV Wenya Liu, Xiulin Wang, Timo Hämäläinen and Fengyu Cong. Exploring Oscillatory Dysconnectivity Networks in Major Depression during Resting State Using Coupled Tensor Decomposition. *submitted to IEEE Transactions on Biomedical Engineering*, 2021.

1 INTRODUCTION

Major depression disorder (MDD) is a multifactorial disorder, and it has become one of the most prevalent psychiatric disorders in the world. Almost one in six people will experience depression at some time in their life. Despite a large number of neurobiological studies, the precise etiology of MDD still remains poorly understood. Noninvasive neuroimaging techniques, like electroencephalogram (EEG), electroencephalogram (MEG), and functional magnetic resonance imaging (fMRI) are urgently needed tools to study the pathoconnectomics of MDD. Among the noninvasive neuroimaging techniques, EEG is an inexpensive technique with high temporal resolution and fine spatial resolution. EEG is able to directly record the electrical activity of neural populations and capture the dynamic changes at a millisecond scale. These advantages make EEG effective in exploring the pathological mechanism of MDD and promising to be applied to clinical diagnosis.

Noninvasive neuroimaging studies have presented rich evidences that the behavioral deficits in MDD are related to structural and functional abnormalities in some brain regions and the connectivity between them, defining depression as a "network disease". The dysfunction of large-scale brain networks in MDD has been widely investigated, including the abnormal intrinsic connectivity networks (ICNs), which support specific cognitive propcesses. The disrupted topological organization of functional brain networks is further quantified through graph theory, which enables to study the correlation with genetic and environmental factors. Existing researches have provided an integrative perspective on mood and cognitive deficits in MDD and potential biomarkers for the diagnosis and treatment of MDD.

However, so far, it is still hard to make the existing findings into clinical use due to many practical problems, such as poor test-retest reliability and sample heterogeneity of data, methodological inconsistency, and so on. Therefore, it is still urgent and necessary to develop novel methods in accordance with the data characteristics.

In this section, we will firstly give a basic introduction to MDD. Then, we will introduce the basic concept of functional connectivity (FC) and its associa-

tion with MDD. Followed we will present the disrupted connectomics in MDD based on graph theory. Finally, we will illustrate the motivation of the conducted research.

1.1 Major depression disorder

In the 1860s, the term *depression* appeared in the medical dictionary to refer to a physiological and metaphorical lowering of emotional functions (Berrios, 1988). In the mid-1970s, to propose diagnostic criteria according to the categories of symptoms, the term *major depression disorder* was introduced by some US clinicians. MDD is a mental disorder characterized by pervasive low mood. The diagnosis of MDD requires at least two weeks of distinct change of mood, characterized by sadness and low energy, low self-esteem, loss of interest in normally enjoyable activities, crying, suicidal thoughts, slowing of speech and action, and pain without a clear cause (Fava and Kendler, 2000; Otte et al., 2016). The exact causes of MDD are not yet understood despite many years' study. It has been demonstrated that the cause of MDD is multifactorial, and it is a comprehensive account of genetic, biochemical, and neurophysiological, and social factors (Belmaker and Agam, 2008; Gotlib and Joormann, 2010). For the clinical diagnosis of MDD, there are two most widely used criteria, including the Diagnostic and Statistical Manual of Mental Disorders V (DSM-5) and the International Statistical Classification of Diseases and Related Health Problems (ICD-10). However, the clinical diagnosis is pretty subjective due to human factors (Gruenberg et al., 2005). MDD is widespread and recurrent. Almost 20% of the population will experience at least one episode of depression during their lifetime, and the relapse rate is over 80% (Gotlib and Hamilton, 2008). Therefore, it is urgent and important to further investigate the pathogenesis and diagnostic tools of MDD.

Over the past decades, researchers have examined the neural mechanisms of MDD using neuroimaging techniques. Some remarkable brain regions have been demonstrated to be related to MDD, such as the amygdala, subgenual anterior cingulate cortex, dorsolateral prefrontal cortex, and so on, which are mainly related to memory, attention, and emotion regulation (Gotlib and Hamilton, 2008). In the 2000s, researchers started to examine the FC of MDD from a neural systems perspective, and they intended to explore the depressive neural network defined by spatially remoted brain regions that are inter-connected at rest or during task (Mayberg et al., 2005; Siegle et al., 2002). Of particular relevance are brain networks related to attention and emotion, such as default mode network (DMN), frontoparietal network(FN), dorsal attention network(DAN), and so on (Kaiser et al., 2015).

However, the correlation of MDD with human connectomics is still a rapidly evolving and highly complex field of study, and this is also an interdisciplinary research area demanding the cooperation of researchers from clinical medicine, cognitive neuroscience, and computational science.

1.2 Functional connectivity

The human brain is a complex network that synchronizes spatially distributed brain regions for collaborative functioning and facilitates the effective segregation and integration during information processing. Cognitive functions build on brain connectivity within large-scale neuronal networks (Varela et al., 2001; Petersen and Sporns, 2015). There are rich evidences from neuropsychological researches that MDD is associated with impairments in executive function, memory, and emotional processing (Gotlib and Joormann, 2010; Gong and He, 2015). Neuroimaging studies demonstrate that those impairments relate to functional and structural abnormalities in many brain regions and the FC between them. MDD involves alterations of functional and structural connectivity in multiple neuronal circuits, and those findings correspond to the current understanding of MDD as a network-based disorder (Gong and He, 2015; Mulders et al., 2015). In this section, we firstly introduce the basic concepts of FC, and then we will introduce the dynamic functional connectivity. Finally, we will review the current findings of the dysconnectivity of large-scale FC of MDD.

1.2.1 Basic concepts of functional connectivity

The human brain contains about one hundred billion neurons interconnected by synapses, establishing a highly intricate brain network. The human brain includes two principles of the functional organization, functional segregation and functional integration. Functional segregation relates to the localization of brain functions which are also , which implies that the brain functions are also anatomically segregated within the cortex, and a specific cortical regions is particularly related to some aspects of perceptual or motor processing (Friston, 2011). Functional integration can mediate the union of specialized brain areas, which describes the cooperative activation of functionally specialized areas during a cognitive process (Friston, 1994). Over the past decades, there is a shift in emphasis from functional segregation to integration. The concept of functional connectivity was introduced from functional integration in the 1990s, which is defined as statistical dependencies among remote neurophysiological events (Friston, 1994).

The brain activity is intrinsic and constantly active. Even in a resting state or task-negative state, the brain will show a high level of spontaneous activity, and different brain regions will communicate by FC. Functional neuroimaging studies propose this kind of spontaneous activity acts as the neuronal baseline activity in the brain, and it plays an essential role by providing important endogenous regulations to sensory-, cognitive-, or motor-driven activities (Damoiseaux et al., 2006; Mantini et al., 2007). One crucial research field initially studied by Prof. Bharat Biswal is resting state networks (RSNs), a group of functional networks which are well reproducible over different subjects and also stable over time within subjects during resting state (Biswal et al., 1995; Damoiseaux et al., 2006; Fukunaga et al., 2006; Fox et al., 2005; Beckmann et al., 2005). The RSNs are mostly identified by

multivariate decompositions of fMRI blood oxygen level dependent (BOLD) signals using the independent component analysis (ICA) method. Each of the RSNs is organized with functionally connected brain regions and is specifically related to some cognitive processes. Both previous EEG and MEG studies have shown that these RSNs also have an electrophysiological basis, and this is a critical step toward understanding the functional role of spontaneous activity (Mantini et al., 2007; Chang et al., 2013; Brookes et al., 2014; Baker et al., 2014; De Pasquale et al., 2010).

Since RSNs occur both during tasks and rest, the term *intrinsic connectivity networks* expands upon the concept of RSNs, which describe a set of large-scale functionally connected brain networks identified both during tasks and rest (Smith et al., 2009; Duyn, 2011). Each of the ICNs owns characteristic spatial signatures to support specific cognitive functions Laird et al. (2011); Seeley et al. (2009). The ICNs include sensory networks, like the visual network and the auditory network, and higher-order networks, like DMN, FN, and DAN. Most of the previous researches focus on identifying the segregated brain functional networks that may serve specialized functions.

1.2.2 Examining the dynamics of functional connectivity

An emerging and hot topic since the 2010s is dynamic functional connectivity (dFC), which considers the brain as a dynamic system. To support ongoing cognition both during tasks and rest, the brain will dynamically integrate and coordinate through the rapid formation and dissolution of a lot of functionally meaningful networks at different time scales (Hutchison et al., 2013; O'Neill et al., 2017). Most of previous researches assume that the FC is static and stationary during the long period of data recording for many minutes or even hours, as reflected in the analysis tools and metrics that are commonly applied (Hutchison et al., 2013). Until recent ten years, researchers started to examine the non-stationarity and dynamic changes over time of resting state and task-specific functional networks, which has provided greater insight into fundamental properties of brain networks and mechanisms of neuronal communications. A landmarkable study to firstly examine the dFC is from Chang and Glover (Chang and Glover, 2010). The resting state consists of different levels of attention, emotion, memory, arousal, and mind-wandering due to the wakefulness of the brain, and under this foundamental fact, they hypothesized that the FC between and within resting state networks will continuously keep changing to support cognitive functions. This study firstly illustrated the dynamics of resting state FC using predefined region of interest (ROI) and proposed the worth to measure the variability of FC. Another landmarkable study to examine dFC using resting state fMRI is from Allen and her colleagues (Allen et al., 2014). They applied group independent component analysis (ICA) and obtained 50 FC components and the corresponding time courses. Then, the dFC is estimated by computing correlations between time courses segmented by sliding time windows. Finally, the clustering method was applied to identify the repeatedly occurred FC patterns.

They demonstrated that some FC patterns were highly replicable over time.

The fMRI studies have provided significant evidence of non-stationary connectivity. However, the fMRI is based on the BOLD fluctuations, which are delayed to neural activity for several seconds due to the latency and longevity of the hemodynamic response. Also, the time difference between different scans only allows examining the FC dynamics at a second timescale. The limited temporal resolution of fMRI makes it unsuitable for imaging dynamic brain activity in the time frame in which these processes occur (He et al., 2019). What's more, it is possible that network dynamics or neural synchrony do not require changes in energy consumption and do not produce a BOLD signal in fMRI (Rossini et al., 2019). In contrast, EEG and MEG techniques can directly record the brain neuronal activities at a millisecond timescale. This temporal richness facilitates investigating the rapid change of FC patterns and captures transiently active networks (Rossini et al., 2019; O'Neill et al., 2017; Mantini et al., 2007). What's more, some studies have already reported that the EEG powers and simultaneously recorded BOLD signals within specific brain networks are significantly correlated in the fluctuations (Mantini et al., 2007). Several studies also demonstrated that most of the fMRI networks could be replicated in EEG and MEG networks(Hipp et al., 2012; Brookes et al., 2011b,a; De Pasquale et al., 2010).

Overall, the dFC has come to dominate the field, and the time-varying aspects of FC are challenging previous descriptions of static interactions within and between large-scale networks. The dFC can reveal the flexibility of functional coordinations between different neural networks and improve our understanding of behavioral shifts and adaptive processes (Allen et al., 2014; Hutchison et al., 2013).

1.2.3 Dysconnectivity networks in major depression disorder

Accumulating neuroimaging studies have concluded that MDD is linked to the dysregulation of multiple distributed functional networks, including cortical and limbic brain regions, but not the aberrant response of a single discrete brain region (Liu et al., 2021; Drevets et al., 2008; Seminowicz et al., 2004; Mayberg, 2003; Zeng et al., 2012; Mulders et al., 2015). However, there are not unifying findings due to the variability across studies in multiple aspects, such as different datasets recorded, different methods applied, different ROIs selected, and so on. The resting-state FC is the most widely used tool to investigate the imbalanced communication among cortical brain networks in MDD. Here, based on the most commonly consistent findings in resting-state studies, we introduce some core networks of particular relevance to MDD, including DMN, central executive network (CEN), and salience network (SN). The SN is theorized to mediate switching between the DMN and CEN, and a triple network model constructed by DMN, CEN, and SN has exhibited an explanatory power for psychiatric disorders (Menon, 2011; Sridharan et al., 2008; Goulden et al., 2014).

(1) Default mode network: The DMN is also known as a task-negative network, because it is prominently activated during rest (Raichle et al., 2001). There

are two sub-networks of DMN including anterior and posterior DMN. The key region of the anterior DMN is the medial prefrontal cortex, and the posterior DMN centers on the posterior cingulate cortex and the precuneus cortex (Andrews-Hanna et al., 2010; Buckner et al., 2008). The DMN is related to internally oriented attention, self-referential processing, emotion regulation, and memory processing (Andrews-Hanna et al., 2014; Cavanna and Trimble, 2006; Leech and Sharp, 2014; Mulders et al., 2015). The hyperconnectivity within DMN is commonly identified during resting state using both seed-based method and ICA method (Kaiser et al., 2015; Mulders et al., 2015).

(2) Central executive network: The CEN, generally known as the FN, is primarily composed of the dorsolateral prefrontal cortex and the lateral posterior parietal cortex. Contrary to the DMN, the CEN is a task-positive network due to strong activation during cognitive tasks. The CEN involves the top-down regulation of attention and emotion (Kaiser et al., 2015; Gong et al., 2016). The aberrant connectivity of the CEN may indicate the deficits in concentrating or regulating emotions (Snyder, 2013).

(3) Salience network: The SN is primarily composed of the anterior insula and dorsal anterior cingulate cortex, and it is activated in detecting various salient stimuli and recruiting relevant functional networks (Menon and Uddin, 2010; Peters et al., 2016). It is demonstrated that the SN contributes to emotional control and processing, social behavior, and self-awareness (Mulders et al., 2015; Menon, 2011; Menon and Toga, 2015). For the MDD group, increased conenctivity within the SN is commonly concluded using both seed-based method and ICA method (Mulders et al., 2015).

Besides the abnormal connectivity within each core network, the changed connectivity between different networks is also widely identified to be related to MDD, which may reflect the disability in altering the interaction between networks (Abbott et al., 2013). For example, the increased connectivity between the anterior DMN and the SN in MDD is commonly reported across different methods, and the decreased connectivity between the posterior DMN and the CEN is also regarded as an important biomarker of MDD (Manoliu et al., 2014; Mulders et al., 2015).

1.3 Graph theory

Over the past 20 years, the topological description of the brain network, well known as the human connectome, is an emerging and hot topic (Sporns et al., 2005, 2004). Attempts to characterize these networks have led to the emergence of a new, multidisciplinary approach, called complex network analysis, which origins from the realm of graph theory born in 1736 (Rubinov and Sporns, 2010). Graph theory facilitates the quantification of brain topology and provides a powerful mathematical framework to characterize or compare the topological orga-

nization of brain networks from different groups. Combined with neuroimaging, graph-based network analysis revealed many nontrivial topological properties that are disrupted in various brain disorders, including MDD, like disrupted global integrity and regional connectivity (Gong and He, 2015). The topological disruption may provide valuable diagnosis biomarkers and new insights into the neuropsychopathology of MDD. In this section, we firstly introduce the basic concepts of graph theory and then summarize the current findings of the disrupted topology of MDD.

1.3.1 Introduction of graph theory

The brain network can be modeled as a graph that comprises nodes (neural elements) connected by edges (connections). The representation of nodes depends on the modality of the collected signals (Stam and Reijneveld, 2007). For electrophysiological techniques, like EEG and MEG, there are two kinds of definitions of the nodes according to the modeling space. In the sensor space, the nodes can be the electrodes, and in the source space, the nodes represent the vertices or brain regions according to the anatomical atlas. For the fMRI modality, the nodes denote the voxels or brain regions according to the parcellation atlas. The edges represent the connection existence (binary graph) or strength (weighted graph) between pairs of nodes measured as structural, functional, or effective connectivity. For different measures of connectivity, the brain network can also be modeled as an undirected graph for FC and a directed graph for effective and structural connectivity.

Gong and He concluded that for both binarized or weighted brain networks, the topological architectures of the brain networks can be depicted at three levels: global properties, regional nodal properties, and modularity (Gong and He, 2015). The global properties, such as clustering coefficient, shortest path length, and global efficiency, represent the ability to rapidly integrate specialized information from distributed brain regions and the capacity of the overall information processing. The regional nodal properties, such as degree and betweenness centralities, reflect the local information processing within the brain regions. The identifying of hubs and communities through local properties can efficiently transfer regional information and facilitate global information integration (Sporns, 2013; He and Evans, 2010; Bullmore and Sporns, 2012, 2009). Modularity indicates a set of non-overlapping modules from the subdivision of brain networks, which can support specific functions (van den Heuvel and Sporns, 2013; Newman, 2006). Modularity is also an important metric to reveal the dynamics of brain organizaiton (Boccaletti et al., 2006).

Graph theory has provided a topological view of network organizations to further reveal and understand the human cognitive function, performance, and behavior (Barrat et al., 2008; Sporns, 2010; Bullmore and Sporns, 2012). The complex anatomical and functional architecture of the brain, such as rich hubs, modular structure, and small-worldness, have provided strong support and evidence that the human brain is an economic system. The brain organization can dy-

namically balance the trade-off between wiring cost and topological value from millisecond to hour timescales. To support different cognitive demands, the brain network will dynamically evolve and adapt by changing the strength of connections and community membership of nodes (Kabbara et al., 2017; Bullmore and Sporns, 2012; Hutchison et al., 2013).

In the view of clinical applications, the topological analysis of brain networks has helped to reconceptualize the pathogenesis and present potential biomarkers of neuropsychiatric disorders, like MDD, schizophrenia, and autism (Bassett and Sporns, 2017; Fornito et al., 2015; Gong and He, 2015; Fornito et al., 2012).

1.3.2 Disrupted topology of major depression disorder

The human brain is a complex network, which is structurally and functionally connected to support information segregation and integration during cognitive tasks. The topological properties have demonstrated that the network resilience of healthy brains can resist various neuropathological lesions. MDD is related to the disrupted topological organization of functional and structural brain networks, which is demonstrated by global, modular, and nodal properties. Different neuroimaging techniques have been applied to investigate the disrupted network topology in MDD, including fMRI, structural magnetic resonance imaging (sMRI), diffusion tensor imaging (DTI), and EEG (Zhang et al., 2011; Meng et al., 2014; Bohr et al., 2013; Tao et al., 2013; Singh et al., 2013; Ajilore et al., 2014; Korgaonkar et al., 2014; Sun et al., 2019; Hasanzadeh et al., 2020). Those previous findings have provided valuable topological biomarkers in the diagnosis and treatment of MDD.

Two remarkable review studies have summarized findings regarding the structural and functional brain connectome for MDD in the duration of 2011-2014 and 2015-2020, respectively (Gong and He, 2015; Yun and Kim, 2021). Summarizing the previous studies, some consistent findings can be concluded. First, the ability of global integrity is lower in MDD compared with healthy controls. Second, brain networks in MDD have a trend to changing to random networks, while the healthy controls have small-world networks. Third, the depressive symptom, illness duration, and treatment response of MDD can affect local network properties.

However, the existing studies on disrupted connectomics in MDD are still limited and urgently needed. The previous results are often inconsistent or even contradictory (Zhi et al., 2018). For example, Zhang et al. reported a increased global efficiency in the MDD group, while Meng et al. showed that the global efficiency is decreased in the MDD group (Zhang et al., 2011; Meng et al., 2014). The inconsistency of current findings can result from multiple factors (Hallquist and Hillary, 2018). From the technical perspective, it could be different modalities (fMRI or sMRI), different definitions of nodes and edges, or different graph metrics. For the clinical reason, it could be different and unbalanced age and gender distribution of MDD patients, different symptoms, different durations of MDD, or different medication statuses. Therefore, it is still a long way to go to

obtain a unified theory of the topological mechanism of MDD, and make it into use for the clinical diagnosis and treatment.

1.4 Research motivations

The motivations of our studies can be concluded from two aspects.

(1) From the view of experimental design, there is a challenge to conventional paradigms with sparsely and abstract stimuli, called naturalistic paradigms. Naturalistic paradigms are also called ecologically valid paradigms, which aim to approximating real-life experiences using naturalistic and continuous stimuli, such as movies, music, and spoken stories. The well-controlled laboratory-style experiments have yielded a fundamental understanding of specialized functions in the brain, but they are always debatable. Because our daily life are dynamically mixed with multimodal information, and the traditional paradigms can not answer how the brains resemble different types of stimuli and integrate the information in the brain. To answer this question, starting from two memorable studies conducted by Hasson and Bartels, increasingly neuroscientists have shifted their focus on naturalistic paradigms (Hasson et al., 2004; Bartels and Zeki, 2004). The landmark achievements on naturalistic paradigms include three reviews and the special issue in journal *Neuroimage, Naturalistic Imaging: The use of ecologically valid conditions to study brain function* (Sonkusare et al., 2019; Vanderwal et al., 2019; Jääskeläinen et al., 2020).

Naturalistic paradigms have shown a clinical potential in mental disorders, such as MDD, autism-spectrum disorder, paranoia, borderline personality disorder (Sonkusare et al., 2019). However, to the best of our knowledge, no studies have investigated the dysconnectivity of large-scale functional networks in MDD during music listening conditions. In Study I, using EEG recorded during listening to modern tango, we studied the sensor-level functional connectivity in MDD, applied graph theory-based methods to measure the topology of brain networks, and tested the potential biomarker of MDD diagnosis (Liu et al., 2020b).

(2) From the view of methodological applications, there is a challenge regarding the multiway and multimodal structure of data. The constructed data by brain networks characterize a multiway structure with the dimension of time $\times$ frequency $\times$ connectivity $\times$ subject. The time domain can examine the temporal dynamics of brain networks, which is well-described in the introduction part (Hutchison et al., 2013). The frequency domain can explore the oscillatory signatures of brain networks. It has been demonstrated that neuronal synchronization and communication between different brain regions is regulated by oscillations, and it is necessary to explore the oscillatory networks. The connectivity domain represents the phase couplings between pairs of brain regions, and the communication of brain regions or neural populations depends on phase interactions (Palva and Palva, 2012). A well-designed experiment always collects data from multiple subjects, constituting an important dimension of the constructed data.

The multimodal structure means the data can be collected from different groups, e.g., the healthy group and the patient group, or different modalities, e.g., fMRI and EEG. Different modalities of data will share common features and also retain individual features (Wang et al., 2020; Wang, 2020; Acar et al., 2017). However, few studies considered the multiway and multimodal structure of data simultaneously.

MDD is associated with abnormal dFC and impaired coordination of oscillatory FC (Kaiser et al., 2016; Demirtaş et al., 2016; Yao et al., 2019; Zhao et al., 2021; Fingelkurts et al., 2007; Whitton et al., 2018). Non-invasive EEG has been demonstrated to be a potentially valuable and reliable tool to study and detect MDD (de Aguiar Neto and Rosa, 2019; Leuchter et al., 2012). Considering the multiway and multimodal nature of constructed data, we proposed a comprehensive and novel framework based on coupled tensor decomposition. In Study II, using the same data in Study I, we proposed a comprehensive framework to explore the source-level dynamic functional connectivity characterized by spatio-temporal-spectral modes of covariation (Liu et al., 2021), which are also hyper- or hypo-connectivity networks in MDD. The extracted dFC networks are taks-relatd, frequency-specific, and music-modulated. In study III, referring study II, we proposed a framework based on coupled tensor decomposition using alpha band resting EEG to explore the sensor-level dysconnectivity networks of MDD. In study IV, we applied the same framework as study III to source-level resting EEG and identified the hyper- or hypo-connectivity networks in MDD during resting state. Studies II, III, and IV have primarily demonstrated the efficiency and feasibility of a coupled tensor decomposition model applied in MDD using EEG. The proposed model and pipeline can be easily applied to other psychiatric disorders.

1.5 Structure of the dissertation

The structure of this dissertation is listed as follows:

Chapter 1 introduces the basic concepts of major depression, functional connectivity, and graph theory, as well as the current findings of previous studies on abnormal large-scale brain networks and disrupted topology in major depression disorder. The motivation of the research is also presented.

Chapter 2 describes the commonly used methods of functional connectivity and the metrics of graph theory.

Chapter 3 briefly summarizes the included articles and lists the contributions of authors to the articles.

Chapter 4 presents the discussion and conclusion of this dissertation, as well as the research limitations and future directions.

2 METHODS

The human brain is organized as a complex network at micro-meso-macro-scale levels. From the view of large-scale functional connectivity, the brain can be modeled by a set of nodes (brain regions) and interconnecting edges (statistical independence). The measurement of statistical independence is a fundamental step to reveal topological architectures and network dynamics. The brain connectome can further provide neuromarkers of mental diseases and task-specific cognitive functions. Figure 1 shows the whole pipeline for functional brain networks modelling and analysis (This figure is cited from (de Vico Fallani et al., 2014)). In this chapter, first, we will introduce the measurements of FC with different kinds of metrics, and then present the topological properties of brain networks measured by graph theory. Finally, we will summarize the commonly used methods to assess the dynamics of functional networks.

2.1 Metrics of functional connectivity

For measuring the connections between predefined network nodes, there are many kinds of hypothesis-free methods, which are suitable as exploratory techniques (Rossini et al., 2019). For example, correlation and coherence are linear methods, which determine the extent to which two variables covary in time space and frequency space, respectively. Information-based methods, like mutual information and transfer entropy, can measure the linear and non-linear interdependence between two signals. Phase synchronization methods, including imaginary part of coherency (ImC), phase locking value (PLV), phase lag index (PLI), and weighted phase lag index (WPLI), measure the phase couplings between two signals also without a linearity assumption. Those metrics can be used as whole-brain approaches, and do not necessarily need the preselected ROI as hypothesis-driven methods, like dynamic causal modeling (Rossini et al., 2019).

The theory has been demonstrated that neural oscillations play a key role in coordinating the activity of spatially remote brain regions. The oscillation

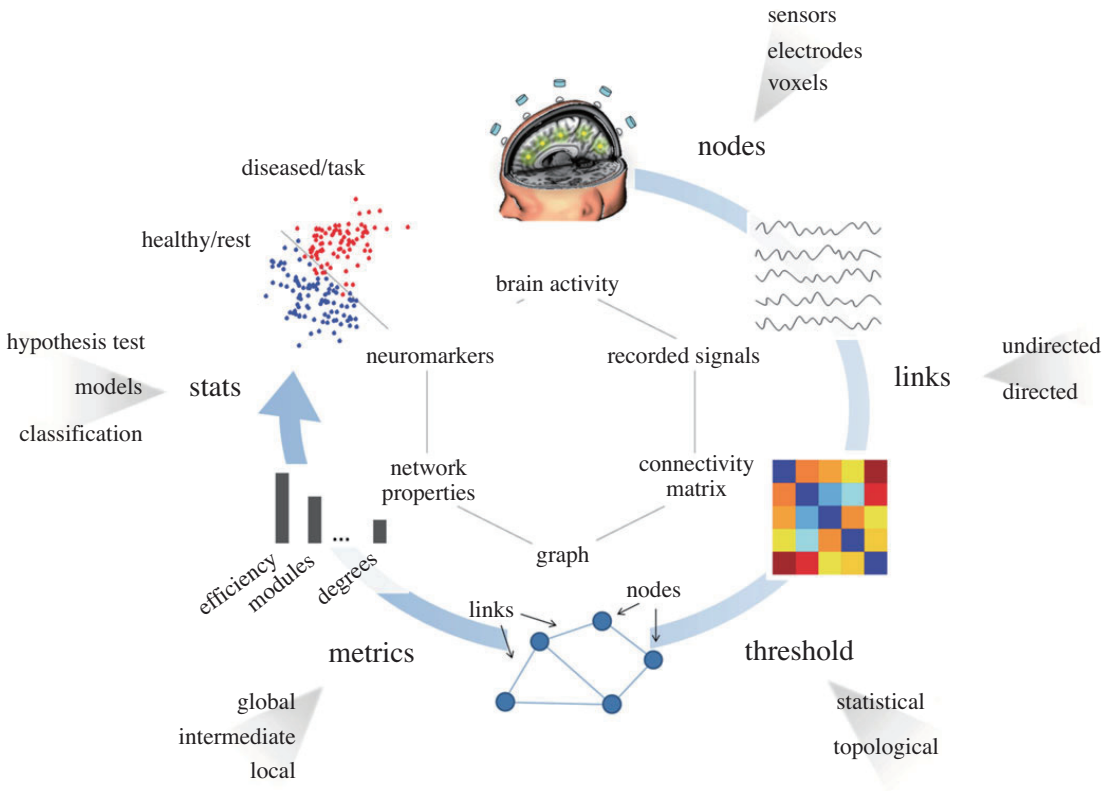

FIGURE 1 Pipeline for functional brain networks modelling and analysis (Cited from (de Vico Fallani et al., 2014)).

can connect different brain regions with resonant communication to construct a functional network. The oscillatory changing can regulate dynamics of neuronal networks, forming the mechanism for creating a flexible and hierarchical communication structure and causing qualitative transitions between different modes of information processing (Fries, 2005; Buzsáki and Draguhn, 2004; Engel et al., 2001; Varela et al., 2001; Salinas and Sejnowski, 2001). Supported by this theory, phase synchronization methods are widely and successfully applied for electrophysiological data (e.g., EEG and MEG). From this point and the EEG signals used in the thesis, in this section, we introduce the phase-based metrics of functional connectivity. For the other metrics, please refer to the review studies (Rossini et al., 2019; He et al., 2019; Engel et al., 2013).

Electrophysiological techniques all suffer from a common problem that the calculating relation between two time series is influenced by the time series especially recorded from nearby electrodes. The recording sensors are not placed in direct contact with the nerve cells generating the signal, and the electric or magnetic fields from an electric primary current source will be transmitted through biological tissue towards measurement sensors. Therefore, the signal collected from one electrode is mixed with the signals from the whole brain, and there are always common sources for two electrodes, which will cause spurious interactions. This effect is called volume conduction (field spread or signal leakage) (Rutkove, 2007; van den Broek et al., 1998; Brunner et al., 2016). It is always

possible that two selected brain regions, presenting a high value of interactions, are not truly connected at all. This phenomenon commonly exists, especially for amplitude-based connectivity metrics. One promising and appealing solution is selecting the measures that are not sensitive to the volume conduction effect, such as ImC, PLI, and WPLI (Nolte et al., 2004; Stam et al., 2007; Vinck et al., 2011). This kind of metrics is based on the theory that volume conduction can cause the instantaneous phase lags of 0 or π, and it can affect the amplitude but not the non-zero phase.

In this section, we will describe phase-based metrics used to quantify connectivity, including metrics that are sensitive (coherence and PLV) and insensitive (ImC, PLI, and WPLI) to the volume conduction effect. We also conclude the advantages and disadvantages of each method. First, we need to define some commonly used representations among those five methods. For time series $x_1(t)$ and $x_2(t)$ from two spatially separated brain regions, there analytical signals $z_1(t)$ and $z_2(t)$ can be obtained through Hilbert transform (or wavelet transform) (Bruns, 2004), as follows:

$$z_1(t) = x_1(t) + i\tilde{x}_1(t) = A_1(t)e^{i\phi_1(t)} \tag{1}$$

and

$$z_2(t) = x_2(t) + i\tilde{x}_2(t) = A_2(t)e^{i\phi_2(t)}, \tag{2}$$

where $\tilde{x}_i(t), i = 1,2$ is the imaginary part, $A_i(t) = \sqrt{x_i(t)^2 + \tilde{x}_i(t)^2}, i = 1,2$ is the instantaneous amplitude, and $\phi_i(t) = arctan\frac{\tilde{x}_i(t)}{x_i(t)}, i = 1,2$ is the instantaneous phase.

2.1.1 Coherence

Coherence is a traditional method to measure the linear relationship of phase synchronization in the spectral domain for electrophysiological signals. The coherence is defined as the cross spectrum $S_{x_1x_2}$ divided by the product of the two power spectra $S_{x_1x_1}$ and $S_{x_2x_2}$ at frequency bin f, as follows:

$$Coh(f) = \frac{|S_{x_1x_2}(f)|^2}{S_{x_1x_1}(f)S_{x_2x_2}(f)}. \tag{3}$$

We can also compute the mean over time of the analytical signals z_1 and z_2 instead of the mean of coherence over all frequencies, which is represented as follows:

$$Coh = \left| \frac{A_1A_2e^{i\Delta\phi}\rangle}{\sqrt{A_1^2\rangle \ A_2^2\rangle}} \right|, \tag{4}$$

where$\langle\cdot\rangle$ represents the mean value and $\Delta\phi = \phi_1 - \phi_2$ represents the instantaneous phase difference. Coherence varies from 0 to 1, representing no coupling and perfect coupling respectively.

Coherence is easy to understand and compute. However, it only reflects the linear correlation between two signals with intermingling phase and amplitude correlations, and it can be easily affected by common inputs due to using the amplitude information (i.e., the volume conduction effect).

2.1.2 Phase locking value

Because coherence mixes amplitude and phase contributions, Lachaux et al. proposed phase locking value (PLV) to quantify the phase relationship by phase-locking statistics, thus excluding the amplitude information (Lachaux et al., 1999). Perfect phase synchronization will produce constant phase differences. After projecting the instantaneous phase differences on the unit circle, PLV measures the consistency of phase differences by phase-locking statistics. The PLV can be computed as follows:

$$PLV = \left\langle e^{i\Delta\phi} \right\rangle . \tag{5}$$

The PLV is also bounded between 0 and 1. The PLV can avoid the mixing of amplitude and phase correlations, and it is less affected by the amplitude variability of the power spectrum. However, PLV can also be influenced by zero-lag phases, and volume-conducted activities can result in a non-zero PLV value.

2.1.3 Imaginary part of coherency

To overcome the influence of volume conduction effect, Nolte et al. proposed the imaginary part of coherency (ImC) index, which can measure the true interaction of two signals even with common sources (Nolte et al., 2004). The ImC is calculated as follows:

$$ImC = \left| \frac{\langle A_1 A_2 sin\Delta\phi \rangle}{\sqrt{\langle A_1^2 \rangle \ \langle A_2^2 \rangle}} \right| , \tag{6}$$

from which we can see a 0 or π phase lag will cause a zero ImC. Therefore, the linear mixing of uncorrelated sources will not result in a non-zero ImC, thus making it insensitive to the volume conduction effect. However, ImC is affected by the value of the phase difference, which makes it failed to accurately measure the consistency of phase differences. It is suitable with a phase lag corresponding to a quarter cycle (Stam et al., 2007; Vinck et al., 2011).

2.1.4 Phase lag index

Regarding the disadvantages of ImC, Stam et al. proposed the phase lag index (PLI) method. The PLI measures the asymmetry of phase difference distribution between two signals. The basic idea is that if two signals do not contain common sources due to volume conduction, the consistent and non-zero phase lag or phase lead will preserve, and if two signals are volume-conducted by common sources, the phase difference distribution will be centered around 0 or π. That is to say, a perfect phase coupling represents that the phase difference is distributed in the interval $-\pi < \Delta\phi < 0$ for consistent phase lag or in the interval $0 < \Delta\phi < \pi$ for consistent phase lead. No coupling means the phase difference distribution is symmetrical. We can calculate the PLI value by

$$PLI = |\langle sign\left[\Delta\phi\right]\rangle| . \tag{7}$$

The PLI is normally taken as the absolute value, making it bounded between 0 and 1. A value of 1 means perfect coupling, and a value of 0 means no coupling or a result from volume conduction (phase differences are centered around 0 or π). We can also remove the absolute operation, and measure the directed interactions or information flow (effective connectivity) regarding the phase lag or phase lead. However, the main disadvantage of PLI is its sensitivity to noise. Phase lag can be easily turned into phase lead by small perturbations from noise, and vice versa. Due to this, the volume conduction effect may not be effectively reduced.

2.1.5 Weighted phase lag index

Considering the disadvantages of ImC and PLI, Vinck et al. proposed a new method, called weight phase lag index (WPLI), which is insensitive to volume conduction, small noise perturbations, and the value of phase differences (Vinck et al., 2011). The WPLI is shown as follows:

$$WPLI = \frac{|\langle Im(S_{x_1x_2})\rangle|}{\langle |Im(S_{x_1x_2})|\rangle}, \tag{8}$$

and it can also be presented as

$$WPLI = \frac{|\langle |Im(S_{x_1x_2})|\, sign\Delta\phi\rangle|}{\langle |Im(S_{x_1x_2})|\rangle}, \tag{9}$$

where $S_{x_1x_2}$ is the the cross-spectrum of two signals. The WPLI ranges between 0 and 1. We can see that compared with PLI, WPLI uses the magnitude of the imaginary part of the cross-spectrum as the weights of phase differences. Therefore, a phase difference near 0 or π will get a smaller weight, thus being insensitive to small noise perturbations.

There are two points that we should clarify. First, ImC, PLI, and WPLI can reduce spurious interactions due to volume conduction to some extent, but the volume conduction can not be entirely eliminated. Second, from the view of statistical meaning, all the five metrics described above should be calculated over a fine number of data points (i.e., signals x_1 and x_2 should have a sufficient length of data points). If we calculate the metrics over time points within a time window, we can get an averaged connectivity value for each time window, and this type of calculation is suitable for EEG or MEG data collected in naturalistic paradigms or resting state. If we calculate the metrics over trials, then we can measure the inter-trial variability of the phase differences and this condition can be applied to event-related EEG or MEG data (Aydore et al., 2013; Rossini et al., 2019; Liu et al., 2020a).

2.2 Metrics of graph theory

The brain network topology based on graph theory has been widely applied to reveal the segregation and integration of neural information in cognition and

explore the mechanism of mental diseases (de Vico Fallani et al., 2014; Sporns, 2013; Yun and Kim, 2021; Park and Friston, 2013). As described by (de Vico Fallani et al., 2014), the topological properties of brain networks can be divided into three categories according to the scales of the brain network. The first category is large-scale metrics of the brain network, which includes the metrics on the entire graph and describes the whole brain network properties. The second one is intermediate-scale metrics, which measure the communities or modules of subgraphs consisted of densely connected nodes. The third category is small-scale metrics, which quantifies the properties of single nodes. The topological metrics selection primarily depends on the research question, like which level of brain network properties fits the research interests. The calculation of the metrics is different according to the constructed networks, such as binary or weighted networks, and directed or undirected networks. For simplicity, we only presented some commonly used metrics for weighted and undirected networks in this section. Please refer to the review studies for exhaustive explanations and mathematical descriptions of all the existing metrics (de Vico Fallani et al., 2014; Rubinov and Sporns, 2010). Figure 2 shows some network metrics for an intuitive understanding of the network topology.

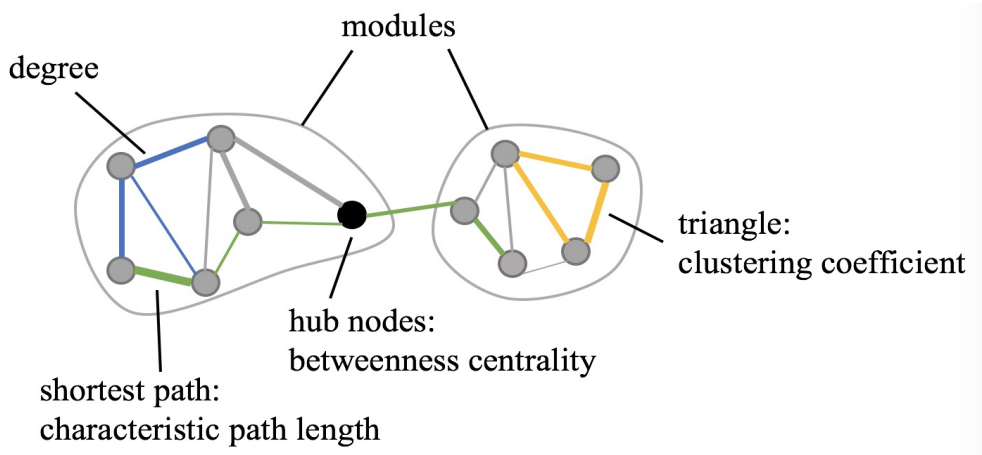

FIGURE 2 Measures of network topology for a weighted and undirected graph.

For a weighted and undirected graph **G** with N nodes, its edge between node i and node j is represented as w_{ij}, which is bounded between 0 and 1. Please note that the self-connection $w_{ii}, i = 1, 2, ..., N$ is zero.

2.2.1 Small-scale metrics

2.2.1.1 Degree

Degree can reflect the importance of a node and represent the number of links connected to a node. It is a fundamental concept based on which many metrics

are defined. The degree of node i is defined as:

$$k_i = \sum_{j=1}^{N} w_{ij}. \tag{10}$$

2.2.1.2 Betweenness centrality

Betweenness centrality of a node measures its participation in many short paths within a network. It is defined as the fraction of all shortest paths in the network that pass through it (Brandes, 2001; Kintali, 2008; Rubinov and Sporns, 2010), as follows:

$$BC_i = \frac{1}{(N-1)(N-2)} \sum_{h=1,h\neq i}^{N} \sum_{j=1,j\neq i,h}^{N} \frac{\rho_{hj}^{(i)}}{\rho_{hj}}, \tag{11}$$

where ρ_{hj} represents the number of shortest paths between node h and node j, and $\rho_{hj}^{(i)}$ means the number of shortest paths between node h and node j which pass through node i.

2.2.2 Intermediate-scale metrics

2.2.2.1 Community

The communities or modules are important indexes of the functional segregation of the network. The human brain have a modular structure with nodes integrated locally through strong short-range edges (Park and Friston, 2013). The modular organization of the brain network indicates segregated neural processing and specialized cognitive functions and enables efficient global communication among modules.

Different from other metrics, the detection of modular structure or community structure typically needs efficient optimization algorithms. There are many methods for community detection, such as the Louvain community detection algorithm, Newman's spectral community detection algorithm, link-based community detection algorithm, clique-percolation community-detection algorithm, and so on (Blondel et al., 2008; Newman, 2006; Ahn et al., 2010; Palla et al., 2005; Rubinov and Sporns, 2010). For the realization of different community detection algorithms, please refer to Brain Connectivity Toolbox (http://www.brain-connectivity-toolbox.net) (Rubinov and Sporns, 2010).

2.2.3 Large-scale metrics

2.2.3.1 Clustering coefficient

Clustering coefficient of the network measures the fraction of triangles around a node. It can reflect functional segregation by depicting the node tendency of

forming local triangles. The Clustering coefficient is defined as:

$$CC = \frac{1}{N}\sum_{i=1}^{N}\frac{2t_i}{k_i(k_i-1))}, \tag{12}$$

where $t_i = \frac{1}{2}\sum_{j=1}^{N}\sum_{h=1}^{N}(w_{ij}w_{ih}w_{jh})^{\frac{1}{3}}$ means the geometric mean of triangles around node i.

2.2.3.2 Characteristic path length

Characteristic path length is a measure of functional integration of the network. It is defined as the average of the shortest weighted path length between all pairs of nodes, as follows:

$$CPL = \frac{1}{N}\sum_{i=1}^{N}\frac{\sum_{j=1,j\neq i}^{N} d_{ij}}{N-1}, \tag{13}$$

where d_{ij} is the shortest weighted path length between node i and j.

2.2.3.3 Small-worldness

Small-worldness measures the balance between functional segregation and functional integration of the network (Humphries and Gurney, 2008). Different from the random network and the regular network, the small-world network is simultaneously highly segregated and integrated, exhibiting low characteristic path length and high clustering coefficient. Both structural connectivity and functional connectivity have reported that the human brain network showed a small-worldness property, which ensures the high efficiency of information transfer with low-wire cost (Hallquist and Hillary, 2018). The small-worldness of the network is calculated as:

$$SW = \frac{CC/CC_{rand}}{CPL/CPL_{rand}}, \tag{14}$$

where CC_{rand} and CPL_{rand} are the clustering coefficient and the characteristic path length of a random network. A small-world network often has $SW > 1$.

2.3 Dynamic functional connectivity

To start, let's take a step back to the evolving hot topic during the recent ten years. Brain functional connectivity is dynamic at different timescales, ranging from the sub-second to the lifespan (Kopell et al., 2014; Calhoun et al., 2014; Di Martino et al., 2014; Betzel and Bassett, 2017; Zalesky et al., 2014). These dynamics of brain network organization have provided new insights into the mechanisms of human cognition and behavior. How do we study the dynamics of brain networks changing over time?

In this section, we introduce some popular and commonly used methods to track the dynamics of brain networks, including clustering-based methods,

decomposition-based methods, and graph-based methods. The first two types of methods aim to find reproducible and transient patterns of FC. The graph-based methods aim to track time-varying changes of FC graphs from the view of topology.

2.3.1 Clustering-based methods

To find the repeated spatial patterns of functional networks along time, a network-level cluster-based approach was proposed as a temporal decomposition procedure. With the FC patterns calculated on windowed segments or at each time point, the cluster-based approach aims to divid them into a number of transiently synchronizing networks. Figure 3 demonstrates the analysis pipeline of the cluster-based method. The most frequently used clustering method is k-means, which is widely applied to extracting repeated FC patterns in fMRI, EEG, andMEG studies (Liu and Duyn, 2013; Allen et al., 2014; Hassan et al., 2015; De Pasquale et al., 2016; O'Neill et al., 2015). For example, in a resting state fMRI study, Liu et al. used k-means clustering analysis to examine the replication of RSN patterns, and the identified multiple spatial patterns may suggest a potential functional relevance (Liu and Duyn, 2013). However, the main difficulties of clustering-based methods are the selection of algorithms (e.g., distance or phase based) and the corresponding parameters (e.g., distance threshold and the cluster number) (Hutchison et al., 2013).

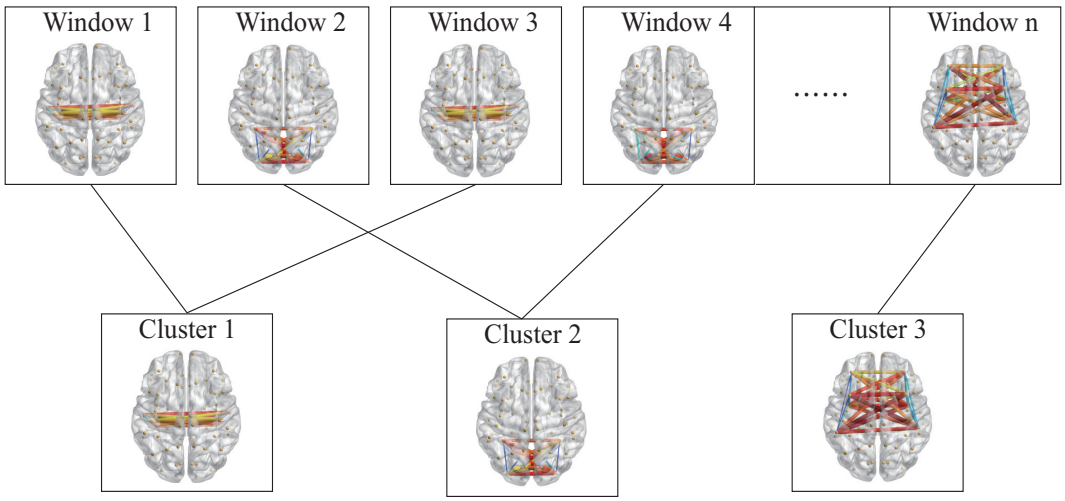

FIGURE 3 The analysis pipeline of the cluster-based method for extracting repeated functional networks.

2.3.2 Decomposition-based methods

According to the structure of the constructed data, the decomposition-based methods can be referred to matrix decomposition or tensor decomposition. This kind of method aims to extract the segregated FC patterns that may serve specialized

functions, like the functional network in ICNs (Gao et al., 2021). Decomposition-based methods will decompose the adjacency matrix/tensor to some network components and corresponding temporal profiles (as well as the subject contribution or spectral modulation according to the structure of the data). The basic assumption of matrix/tensor decomposition-based methods is that for every time point or each time window, the functional connectivity network is a linear combination or coactivation of several network components, which represent the repeating FC patterns.

2.3.2.1 Matrix decomposition

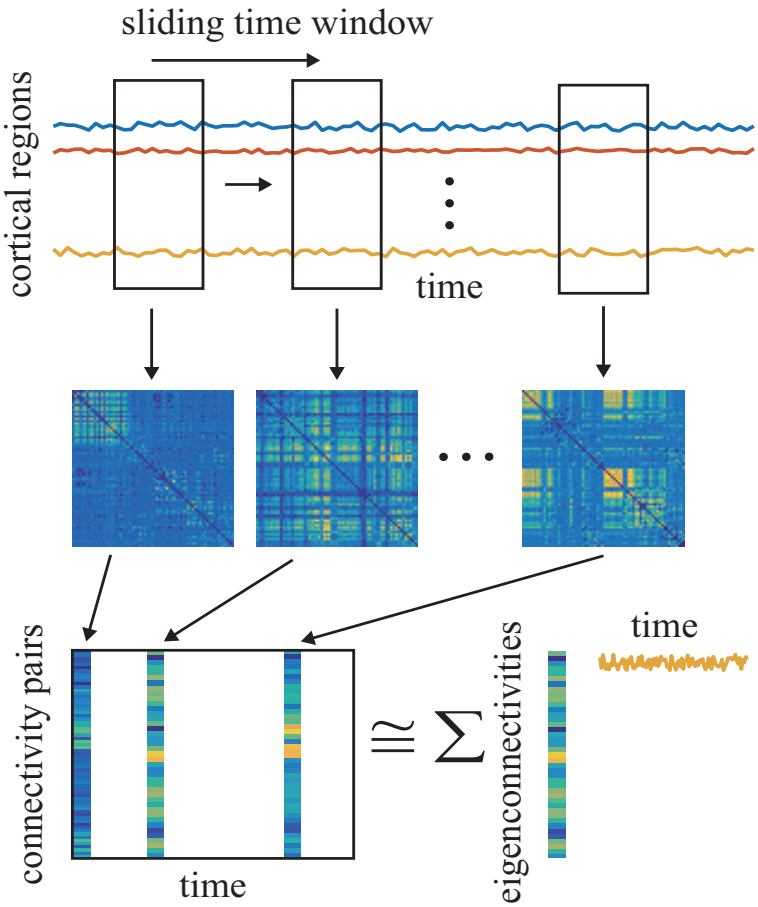

FIGURE 4 The analysis pipeline of matrix decomposition methods for extracting repeated functional networks.

Matrix decomposition methods, like PCA, ICA, and nonnegative matrix factorization, have been widely and successfully applied to identify repeating and meaningful functional networks (Leonardi et al., 2013; Brookes et al., 2012; O'Neill et al., 2017; Zhu et al., 2020b; Brookes et al., 2011b; Koelewijn et al., 2017; Nugent et al., 2017; Zhou et al., 2020; Smitha et al., 2017; O'Neill, 2016). The analysis pipeline of the matrix decomposition method is shown in Figure 4. The functional connectivity is first computed using a sliding window method (time point

to time point connectivity is also possible), and then matrix decomposition methods can be applied on this temporally concatenated adjacency matrix. Finally, we can get a set of time-dependent network components. Please note that group analysis is also possible if we fold the time and subject dimensions. However, this "artificially flatten" operation will remove the specific information endorsed by higher-order structure and make it difficult in results interpretation (Cichocki, 2013). What's more, the ICA and PCA will impose independent or uncorrelated constraints on the network components, which also makes it difficult to explain the results.

2.3.2.2 Tensor decomposition

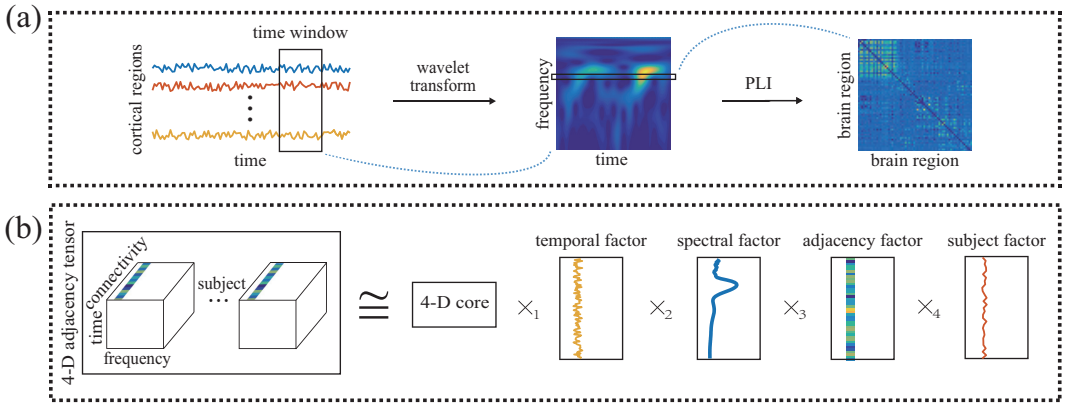

FIGURE 5 The analysis pipeline of tensor decomposition methods for extracting repeated functional networks. (a) The construction of a 4-D adjacency tensor with the dimension of time × frequency × connectivity × subject. (b) The CP decomposition of the adjacency tensor.

Tensor decomposition is an extension of matrix decomposition regarding the multiway or multidimensional structure of data. In recent years, tensor decomposition has been widely used in brain imaging data. Please refer (Cichocki, 2013; Cong et al., 2015; Zhou et al., 2016) for reviews. For electrophysiological data (EEG or MEG), the data can be constructed to a high-order tensor, which may include the dimension of time, space, frequency, subject, group/condition, trials. This multi-dimensional nature points to the adoption of tensor decomposition models instead of matrix decomposition models (Mørup, 2011; Mørup et al., 2007, 2006; Cong et al., 2015; Wang et al., 2018).

For the application of tensor decomposition in revealing functional network dynamics, considering the temporal dynamics and spectral modulations of spatial couplings (e.g., functional connectivity) for multiple participants from different groups in a cognitive task, a multi-way dataset structure is naturally formed. Recently, the tensor decomposition method based on the CP or PARAFAC2 model has been applied to dynamic functional connectivity using fMRI, EEG, and MEG data (Spyrou et al., 2018; Zhu et al., 2020a, 2019; Pester et al., 2015; Hu et al.,

2021b,a; Roald et al., 2020; Escudero et al., 2015). Those models can extract meaningful components and reveal the interactions between different modes. For example, Figure 5 shows the analysis pipeline of tensor decomposition methods for extracting repeated functional networks using resting EEG data. First, the time-frequency representation is performed on the windowed segment of cortical signals, and then metrics, like PLI, can be applied to calculate the functional connectivity in each time window and at each frequency bin. Therefore, a 4-D adjacency tensor can be formed. Next, the CP decomposition can be performed to decompose the tensor into four factor matrices, representing the temporal, spectral, adjacency, and subject components that are intercorrelated. That is to say, the extracted functional networks are time-varying, frequency-specific, and subject-contributed.

However, in previous studies, the CP model is applied under the assumption of spatial, temporal, and spectral consistency, potentially indicating that all the subjects have the same frequency-specific brain networks with the same temporal dynamics, and this assumption is irrational, expecially for signals recorded from resting state (Wang et al., 2020; Wang, 2020; Liu et al., 2021; Zhou et al., 2016; Jonmohamadi et al., 2020). Regarding this problem, a coupled CP decomposition model for linked component analysis is applied (Liu et al., 2021). This model is flexible to assume the incomplete consistency in different modes and extract the shared and unshared information between data blocks. Figure 6 shows the illustration of a mode-1 coupled CP decomposition model for a set of third-order tensors.

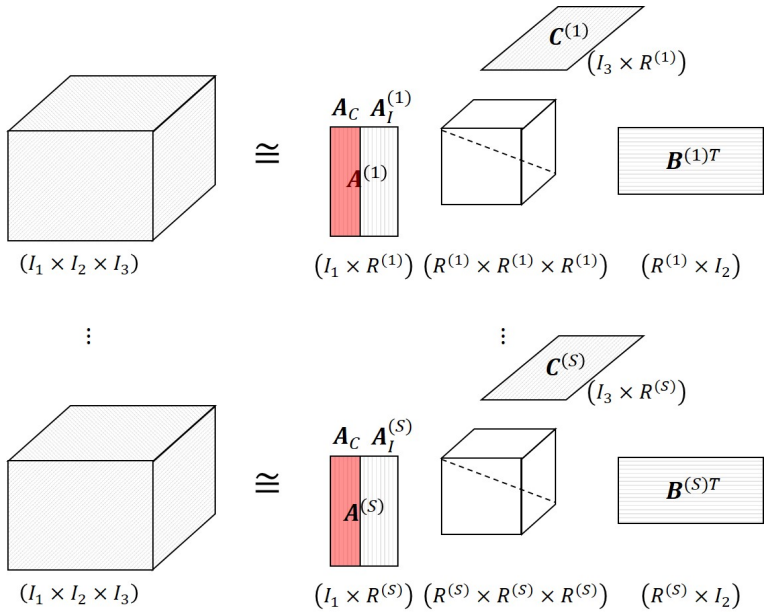

FIGURE 6 Illustration of the mode-1 coupled CP decomposition model for a set of third-order tensors (cited from (Wang, 2020)).

2.3.3 Graph-based methods

Modeling the complex brain networks as graphs where nodes are connected by edges has provided new insights into the organization, development, and function of the brain (Bullmore and Bassett, 2011; Sporns et al., 2004). A promising approach to assess network variations is the multi-layer network model, which is flexible enough to deal with networks varying along different dimensions. For example, if the layers represent FC in different frequency bands, cross-frequency interactions during integration and segregation of brain activities could be investigated (Guillon et al., 2017; de Vico Fallani et al., 2014; De Domenico, 2017). The most popular application of the multi-layer network model is studying the temporal dynamics of functional networks, where a layer is defined as the network at a time point or with a time window, and then some metrics of the network's topology are used to represent the network dynamics between layers (De Domenico, 2017; Sizemore and Bassett, 2018).

After establishing the multi-layer structure of multiple brain networks from different time points or windows, how can we evaluate the spatiotemporal dynamics based on graph metrics? According to a review study, we summarize some measures, including time-respecting paths, latency, centrality, and temporal community structure (Sizemore and Bassett, 2018). The time-respecting path is a set of collections of time-resolved connections of nodes. This measure is particularly useful to study the dynamic information flow due to the time-dependence of the path. The latency and centrality is a measure of the efficiency of reachability between two nodes. The temporal community structure method is based on community detection algorithms. One node can dynamically travel through different communities by changing the membership, and the temporal community structure method can be evaluated by node flexibility (the frequency of one node changing communities), node promiscuity (the switching rate of one node participating communities), and node cohesion (the number of times one node changing communities mutually with another node).

3 OVERVIEW OF INCLUDED ARTICLES

3.1 Article I: "Functional Connectivity of Major Depression Disorder Using Ongoing EEG during Music Perception"

Wenya Liu, Chi Zhang, Xiaoyu Wang, Jing Xu, Yi Chang, Tapani Ristaniemi, and Fengyu Cong. (2020). Functional connectivity of major depression disorder using ongoing EEG during music perception. *Clinical Neurophysiology*, 131(10), 2413-2422.

3.1.1 Methods

The 64-channel EEG data were collected from 19 healthy participants and 20 MDD participants when they were listening to a piece of 512-second modern tango. First, we preprocessed the data and filtered the data into five typically analyzed frequency bands, including delta (0.5–4 Hz), theta (4–8 Hz), alpha (8–13 Hz), beta(13–30 Hz), and gamma (30–80 Hz) bands. Second, for each frequency band, we segmented the data using non-overlapping sliding windows with the length of 10 seconds and applied PLI method to calculate FC within each time window. Three graph theory-based measures, including degree, clustering coefficient, and characteristic path length, were also calculated to measure the topolgical properties of FC within each time window. Third, the network-based statistic method was applied to find the statistically significant difference of FC connections between the healthy group and the MDD group for each frequency band, and the *t*-test was used to examine the lateralization effect with the degree values. Forth, we validated the discriminate ability of delta and beta frequency bands by six classifiers, including decision tree, Gaussian mixture model, k-nearest neighbor, naïve Bayes, random forest, and support vector machine.

3.1.2 Results

During listening to music, MDD patients showed a decreased connectivity pattern in the delta band (p = 0.045), and 13 significant connections were found with distribution within right central brain areas and between right temporal and left parietal brain regions. In the beta band, the MDD group showed an increased connectivity pattern (p = 0.0344), and there were 43 long-distance connections showed significant differences between two groups, which were distributed mostly within frontal brain areas and between frontal and parieta-occipital brain area, as shown in Figure 7. The healthy group exhibited a left hemisphere-dominant phenomenon, but the MDD group did not have such a lateralization effect. The beta band showed the best discriminate ability using the support vector machine classifier, and obtained the classification performance of the accuracy of 89.7 %, sensitivity of 89.4 %, and specificity of 89.9 %.

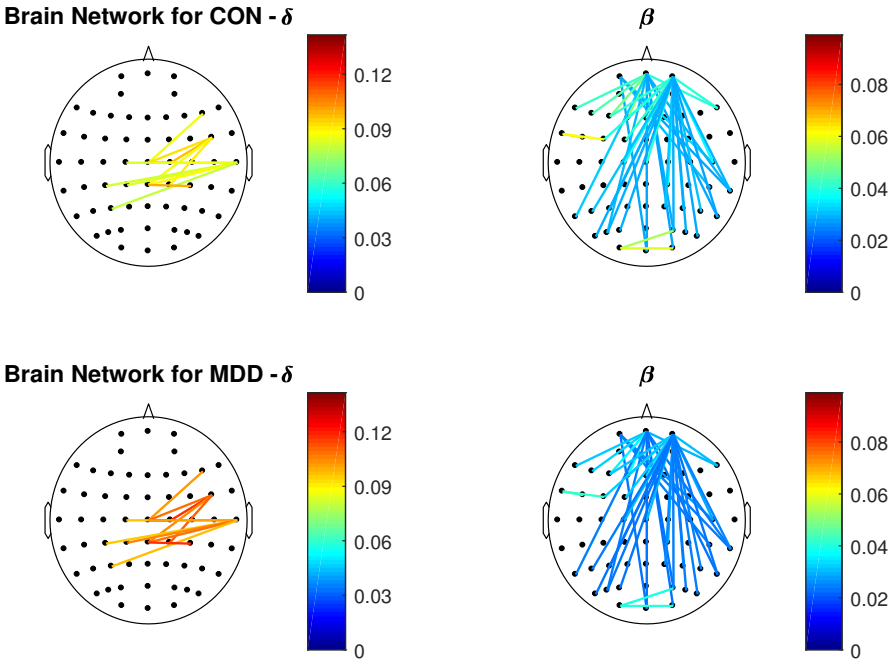

FIGURE 7 The significant brain network connections in delta and beta frequency bands of the healthy group and the MDD group.

3.1.3 Contribution

Wenya Liu proposed the ideas of the whole study, analyzed the data, and wrote and revised the manuscript. Xiaoyu Wang preprocessed the data. Jing Xu and Yi Chang helped to collect the data and discussed the results. Fengyu Cong, Tapani Ristaniemi, and Chi Zhang supervised the whole study and revised the manuscript.

3.2 Article II: "Identifying Oscillatory Hyperconnectivity and Hypoconnectivity Networks in Major Depression Using Coupled Tensor Decomposition"

Wenya Liu, Xiulin Wang, Jing Xu, Yi Chang, Timo Hämäläinen, and Fengyu Cong. (2021). Identifying Oscillatory Hyperconnectivity and Hypoconnectivity Networks in Major Depression Using Coupled Tensor Decomposition. *Accepted by IEEE Transactions on Neural Systems & Rehabilitation Engineering*.

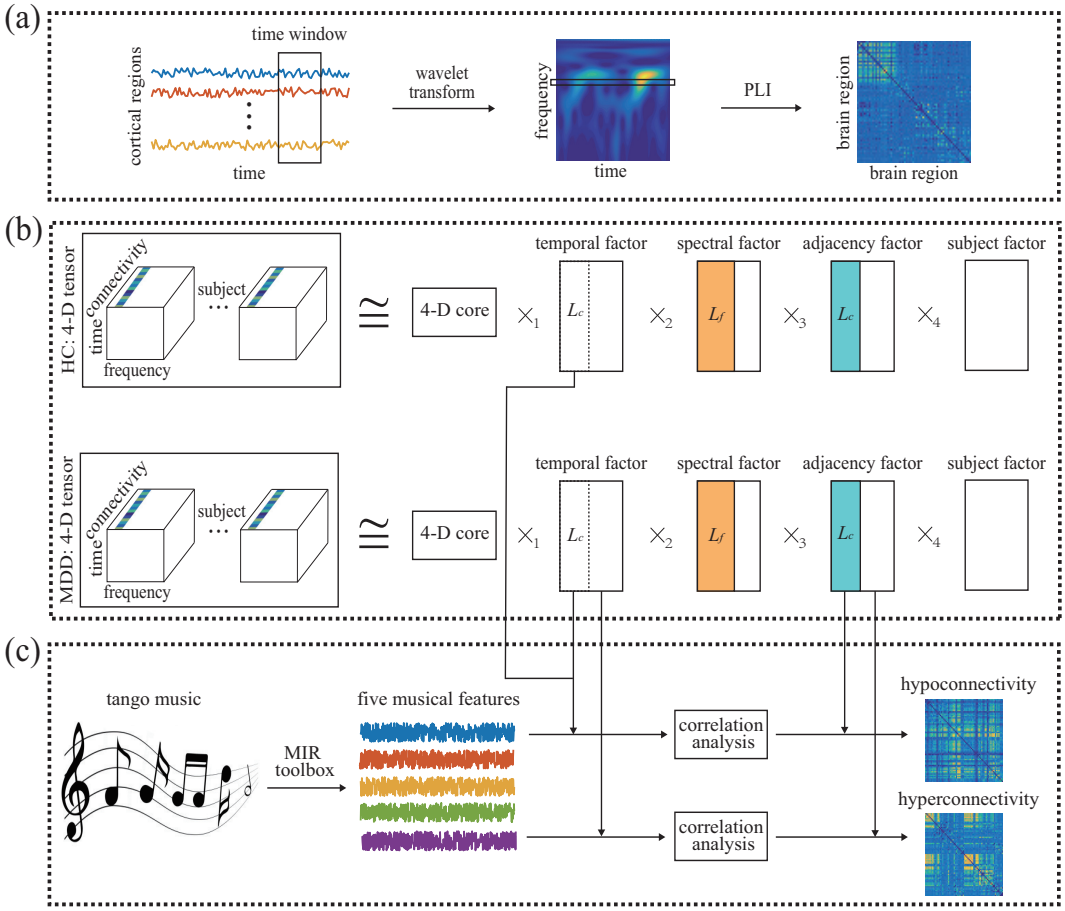

FIGURE 8 Diagram of the analysis pipeline. (a) Adjacency matrix construction in each time window and each frequency bin. (b) Adjacency tensor construction and decomposition. (c) The identification of hyperconnectivity and hypoconnectivity networks by music modulation.

3.2.1 Methods

The 64-channel EEG data were collected from 19 healthy participants and 20 MDD participants when they were listening to a piece of 512-second modern tango, as the same in study I. First, the data were preprocessed and filtered to a frequency band of 1-30 Hz. Second, we applied the minimum norm estimate

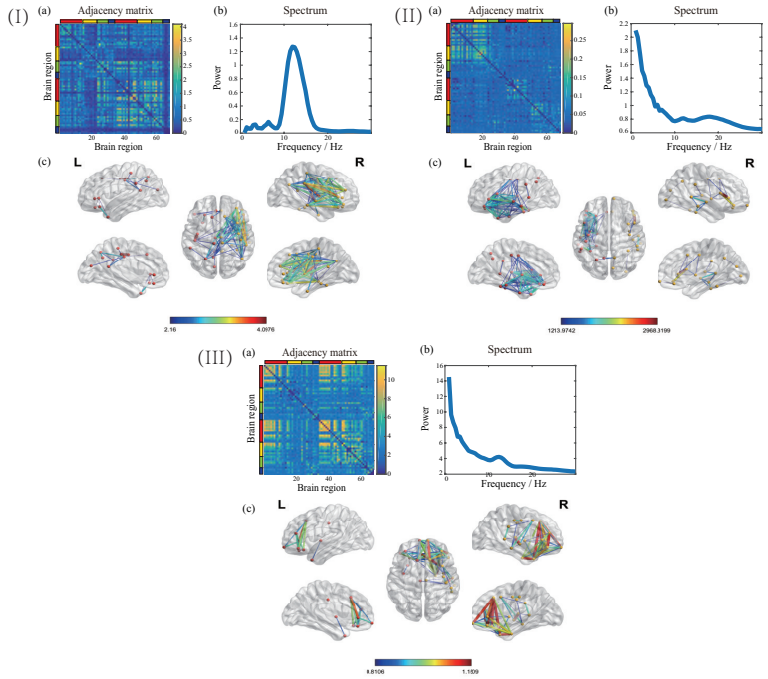

FIGURE 9 Three oscillatory hyperconnectivity networks. (a) Adjacency matrix representation of the network. (b) The spectral component of the network. (c) Cortical space representation of the network in Lateral, medial and dorsal view.

method for source reconstruction, and parcellate the cortical surface into 68 brain regions with the DesikanKilliany anatomical atlas. Third, we segmented the data by a sliding window with the window length of 3 s and the overlap of 2 s, and calculated the time-frequency representation within each time window by wavelet transform. The PLI method was applied to measure the pairwise functional connectivity within each sliding window and at each frequency bin. Fourth, we constructed two fourth-order adjacency tensors with the dimension of time $\times$ frequency $\times$ connectivity $\times$ subject, and applied a low-rank double-coupled nonnegative tensor decomposition method to extract functional networks characterized by spatio-temporal-spectral modes of covariation. Fifth, the correlation analysis based on the permutation test was used to identify the music-induced functional networks and the hyper- and hypo-connectivity networks in MDD. The analysis pipeline is shown in Figure 8.

3.2.2 Results

We concluded three oscillatory hyperconnectivity networks and three oscillatory hypoconnectivity networks in MDD, as shown in Figure 9 and Figure 10. The hyperconnectivity networks include the DMN related network modulated by alpha and beta (10-16 Hz) bands, a left auditory related network modulated by the delta band, and a prefrontal network modulated by the delta band. The hyperconnectivity networks include two fronto-parietal networks modulated by oscillations

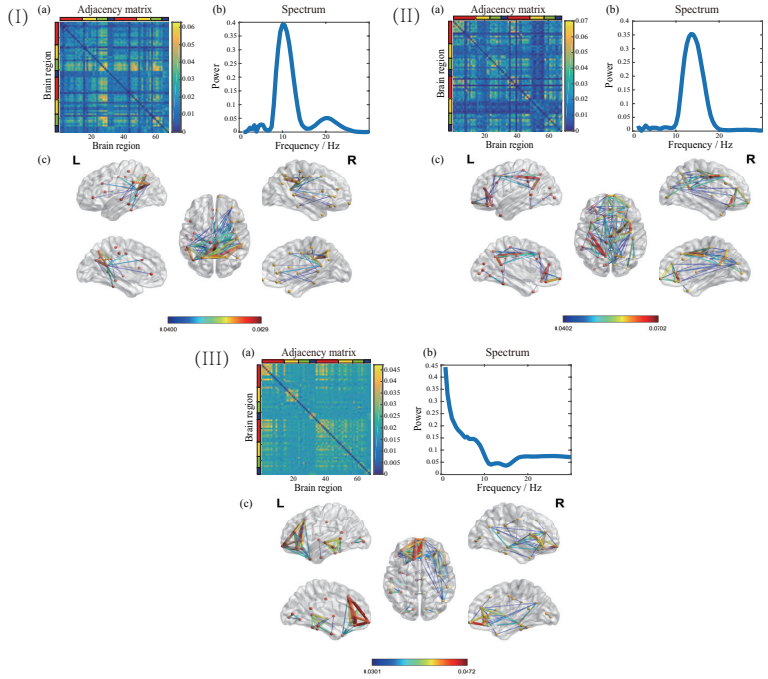

FIGURE 10 Three oscillatory hypoconnectivity networks. (a) Adjacency matrix representation of the network. (b) The spectral component of the network. (c) Cortical space representation of the network in Lateral, medial and dorsal view.

of 8-14 Hz and 10-19 Hz and a prefrontal network modulated by the delta band.

3.2.3 Contribution

Wenya Liu proposed the ideas of the whole study, analyzed the data, and wrote and revised the manuscript. Xiulin Wang provided the code of coupled tensor decomposition, wrote the section of coupled tensor decomposition, and revised the manuscript. Jing Xu and Yi Chang helped to collect the data and discussed the results. Fengyu Cong and Timo Hämäläinen supervised the whole study and revised the manuscript.

3.3 Article III: "Alpha Band Dysconnectivity Networks in Major Depression during Resting State"

Wenya Liu, Xiulin Wang, Fengyu Cong, and Timo Hämäläinen. (2021). Alpha Band Dysconnectivity Networks in Major Depression during Resting State. *29th European Signal Processing Conference (EUSIPCO)*, Dublin, Ireland. Accepted.

3.3.1 Methods

In this study, we used an open access dataset, called Multi-modal Open Dataset for Mental-disorder Analysis (MODMA) dataset with 128-channel resting state EEG data. First, we preprocessed the data and filtered the data to the alpha band (8-13 Hz). Second, PLI was applied to calculate the sensor-level pairwise functional connectivity within each sliding window (window length: 3 s, overlap: 2 s). Third, we constructed two third-order adjacency tensors with the dimension of time $\times$ connectivity $\times$ subject, and applied a low-rank double-coupled nonnegative tensor decomposition method to extract dynamic brain networks. Fourth, we used the k-means clustering method to identify the individual networks characterized with MDD.

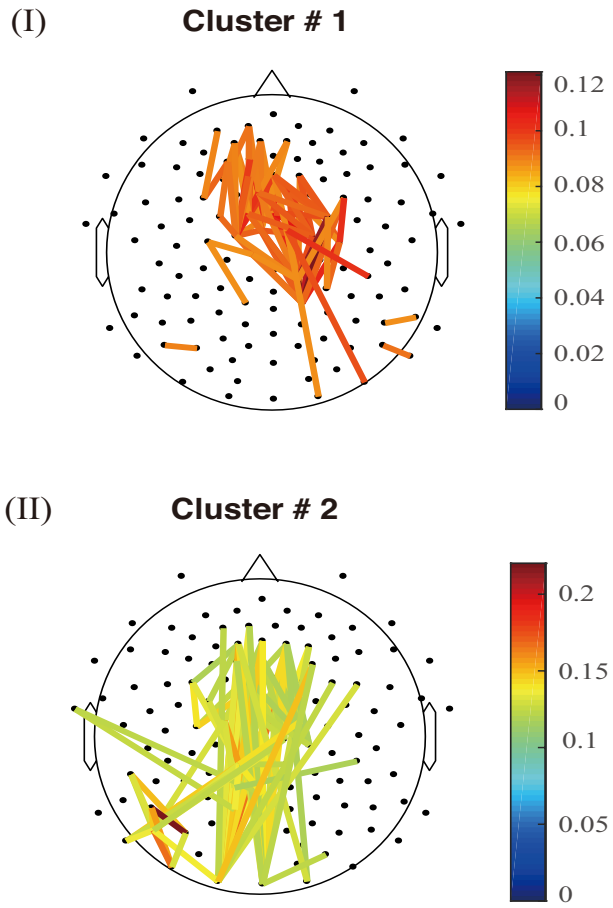

FIGURE 11 The two clusters of dysconnectivity networks in MDD during resting state.

3.3.2 Results

We summarized two alpha-band time-varying networks, which represent the hyperconnectivity networks in MDD during resting state, as shown in Figure 11. Figure 11(I) showed a fronto-parietal network which was related to attention and emotion regulation, and Figure 11(II) showed a frontal-occipital dysconnectivity

network which also has been demonstrated to be associate with attention.

3.3.3 Contribution

Wenya Liu proposed the ideas of the whole study, analyzed the data, and wrote and revised the manuscript. Xiulin Wang provided the code of coupled tensor decomposition and revised the manuscript. Fengyu Cong and Timo Hämäläinen supervised the whole study and revised the manuscript.

3.4 Article IV: "Exploring Oscillatory Dysconnectivity Networks in Major Depression during Resting State Using Coupled Tensor Decomposition"

Wenya Liu, Xiulin Wang, Timo Hämäläinen, and Fengyu Cong. (2021). Alpha Band Dysconnectivity Networks in Major Depression during Resting State. *submitted to IEEE Transactions on Biomedical Engineering*.

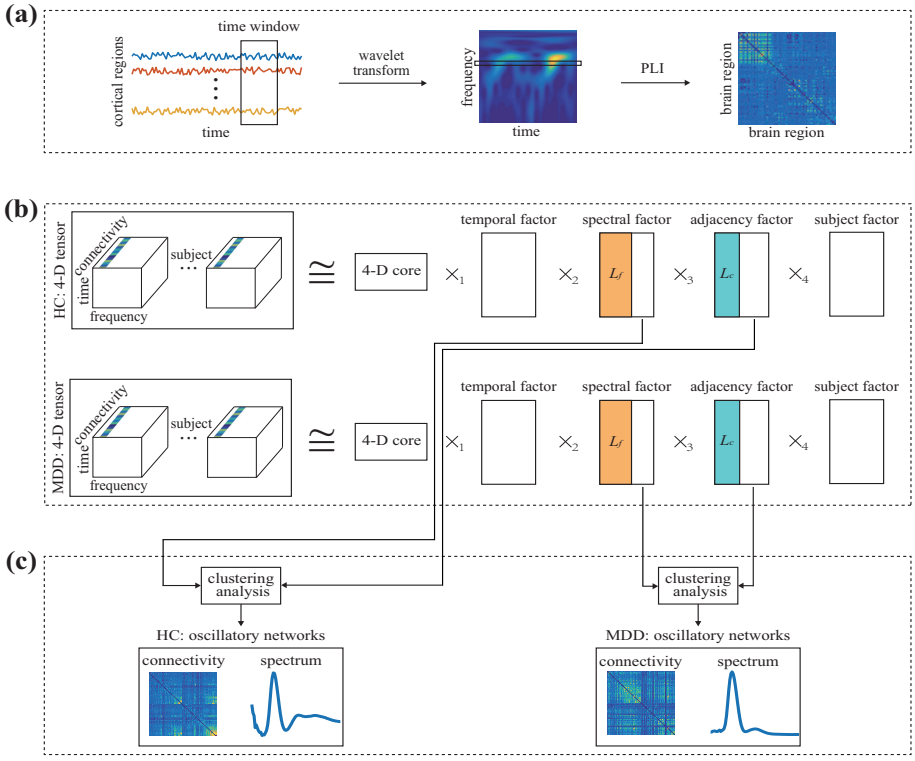

FIGURE 12 Diagram of the analysis pipeline. (a) Adjacency matrix construction in each time window and at each frequency bin. (b) Adjacency tensor construction and decomposition. (c) The identification of oscillatory networks specified for each group by clustering analysis.

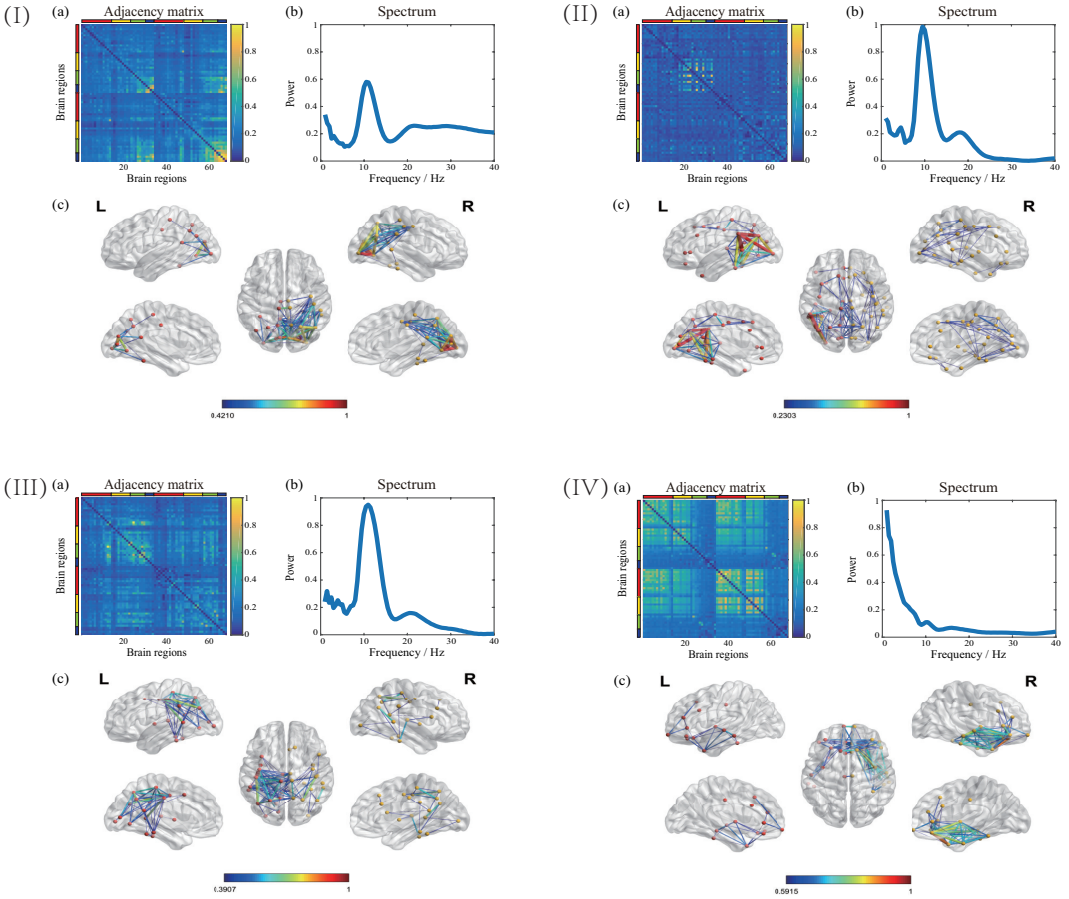

FIGURE 13 Four oscillatory networks specified in the HC group. (a) Adjacency matrix representation of the network. (b) The spectral component of the network. (c) Cortical space representation of the network in lateral, medial and dorsal view.

3.4.1 Methods

In this study, we used an open access dataset, called Multi-modal Open Dataset for Mental-disorder Analysis (MODMA) dataset with 128-channel resting state EEG data, as the same in study III. First, the data were preprocessed using the EEGLAB toolbox and then filtered to 1-40 Hz with the FIR band-pass filter. Second, we performed source localization using the weighted minimum norm estimate method, and segmented the cortical surface into 68 brain regions with the DesikanKilliany anatomical atlas. Third, the cortical source data were segmented by a sliding window with a window length of 3 s and an overlap of 2 s, and wavelet transform was applied to obtain the time-frequency representation in each window. Then, we applied the PLI method to measure the phase-coupling between all pairs of brain regions in each time window and at each frequency bin. Fourth, two fourth-order adjacency tensors was constructed with the dimension of time $\times$ frequency $\times$ connectivity $\times$ subject, and we applied a low-rank coupled tensor decomposition method with nonnegative constraints on all modes and double-coupled constraints on spectral and adjacency modes. Fifth, k-means

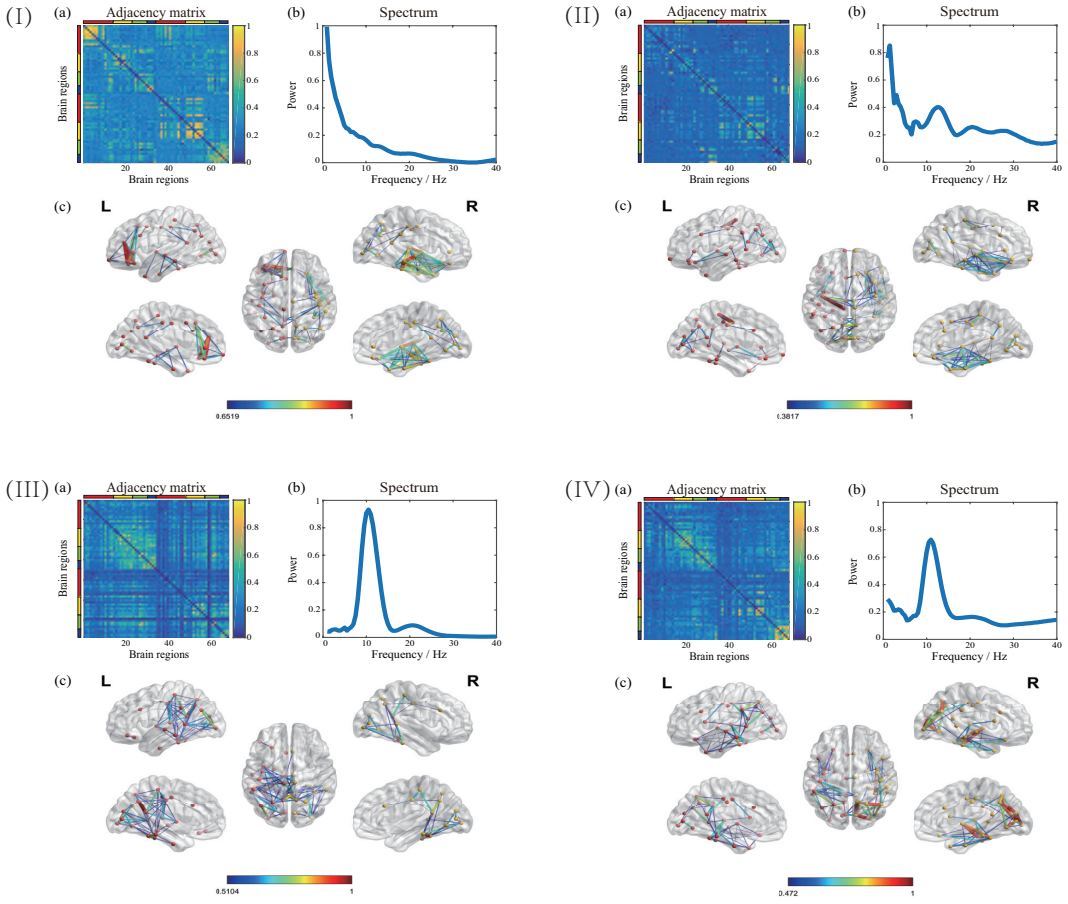

FIGURE 14 Four oscillatory networks specified in the MDD group. (a) Adjacency matrix representation of the network. (b) The spectral component of the network. (c) Cortical space representation of the network in lateral, medial and dorsal view.

clustering analysis was conducted to cluster the oscillatory networks that characterize individual networks in the healthy group and the MDD group, respectively. The analysis pipeline is shown in Figure 12.

3.4.2 Results

We clustered four oscillatory networks that characterized the individual networks in the HC group and the hypoconnectivity networks in MDD, as shown in Figure 13. Figure 13I-III were alpha rhythm modulated networks. Figure 13I showed a right visual network, Figure 13II showed a left hemisphere dominated temporoparietal network, and Figure 13III showed a sensorimotor network. A bilateral frontotemporal network was identified to be modulated by delta band, as shown in Figure 13IV. We clustered four oscillatory networks, which are specified and overactive in the MDD group, as shown in Figure 14. Figure 14I and Figure 14II indicated delta oscillatory networks. Figure 14I showed a left prefrontal and right auditory network, and Figure 14II showed a right frontotemporal network. The networks shown in Figure 14III and Figure 14IV were modulated by late al-

pha oscillations. Figure 14III showed a posterior network, which involved key areas of DMN, and Figure 14IV represented a DAN-related network that also includes functionally connected visual cortex.

3.4.3 Contribution

Wenya Liu proposed the ideas of the whole study, analyzed the data, and wrote and revised the manuscript. Xiulin Wang provided the code of coupled tensor decomposition and revised the manuscript. Fengyu Cong and Timo Hämäläinen supervised the whole study and revised the manuscript.

4 DISCUSSION

This thesis investigated the dysconnectivity of oscillatory networks in MDD during music listening and resting state at both source-level and sensor-level. This chapter will conclude our findings of MDD, and discuss some limitations in the view of methodology. We will also point out some future directions of current research.

4.1 Summarization of findings of major depression disorder

Study I and Study II investigated the abnormal oscillatory networks in MDD during music listening in sensor space and cortical source space, respectively. Study III and Study IV studied the altered oscillatory networks during resting state in sensor space and cortical source space, respectively. The findings of those studies point to the altered functional connectivity that is related to sensory networks and higher-order cognitive networks. The related sensory networks include the auditory network and the visual network. This dysfunction of sensory networks may indicate that the MDD patients are less involved in the surrounding environments, which may reflect the loss of interest in the outside world. The altered higher-order cognitive networks mainly include the DMN, the FN, the prefrontal network. The dysconnectivity of those higher-order cognitive networks is related to the function of attention, memory, and emotion, which are commonly reported in previous researches. Those network dysfunctions are associated with many MDD symptoms, including feelings of sadness, anxiety, and disability in concentrating and remembering things.

Although there are already many years of multidisciplinary studies of MDD, there are no unifying results among those studies due to the different research problems, techniques, and applied methodologies. From the view of neuroscience, the neural dysfunction of MDD is too complex, and it does not cohere to write a straightforward story about MDD. One urgent task is developing advanced methodologies to reveal the MDD mechanisms from data as accurately as possi-

ble. Another pressing task is to specify the neural dysfunctions with depression subtypes and symptom profiles.

4.2 Limitations of methodological applications

The results depend on many steps of methodological applications, such as the selection of sliding windows and phase synchronization metrics. The sliding window technique is typically applied in naturalistic paradigms and resting state when analyzing the dynamic brain networks. However, the selection of the window length and overlapping intrinsically affects the timescales of the dynamic fluctuations of the FC, thus limiting the explanation of the results. Different phase synchronization metrics can result in different connectivity maps. It is unknown how much the volume conduction effect can confound the true interactions and how much different phase synchronization metrics can correct the spurious connections. Although the zero-lag insensitive metrics can reduce the volume conduction effect, one should never expect the complete elimination of ghost interactions. Therefore, the results should be carefully explained particularly for sensor-level analysis.

One highlighted contribution of this thesis is that we introduced the coupled tensor decomposition model regarding the multiway and multiset data structure. Under the assumption that there are partially neural dysfunctions partially altered functional networks in MDD compared with healthy controls, we identified the time-varying and frequency-specific networks in MDD at the group level. At this point, we clarify some limitations of the proposed method. First, further studies should address the stabilities of the algorithm. Our results are summarized from many times' runs of the coupled tensor decomposition method, and the results may be confounded from various local optimal solutions. Therefore, more accurate optimization algorithms should be tested and developed. Second, the selection of the number of coupled components is a key issue that directly affects the results, and there is not enough prior information to be utilized. In our study, we firstly decomposed the individual tensor and then correlated the components between blocks. This is one potential solution to determine the coupled components, but the selection is still very subjective. Third, the proposed framework enables the exploration of group-featured information in MDD, but we ignored the subject differences within each group. However, the subject differences are crucial for the development of new diagnostics and personalized interventions for neuropsychiatric disorders. Our proposed method can realize the identifying of subject differences, but this will bring more challenges to parameter selections and result explanations. This unsolved issue should be taken into consideration for future extension of our work.

4.3 Future directions

As described above, individual differences are important for clinical use. Previous studies have investigated the network dysfunction of MDD between heterogeneous clinical groups. Recently, increasing interests focus on characterizing the individual-specific brain networks and topological features (Satterthwaite et al., 2018; Finn et al., 2017; Scheinost et al., 2019). Advanced methodologies and experimental design should be developed to explicitly explore the group features that are consistent across individuals and individual features that are specific for each subject.

For electrophysiological techniques, like EEG and MEG, the spatial resolution is relatively poor, and the source modeling is somehow controversial due to the non-uniqueness in inverse problem, and the recorded signals from the scalp are not sensitive to the neuronal activities in the deep brain (Rossini et al., 2019). While fMRI has perfect spatial resolution but poor temporal resolution due to the hemodynamic response, and this limited the studies of dynamic brain networks. Therefore, combining different brain techniques and fully making use of their advantages are promising research directions. The coupled tensor decomposition applied in our studies is a potentially powerful method for the fusion of different modalities, because the coupled tensor decomposition model is flexible enough to jointly analyze multiset data with coupling information and different data structures.

Differences in functional connectivity during task and rest should also be further studied, especially between the naturalistic stimuli and resting state. The energy consumption during ongoing tasks only increases 5% compared with resting conditions, and there is a high similarity of functional networks between rest and task (Gonzalez-Castillo and Bandettini, 2018). How the task-related networks are modulated by the resting-state networks is a promising direction to study. What's more, for the high-resolution EEG and MEG techniques, the recorded signals are very similar to those of resting state. Further studies should also focus on the separation of task-related brain activities and spontaneous activities, and find the dissimilarities and underpinning of the dynamic networks in naturalistic tasks.

The network communication is regulated by neuronal oscillations. The cross-frequency coupling serves as a systems-level neuronal mechanism to temporally coordinate network transitions and communications (Palva and Palva, 2012). It is suggested that different neuronal processes carried out concurrently in multiple frequency bands are integrated to support coherent cognitive functions (Palva and Palva, 2018). Cross-frequency phase synchrony, phase-amplitude coupling, and cross-frequency amplitude–amplitude correlations are three forms of cross-frequency coupling. However, a clear mechanism of cross-frequency coupling still remains unknown. Abnormal cross-frequency network communications may lead to cognitive disorders. This thesis investigated within-frequency-synchronized networks. Further researches could explore the cross-frequency interaction of

different brain networks and their dysfunction in MDD, and the corresponding methodologies should also be developed.

5 CONCLUSION

This thesis investigated the oscillatory networks in MDD using EEG recorded during music listening conditions and resting state. Study I is the first attempt to examine the altered functional connectivity using EEG during music perception. The results of beta-band dysconnectivity have provided potential and promising biomarkers for the clinical diagnosis of MDD. Regarding the multiway and multimodal nature of the EEG brain networks, we firstly applied a coupled tensor decomposition model to extract the brain networks, which are time-varying, frequency-specific, and group-featured. We validated the efficiency and feasibility of this model by synthetic data and applied this model to EEG data recorded in the naturalistic paradigm and resting state (study II-IV). The altered functional networks of MDD include sensory networks and higher-order cognitive networks, such as the auditory network, the DMN, the FN, and so on. Those brain networks are mostly related to emotional regulation, attention, and memory, and the associated dysfunctions in MDD are also commonly demonstrated in the literature. The dysconnectivity networks identified in our studies are notable in delta, alpha, and beta oscillations, which are well supported by previous researches. The dysconnectivity of oscillatory networks reported in our studies may provide new insights into the pathoconnectomics of MDD and potential biomarkers of MDD diagnosis.

As stated in our thesis, there have been mixed or even contradictory results about the network dysfunctions of MDD due to many aspects of limitations. Undoubtedly, it would be of great interest to draw a comprehensive picture of the altered connectomes of MDD and make practical contributions to the clinical diagnosis and treatment.

YHTEENVETO (SUMMARY IN FINNISH)

Tässä opinnäytetyössä tutkittiin suuren masennushäiriön (MDD:n Major Depression Disorder) värähtelyverkkoja käyttämällä musiikin kuuntelu- ja lepotilassa tallennettua EEG:tä. Tutkimus on ensimmäinen yritys tutkia muuttunutta toiminnallista yhteyttä EEG:llä musiikin havaitsemisen aikana. Beeta-kaistan toimintahäiriön tulokset ovat tarjonneet potentiaalisia ja lupaavia biomarkkereita MDD:n kliiniseen diagnosointiin. Mitä tulee EEG-aivoverkkojen monisuuntaiseen ja multimodaaliseen luonteeseen, käytimme ensin kytkettyä tensorin hajoamismallia aivoverkkojen poimimiseksi, jotka ovat ajoittain vaihtelevia, taajuuskohtaisia ja ryhmäkohtaisia. Vahvistimme tämän mallin tehokkuuden ja toteutettavuuden synteettisillä tiedoilla ja sovelsimme tätä mallia EEG-tietoihin, jotka on tallennettu naturalistiseen paradigmaan ja lepotilaan. MDD:n muuttuneet toiminnalliset verkot sisältävät aistiverkkoja ja korkeamman asteen kognitiivisia verkkoja, kuten kuuloverkko, DMN, FN ja niin edelleen. Nämä aivoverkot liittyvät enimmäkseen emotionaaliseen säätelyyn, huomioon ja muistiin, ja niihin liittyvät MDD -toimintahäiriöt ovat myös yleisesti osoitettu kirjallisuudessa. Tutkimuksissamme tunnistetut häiriöverkot ovat merkittäviä delta-, alfa- ja beeta -värähtelyissä, joita aiemmat tutkimukset tukevat hyvin. Tutkimuksissamme raportoitu värähtelyverkkojen epäyhteysyhteys antaa uutta tietoa MDD:n patokonnektomiasta ja MDD -diagnoosin mahdollisista biomarkkereista.

Kuten väitöskirjassa todettiin, MDD:n verkkohäiriöistä on saatu ristiriitaisia tuloksia monien rajoitusten vuoksi. Olisi erittäin mielenkiintoista piirtää kattava kuva MDD:n muuttuneista yhteyksistä ja antaa sitä kautta käytännön apua kliiniseen diagnosointiin ja hoitoon.

REFERENCES

Abbott, C. C., Lemke, N. T., Gopal, S., Thoma, R. J., Bustillo, J., Calhoun, V. D., and Turner, J. A. (2013). Electroconvulsive therapy response in major depressive disorder: a pilot functional network connectivity resting state fmri investigation. *Frontiers in psychiatry*, 4:10.

Acar, E., Levin-Schwartz, Y., Calhoun, V. D., and Adali, T. (2017). Tensor-based fusion of eeg and fmri to understand neurological changes in schizophrenia. In *2017 IEEE International Symposium on Circuits and Systems (ISCAS)*, pages 1–4. IEEE.

Ahn, Y.-Y., Bagrow, J. P., and Lehmann, S. (2010). Link communities reveal multiscale complexity in networks. *nature*, 466(7307):761–764.

Ajilore, O., Lamar, M., Leow, A., Zhang, A., Yang, S., and Kumar, A. (2014). Graph theory analysis of cortical-subcortical networks in late-life depression. *The American Journal of Geriatric Psychiatry*, 22(2):195–206.

Allen, E. A., Damaraju, E., Plis, S. M., Erhardt, E. B., Eichele, T., and Calhoun, V. D. (2014). Tracking whole-brain connectivity dynamics in the resting state. *Cerebral cortex*, 24(3):663–676.

Andrews-Hanna, J. R., Reidler, J. S., Sepulcre, J., Poulin, R., and Buckner, R. L. (2010). Functional-anatomic fractionation of the brain's default network. *Neuron*, 65(4):550–562.

Andrews-Hanna, J. R., Smallwood, J., and Spreng, R. N. (2014). The default network and self-generated thought: component processes, dynamic control, and clinical relevance. *Annals of the New York Academy of Sciences*, 1316(1):29.

Aydore, S., Pantazis, D., and Leahy, R. M. (2013). A note on the phase locking value and its properties. *Neuroimage*, 74:231–244.

Baker, A. P., Brookes, M. J., Rezek, I. A., Smith, S. M., Behrens, T., Smith, P. J. P., and Woolrich, M. (2014). Fast transient networks in spontaneous human brain activity. *Elife*, 3:e01867.

Barrat, A., Barthelemy, M., and Vespignani, A. (2008). *Dynamical processes on complex networks*. Cambridge university press.

Bartels, A. and Zeki, S. (2004). Functional brain mapping during free viewing of natural scenes. *Human brain mapping*, 21(2):75–85.

Bassett, D. S. and Sporns, O. (2017). Network neuroscience. *Nature neuroscience*, 20(3):353–364.

Beckmann, C. F., DeLuca, M., Devlin, J. T., and Smith, S. M. (2005). Investigations into resting-state connectivity using independent component analysis. *Philosophical Transactions of the Royal Society B: Biological Sciences*, 360(1457):1001–1013.

Belmaker, R. and Agam, G. (2008). Major depressive disorder. *New England Journal of Medicine*, 358(1):55–68.

Berrios, G. E. (1988). Melancholia and depression during the 19th century: a conceptual history. *The British Journal of Psychiatry*, 153(3):298–304.

Betzel, R. F. and Bassett, D. S. (2017). Multi-scale brain networks. *Neuroimage*, 160:73–83.

Biswal, B., Zerrin Yetkin, F., Haughton, V. M., and Hyde, J. S. (1995). Functional connectivity in the motor cortex of resting human brain using echo-planar mri. *Magnetic resonance in medicine*, 34(4):537–541.

Blondel, V. D., Guillaume, J.-L., Lambiotte, R., and Lefebvre, E. (2008). Fast unfolding of communities in large networks. *Journal of statistical mechanics: theory and experiment*, 2008(10):P10008.

Boccaletti, S., Latora, V., Moreno, Y., Chavez, M., and Hwang, D.-U. (2006). Complex networks: Structure and dynamics. *Physics reports*, 424(4-5):175–308.

Bohr, I. J., Kenny, E., Blamire, A., O'Brien, J. T., Thomas, A., Richardson, J., and Kaiser, M. (2013). Resting-state functional connectivity in late-life depression: higher global connectivity and more long distance connections. *Frontiers in psychiatry*, 3:116.

Brandes, U. (2001). A faster algorithm for betweenness centrality. *Journal of mathematical sociology*, 25(2):163–177.

Brookes, M. J., Hale, J. R., Zumer, J. M., Stevenson, C. M., Francis, S. T., Barnes, G. R., Owen, J. P., Morris, P. G., and Nagarajan, S. S. (2011a). Measuring functional connectivity using meg: methodology and comparison with fcmri. *Neuroimage*, 56(3):1082–1104.

Brookes, M. J., Liddle, E. B., Hale, J. R., Woolrich, M. W., Luckhoo, H., Liddle, P. F., and Morris, P. G. (2012). Task induced modulation of neural oscillations in electrophysiological brain networks. *Neuroimage*, 63(4):1918–1930.

Brookes, M. J., O'Neill, G. C., Hall, E. L., Woolrich, M. W., Baker, A., Corner, S. P., Robson, S. E., Morris, P. G., and Barnes, G. R. (2014). Measuring temporal, spectral and spatial changes in electrophysiological brain network connectivity. *Neuroimage*, 91:282–299.

Brookes, M. J., Woolrich, M., Luckhoo, H., Price, D., Hale, J. R., Stephenson, M. C., Barnes, G. R., Smith, S. M., and Morris, P. G. (2011b). Investigating the electrophysiological basis of resting state networks using magnetoencephalography. *Proceedings of the National Academy of Sciences*, 108(40):16783–16788.

Brunner, C., Billinger, M., Seeber, M., Mullen, T. R., and Makeig, S. (2016). Volume conduction influences scalp-based connectivity estimates. *Frontiers in computational neuroscience*, 10:121.

Bruns, A. (2004). Fourier-, hilbert-and wavelet-based signal analysis: are they really different approaches? *Journal of neuroscience methods*, 137(2):321–332.

Buckner, R. L., Andrews-Hanna, J. R., and Schacter, D. L. (2008). The brain's default network: anatomy, function, and relevance to disease.

Bullmore, E. and Sporns, O. (2009). Complex brain networks: graph theoretical analysis of structural and functional systems. *Nature reviews neuroscience*, 10(3):186–198.

Bullmore, E. and Sporns, O. (2012). The economy of brain network organization. *Nature Reviews Neuroscience*, 13(5):336–349.

Bullmore, E. T. and Bassett, D. S. (2011). Brain graphs: graphical models of the human brain connectome. *Annual review of clinical psychology*, 7:113–140.

Buzsáki, G. and Draguhn, A. (2004). Neuronal oscillations in cortical networks. *science*, 304(5679):1926–1929.

Calhoun, V. D., Miller, R., Pearlson, G., and Adalı, T. (2014). The chronnectome: time-varying connectivity networks as the next frontier in fmri data discovery. *Neuron*, 84(2):262–274.

Cavanna, A. E. and Trimble, M. R. (2006). The precuneus: a review of its functional anatomy and behavioural correlates. *Brain*, 129(3):564–583.

Chang, C. and Glover, G. H. (2010). Time–frequency dynamics of resting-state brain connectivity measured with fmri. *Neuroimage*, 50(1):81–98.

Chang, C., Liu, Z., Chen, M. C., Liu, X., and Duyn, J. H. (2013). Eeg correlates of time-varying bold functional connectivity. *Neuroimage*, 72:227–236.

Cichocki, A. (2013). Tensor decompositions: a new concept in brain data analysis? *arXiv preprint arXiv:1305.0395*.

Cong, F., Lin, Q.-H., Kuang, L.-D., Gong, X.-F., Astikainen, P., and Ristaniemi, T. (2015). Tensor decomposition of eeg signals: a brief review. *Journal of neuroscience methods*, 248:59–69.

Damoiseaux, J. S., Rombouts, S., Barkhof, F., Scheltens, P., Stam, C. J., Smith, S. M., and Beckmann, C. F. (2006). Consistent resting-state networks across healthy subjects. *Proceedings of the national academy of sciences*, 103(37):13848–13853.

de Aguiar Neto, F. S. and Rosa, J. L. G. (2019). Depression biomarkers using non-invasive eeg: A review. *Neuroscience & Biobehavioral Reviews*, 105:83–93.

De Domenico, M. (2017). Multilayer modeling and analysis of human brain networks. *Giga Science*, 6(5):gix004.

De Pasquale, F., Della Penna, S., Snyder, A. Z., Lewis, C., Mantini, D., Marzetti, L., Belardinelli, P., Ciancetta, L., Pizzella, V., Romani, G. L., et al. (2010). Temporal dynamics of spontaneous meg activity in brain networks. *Proceedings of the National Academy of Sciences*, 107(13):6040–6045.

De Pasquale, F., Della Penna, S., Sporns, O., Romani, G., and Corbetta, M. (2016). A dynamic core network and global efficiency in the resting human brain. *Cerebral Cortex*, 26(10):4015–4033.

de Vico Fallani, F., Richiardi, J., Chavez, M., and Achard, S. (2014). Graph analysis of functional brain networks: practical issues in translational neuroscience. *Philosophical Transactions of the Royal Society B: Biological Sciences*, 369(1653):20130521.

Demirtaş, M., Tornador, C., Falcón, C., López-Solà, M., Hernández-Ribas, R., Pujol, J., Menchón, J. M., Ritter, P., Cardoner, N., Soriano-Mas, C., et al. (2016). Dynamic functional connectivity reveals altered variability in functional connectivity among patients with major depressive disorder. *Human brain mapping*, 37(8):2918–2930.

Di Martino, A., Fair, D. A., Kelly, C., Satterthwaite, T. D., Castellanos, F. X., Thomason, M. E., Craddock, R. C., Luna, B., Leventhal, B. L., Zuo, X.-N., et al. (2014). Unraveling the miswired connectome: a developmental perspective. *Neuron*, 83(6):1335–1353.

Drevets, W. C., Price, J. L., and Furey, M. L. (2008). Brain structural and functional abnormalities in mood disorders: implications for neurocircuitry models of depression. *Brain structure and function*, 213(1-2):93–118.

Duyn, J. (2011). Spontaneous fmri activity during resting wakefulness and sleep. *Progress in brain research*, 193:295–305.

Engel, A. K., Fries, P., and Singer, W. (2001). Dynamic predictions: oscillations and synchrony in top–down processing. *Nature Reviews Neuroscience*, 2(10):704–716.

Engel, A. K., Gerloff, C., Hilgetag, C. C., and Nolte, G. (2013). Intrinsic coupling modes: multiscale interactions in ongoing brain activity. *Neuron*, 80(4):867–886.

Escudero, J., Acar, E., Fernández, A., and Bro, R. (2015). Multiscale entropy analysis of resting-state magnetoencephalogram with tensor factorisations in alzheimer's disease. *Brain research bulletin*, 119:136–144.

Fava, M. and Kendler, K. S. (2000). Major depressive disorder. *Neuron*, 28(2):335–341.

Fingelkurts, A. A., Fingelkurts, A. A., Rytsälä, H., Suominen, K., Isometsä, E., and Kähkönen, S. (2007). Impaired functional connectivity at eeg alpha and theta frequency bands in major depression. *Human brain mapping*, 28(3):247–261.

Finn, E. S., Scheinost, D., Finn, D. M., Shen, X., Papademetris, X., and Constable, R. T. (2017). Can brain state be manipulated to emphasize individual differences in functional connectivity? *Neuroimage*, 160:140–151.

Fornito, A., Zalesky, A., and Breakspear, M. (2015). The connectomics of brain disorders. *Nature Reviews Neuroscience*, 16(3):159–172.

Fornito, A., Zalesky, A., Pantelis, C., and Bullmore, E. T. (2012). Schizophrenia, neuroimaging and connectomics. *Neuroimage*, 62(4):2296–2314.

Fox, M. D., Snyder, A. Z., Vincent, J. L., Corbetta, M., Van Essen, D. C., and Raichle, M. E. (2005). The human brain is intrinsically organized into dynamic, anticorrelated functional networks. *Proceedings of the National Academy of Sciences*, 102(27):9673–9678.

Fries, P. (2005). A mechanism for cognitive dynamics: neuronal communication through neuronal coherence. *Trends in cognitive sciences*, 9(10):474–480.

Friston, K. J. (1994). Functional and effective connectivity in neuroimaging: a synthesis. *Human brain mapping*, 2(1-2):56–78.

Friston, K. J. (2011). Functional and effective connectivity: a review. *Brain connectivity*, 1(1):13–36.

Fukunaga, M., Horovitz, S. G., van Gelderen, P., de Zwart, J. A., Jansma, J. M., Ikonomidou, V. N., Chu, R., Deckers, R. H., Leopold, D. A., and Duyn, J. H. (2006). Large-amplitude, spatially correlated fluctuations in bold fmri signals during extended rest and early sleep stages. *Magnetic resonance imaging*, 24(8):979–992.

Gao, Q., Xiang, Y., Zhang, J., Luo, N., Liang, M., Gong, L., Yu, J., Cui, Q., Sepulcre, J., and Chen, H. (2021). A reachable probability approach for the analysis of spatio-temporal dynamics in the human functional network. *NeuroImage*, page 118497.

Gong, D., He, H., Ma, W., Liu, D., Huang, M., Dong, L., Gong, J., Li, J., Luo, C., and Yao, D. (2016). Functional integration between salience and central executive networks: a role for action video game experience. *Neural Plasticity*, 2016.

Gong, Q. and He, Y. (2015). Depression, neuroimaging and connectomics: a selective overview. *Biological psychiatry*, 77(3):223–235.

Gonzalez-Castillo, J. and Bandettini, P. A. (2018). Task-based dynamic functional connectivity: Recent findings and open questions. *Neuroimage*, 180:526–533.

Gotlib, I. H. and Hamilton, J. P. (2008). Neuroimaging and depression: Current status and unresolved issues. *Current Directions in Psychological Science*, 17(2):159–163.

Gotlib, I. H. and Joormann, J. (2010). Cognition and depression: current status and future directions. *Annual review of clinical psychology*, 6:285–312.

Goulden, N., Khusnulina, A., Davis, N. J., Bracewell, R. M., Bokde, A. L., McNulty, J. P., and Mullins, P. G. (2014). The salience network is responsible for switching between the default mode network and the central executive network: replication from dcm. *Neuroimage*, 99:180–190.

Gruenberg, A. M., Goldstein, R. D., Pincus, H. A., et al. (2005). Classification of depression: research and diagnostic criteria: Dsm-iv and icd-10. *Biology of Depression*, 11:43.

Guillon, J., Attal, Y., Colliot, O., La Corte, V., Dubois, B., Schwartz, D., Chavez, M., and Fallani, F. D. V. (2017). Loss of inter-frequency brain hubs in alzheimer's. In *BOOK OF ABSTRACTS*, page 90.

Hallquist, M. N. and Hillary, F. G. (2018). Graph theory approaches to functional network organization in brain disorders: A critique for a brave new small-world. *Network Neuroscience*, 3(1):1–26.

Hasanzadeh, F., Mohebbi, M., and Rostami, R. (2020). Graph theory analysis of directed functional brain networks in major depressive disorder based on eeg signal. *Journal of neural engineering*, 17(2):026010.

Hassan, M., Benquet, P., Biraben, A., Berrou, C., Dufor, O., and Wendling, F. (2015). Dynamic reorganization of functional brain networks during picture naming. *Cortex*, 73:276–288.

Hasson, U., Nir, Y., Levy, I., Fuhrmann, G., and Malach, R. (2004). Intersubject synchronization of cortical activity during natural vision. *science*, 303(5664):1634–1640.

He, B., Astolfi, L., Valdés-Sosa, P. A., Marinazzo, D., Palva, S. O., Bénar, C.-G., Michel, C. M., and Koenig, T. (2019). Electrophysiological brain connectivity: theory and implementation. *IEEE Transactions on Biomedical Engineering*, 66(7):2115–2137.

He, Y. and Evans, A. (2010). Graph theoretical modeling of brain connectivity. *Current opinion in neurology*, 23(4):341–350.

Hipp, J. F., Hawellek, D. J., Corbetta, M., Siegel, M., and Engel, A. K. (2012). Large-scale cortical correlation structure of spontaneous oscillatory activity. *Nature neuroscience*, 15(6):884–890.

Hu, G., Li, H., Zhao, W., Hao, Y., Bai, Z., Nickerson, L. D., and Cong, F. (2021a). Discovering hidden brain network responses to naturalistic stimuli via tensor component analysis of multi-subject fmri data. *bioRxiv*.

Hu, G., Wang, D., Luo, S., Hao, Y., Nickerson, L. D., and Cong, F. (2021b). Frequency specific co-activation pattern analysis via sparse nonnegative tensor decomposition. *Journal of Neuroscience Methods*, 362:109299.

Humphries, M. D. and Gurney, K. (2008). Network 'small-world-ness': a quantitative method for determining canonical network equivalence. *PloS one*, 3(4):e0002051.

Hutchison, R. M., Womelsdorf, T., Allen, E. A., Bandettini, P. A., Calhoun, V. D., Corbetta, M., Della Penna, S., Duyn, J. H., Glover, G. H., Gonzalez-Castillo, J., et al. (2013). Dynamic functional connectivity: promise, issues, and interpretations. *Neuroimage*, 80:360–378.

Jääskeläinen, I. P., Sams, M., Glerean, E., and Ahveninen, J. (2020). Movies and narratives as naturalistic stimuli in neuroimaging. *NeuroImage*, page 117445.

Jonmohamadi, Y., Muthukumaraswamy, S., Chen, J., Roberts, J., Crawford, R., and Pandey, A. (2020). Extraction of common task features in eeg-fmri data using coupled tensor-tensor decomposition. *Brain Topography*, 33(5):636–650.

Kabbara, A., Falou, W. E., Khalil, M., Wendling, F., and Hassan, M. (2017). The dynamic functional core network of the human brain at rest. *Scientific reports*, 7(1):1–16.

Kaiser, R. H., Andrews-Hanna, J. R., Wager, T. D., and Pizzagalli, D. A. (2015). Large-scale network dysfunction in major depressive disorder: a meta-analysis of resting-state functional connectivity. *JAMA psychiatry*, 72(6):603–611.

Kaiser, R. H., Whitfield-Gabrieli, S., Dillon, D. G., Goer, F., Beltzer, M., Minkel, J., Smoski, M., Dichter, G., and Pizzagalli, D. A. (2016). Dynamic resting-state functional connectivity in major depression. *Neuropsychopharmacology*, 41(7):1822–1830.

Kintali, S. (2008). Betweenness centrality: Algorithms and lower bounds. *arXiv preprint arXiv:0809.1906*.

Koelewijn, L., Bompas, A., Tales, A., Brookes, M. J., Muthukumaraswamy, S. D., Bayer, A., and Singh, K. D. (2017). Alzheimer's disease disrupts alpha and beta-band resting-state oscillatory network connectivity. *Clinical Neurophysiology*, 128(11):2347–2357.

Kopell, N. J., Gritton, H. J., Whittington, M. A., and Kramer, M. A. (2014). Beyond the connectome: the dynome. *Neuron*, 83(6):1319–1328.

Korgaonkar, M. S., Fornito, A., Williams, L. M., and Grieve, S. M. (2014). Abnormal structural networks characterize major depressive disorder: a connectome analysis. *Biological psychiatry*, 76(7):567–574.

Lachaux, J.-P., Rodriguez, E., Martinerie, J., and Varela, F. J. (1999). Measuring phase synchrony in brain signals. *Human brain mapping*, 8(4):194–208.

Laird, A. R., Fox, P. M., Eickhoff, S. B., Turner, J. A., Ray, K. L., McKay, D. R., Glahn, D. C., Beckmann, C. F., Smith, S. M., and Fox, P. T. (2011). Behavioral interpretations of intrinsic connectivity networks. *Journal of cognitive neuroscience*, 23(12):4022–4037.

Leech, R. and Sharp, D. J. (2014). The role of the posterior cingulate cortex in cognition and disease. *Brain*, 137(1):12–32.

Leonardi, N., Richiardi, J., Gschwind, M., Simioni, S., Annoni, J.-M., Schluep, M., Vuilleumier, P., and Van De Ville, D. (2013). Principal components of functional connectivity: a new approach to study dynamic brain connectivity during rest. *NeuroImage*, 83:937–950.

Leuchter, A. F., Cook, I. A., Hunter, A. M., Cai, C., and Horvath, S. (2012). Resting-state quantitative electroencephalography reveals increased neurophysiologic connectivity in depression. *PloS one*, 7(2):e32508.

Liu, W., Wang, X., Ristaniemi, T., and Cong, F. (2020a). Identifying task-based dynamic functional connectivity using tensor decomposition. In *International Conference on Neural Information Processing*, pages 361–369. Springer.

Liu, W., Wang, X., Xu, J., Chang, Y., Hamalainen, T., and Cong, F. (2021). Identifying oscillatory hyperconnectivity and hypoconnectivity networks in major depression using coupled tensor decomposition. *bioRxiv*.

Liu, W., Zhang, C., Wang, X., Xu, J., Chang, Y., Ristaniemi, T., and Cong, F. (2020b). Functional connectivity of major depression disorder using ongoing eeg during music perception. *Clinical Neurophysiology*, 131(10):2413–2422.

Liu, X. and Duyn, J. H. (2013). Time-varying functional network information extracted from brief instances of spontaneous brain activity. *Proceedings of the National Academy of Sciences*, 110(11):4392–4397.

Manoliu, A., Meng, C., Brandl, F., Doll, A., Tahmasian, M., Scherr, M., Schwerthöffer, D., Zimmer, C., Förstl, H., Bäuml, J., et al. (2014). Insular dysfunction within the salience network is associated with severity of symptoms and aberrant inter-network connectivity in major depressive disorder. *Frontiers in human neuroscience*, 7:930.

Mantini, D., Perrucci, M. G., Del Gratta, C., Romani, G. L., and Corbetta, M. (2007). Electrophysiological signatures of resting state networks in the human brain. *Proceedings of the National Academy of Sciences*, 104(32):13170–13175.

Mayberg, H. S. (2003). Modulating dysfunctional limbic-cortical circuits in depression: towards development of brain-based algorithms for diagnosis and optimised treatment. *British medical bulletin*, 65(1):193–207.

Mayberg, H. S., Lozano, A. M., Voon, V., McNeely, H. E., Seminowicz, D., Hamani, C., Schwalb, J. M., and Kennedy, S. H. (2005). Deep brain stimulation for treatment-resistant depression. *Neuron*, 45(5):651–660.

Meng, C., Brandl, F., Tahmasian, M., Shao, J., Manoliu, A., Scherr, M., Schwerthöffer, D., Bäuml, J., Förstl, H., Zimmer, C., et al. (2014). Aberrant topology of striatum's connectivity is associated with the number of episodes in depression. *Brain*, 137(2):598–609.

Menon, V. (2011). Large-scale brain networks and psychopathology: a unifying triple network model. *Trends in cognitive sciences*, 15(10):483–506.

Menon, V. and Toga, A. W. (2015). Brain mapping: an encyclopedic reference. *Academic Press: Cambridge, MA, USA*, pages 597–611.

Menon, V. and Uddin, L. Q. (2010). Saliency, switching, attention and control: a network model of insula function. *Brain structure and function*, 214(5-6):655–667.

Mørup, M. (2011). Applications of tensor (multiway array) factorizations and decompositions in data mining. *Wiley Interdisciplinary Reviews: Data Mining and Knowledge Discovery*, 1(1):24–40.

Mørup, M., Hansen, L. K., and Arnfred, S. M. (2007). Erpwavelab: A toolbox for multi-channel analysis of time–frequency transformed event related potentials. *Journal of neuroscience methods*, 161(2):361–368.

Mørup, M., Hansen, L. K., Herrmann, C. S., Parnas, J., and Arnfred, S. M. (2006). Parallel factor analysis as an exploratory tool for wavelet transformed event-related eeg. *NeuroImage*, 29(3):938–947.

Mulders, P. C., van Eijndhoven, P. F., Schene, A. H., Beckmann, C. F., and Tendolkar, I. (2015). Resting-state functional connectivity in major depressive disorder: a review. *Neuroscience & Biobehavioral Reviews*, 56:330–344.

Newman, M. E. (2006). Modularity and community structure in networks. *Proceedings of the national academy of sciences*, 103(23):8577–8582.

Nolte, G., Bai, O., Wheaton, L., Mari, Z., Vorbach, S., and Hallett, M. (2004). Identifying true brain interaction from eeg data using the imaginary part of coherency. *Clinical neurophysiology*, 115(10):2292–2307.

Nugent, A. C., Luber, B., Carver, F. W., Robinson, S. E., Coppola, R., and Zarate Jr, C. A. (2017). Deriving frequency-dependent spatial patterns in meg-derived resting state sensorimotor network: A novel multiband ica technique. *Human brain mapping*, 38(2):779–791.

O'Neill, G. C. (2016). *Dynamic electrophysiological connectomics*. PhD thesis, University of Nottingham.

O'Neill, G. C., Bauer, M., Woolrich, M. W., Morris, P. G., Barnes, G. R., and Brookes, M. J. (2015). Dynamic recruitment of resting state sub-networks. *Neuroimage*, 115:85–95.

Otte, C., Gold, S. M., Penninx, B. W., Pariante, C. M., Etkin, A., Fava, M., Mohr, D. C., and Schatzberg, A. F. (2016). Major depressive disorder. *Nature reviews Disease primers*, 2(1):1–20.

O'Neill, G. C., Tewarie, P. K., Colclough, G. L., Gascoyne, L. E., Hunt, B. A., Morris, P. G., Woolrich, M. W., and Brookes, M. J. (2017). Measurement of dynamic task related functional networks using meg. *NeuroImage*, 146:667–678.

Palla, G., Derényi, I., Farkas, I., and Vicsek, T. (2005). Uncovering the overlapping community structure of complex networks in nature and society. *nature*, 435(7043):814–818.

Palva, J. M. and Palva, S. (2018). Functional integration across oscillation frequencies by cross-frequency phase synchronization. *European Journal of Neuroscience*, 48(7):2399–2406.

Palva, S. and Palva, J. M. (2012). Discovering oscillatory interaction networks with m/eeg: challenges and breakthroughs. *Trends in cognitive sciences*, 16(4):219–230.

Park, H.-J. and Friston, K. (2013). Structural and functional brain networks: from connections to cognition. *Science*, 342(6158).

Pester, B., Ligges, C., Leistritz, L., Witte, H., and Schiecke, K. (2015). Advanced insights into functional brain connectivity by combining tensor decomposition and partial directed coherence. *PloS one*, 10(6):e0129293.

Peters, S. K., Dunlop, K., and Downar, J. (2016). Cortico-striatal-thalamic loop circuits of the salience network: a central pathway in psychiatric disease and treatment. *Frontiers in systems neuroscience*, 10:104.

Petersen, S. E. and Sporns, O. (2015). Brain networks and cognitive architectures. *Neuron*, 88(1):207–219.

Raichle, M. E., MacLeod, A. M., Snyder, A. Z., Powers, W. J., Gusnard, D. A., and Shulman, G. L. (2001). A default mode of brain function. *Proceedings of the National Academy of Sciences*, 98(2):676–682.

Roald, M., Bhinge, S., Jia, C., Calhoun, V., Adalı, T., and Acar, E. (2020). Tracing network evolution using the parafac2 model. In *ICASSP 2020-2020 IEEE International Conference on Acoustics, Speech and Signal Processing (ICASSP)*, pages 1100–1104. IEEE.

Rossini, P., Di Iorio, R., Bentivoglio, M., Bertini, G., Ferreri, F., Gerloff, C., Ilmoniemi, R., Miraglia, F., Nitsche, M., Pestilli, F., et al. (2019). Methods for analysis of brain connectivity: An ifcn-sponsored review. *Clinical Neurophysiology*, 130(10):1833–1858.

Rubinov, M. and Sporns, O. (2010). Complex network measures of brain connectivity: uses and interpretations. *Neuroimage*, 52(3):1059–1069.

Rutkove, S. B. (2007). Introduction to volume conduction. In *The clinical neurophysiology primer*, pages 43–53. Springer.

Salinas, E. and Sejnowski, T. J. (2001). Correlated neuronal activity and the flow of neural information. *Nature reviews neuroscience*, 2(8):539–550.

Satterthwaite, T. D., Xia, C. H., and Bassett, D. S. (2018). Personalized neuroscience: Common and individual-specific features in functional brain networks. *Neuron*, 98(2):243–245.

Scheinost, D., Noble, S., Horien, C., Greene, A. S., Lake, E. M., Salehi, M., Gao, S., Shen, X., O'Connor, D., Barron, D. S., et al. (2019). Ten simple rules for predictive modeling of individual differences in neuroimaging. *NeuroImage*, 193:35–45.

Seeley, W. W., Crawford, R. K., Zhou, J., Miller, B. L., and Greicius, M. D. (2009). Neurodegenerative diseases target large-scale human brain networks. *Neuron*, 62(1):42–52.

Seminowicz, D. A., Mayberg, H. S., McIntosh, A. R., Goldapple, K., Kennedy, S., Segal, Z., and Rafi-Tari, S. (2004). Limbic–frontal circuitry in major depression: a path modeling metanalysis. *Neuroimage*, 22(1):409–418.

Siegle, G. J., Steinhauer, S. R., Thase, M. E., Stenger, V. A., and Carter, C. S. (2002). Can't shake that feeling: event-related fmri assessment of sustained amygdala activity in response to emotional information in depressed individuals. *Biological psychiatry*, 51(9):693–707.

Singh, M. K., Kesler, S. R., Hosseini, S. H., Kelley, R. G., Amatya, D., Hamilton, J. P., Chen, M. C., and Gotlib, I. H. (2013). Anomalous gray matter structural networks in major depressive disorder. *Biological psychiatry*, 74(10):777–785.

Sizemore, A. E. and Bassett, D. S. (2018). Dynamic graph metrics: Tutorial, toolbox, and tale. *NeuroImage*, 180:417–427.

Smith, S. M., Fox, P. T., Miller, K. L., Glahn, D. C., Fox, P. M., Mackay, C. E., Filippini, N., Watkins, K. E., Toro, R., Laird, A. R., et al. (2009). Correspondence of the brain's functional architecture during activation and rest. *Proceedings of the national academy of sciences*, 106(31):13040–13045.

Smitha, K., Akhil Raja, K., Arun, K., Rajesh, P., Thomas, B., Kapilamoorthy, T., and Kesavadas, C. (2017). Resting state fmri: A review on methods in resting state connectivity analysis and resting state networks. *The neuroradiology journal*, 30(4):305–317.

Snyder, H. R. (2013). Major depressive disorder is associated with broad impairments on neuropsychological measures of executive function: a meta-analysis and review. *Psychological bulletin*, 139(1):81.

Sonkusare, S., Breakspear, M., and Guo, C. (2019). Naturalistic stimuli in neuroscience: critically acclaimed. *Trends in cognitive sciences*, 23(8):699–714.

Sporns, O. (2010). *Networks of the Brain*. MIT press.

Sporns, O. (2013). Network attributes for segregation and integration in the human brain. *Current opinion in neurobiology*, 23(2):162–171.

Sporns, O., Chialvo, D. R., Kaiser, M., and Hilgetag, C. C. (2004). Organization, development and function of complex brain networks. *Trends in cognitive sciences*, 8(9):418–425.

Sporns, O., Tononi, G., and Kötter, R. (2005). The human connectome: a structural description of the human brain. *PLoS computational biology*, 1(4):e42.

Spyrou, L., Parra, M., and Escudero, J. (2018). Complex tensor factorization with parafac2 for the estimation of brain connectivity from the eeg. *IEEE Transactions on Neural Systems and Rehabilitation Engineering*, 27(1):1–12.

Sridharan, D., Levitin, D. J., and Menon, V. (2008). A critical role for the right fronto-insular cortex in switching between central-executive and default-mode networks. *Proceedings of the National Academy of Sciences*, 105(34):12569–12574.

Stam, C. J., Nolte, G., and Daffertshofer, A. (2007). Phase lag index: assessment of functional connectivity from multi channel eeg and meg with diminished bias from common sources. *Human brain mapping*, 28(11):1178–1193.

Stam, C. J. and Reijneveld, J. C. (2007). Graph theoretical analysis of complex networks in the brain. *Nonlinear biomedical physics*, 1(1):1–19.

Sun, S., Li, X., Zhu, J., Wang, Y., La, R., Zhang, X., Wei, L., and Hu, B. (2019). Graph theory analysis of functional connectivity in major depression disorder with high-density resting state eeg data. *IEEE Transactions on Neural Systems and Rehabilitation Engineering*, 27(3):429–439.

Tao, H., Guo, S., Ge, T., Kendrick, K. M., Xue, Z., Liu, Z., and Feng, J. (2013). Depression uncouples brain hate circuit. *Molecular psychiatry*, 18(1):101–111.

van den Broek, S. P., Reinders, F., Donderwinkel, M., and Peters, M. (1998). Volume conduction effects in eeg and meg. *Electroencephalography and clinical neurophysiology*, 106(6):522–534.

van den Heuvel, M. P. and Sporns, O. (2013). Network hubs in the human brain. *Trends in cognitive sciences*, 17(12):683–696.

Vanderwal, T., Eilbott, J., and Castellanos, F. X. (2019). Movies in the magnet: Naturalistic paradigms in developmental functional neuroimaging. *Developmental cognitive neuroscience*, 36:100600.

Varela, F., Lachaux, J.-P., Rodriguez, E., and Martinerie, J. (2001). The brainweb: phase synchronization and large-scale integration. *Nature reviews neuroscience*, 2(4):229–239.

Vinck, M., Oostenveld, R., Van Wingerden, M., Battaglia, F., and Pennartz, C. M. (2011). An improved index of phase-synchronization for electrophysiological data in the presence of volume-conduction, noise and sample-size bias. *Neuroimage*, 55(4):1548–1565.

Wang, D., Zhu, Y., Ristaniemi, T., and Cong, F. (2018). Extracting multi-mode erp features using fifth-order nonnegative tensor decomposition. *Journal of neuroscience methods*, 308:240–247.

Wang, X. (2020). Coupled nonnegative matrix/tensor factorization in brain imaging data. *JYU dissertations*.

Wang, X., Liu, W., Toiviainen, P., Ristaniemi, T., and Cong, F. (2020). Group analysis of ongoing eeg data based on fast double-coupled nonnegative tensor decomposition. *Journal of neuroscience methods*, 330:108502.

Whitton, A. E., Deccy, S., Ironside, M. L., Kumar, P., Beltzer, M., and Pizzagalli, D. A. (2018). Electroencephalography source functional connectivity reveals abnormal high-frequency communication among large-scale functional networks in depression. *Biological Psychiatry: Cognitive Neuroscience and Neuroimaging*, 3(1):50–58.

Yao, Z., Shi, J., Zhang, Z., Zheng, W., Hu, T., Li, Y., Yu, Y., Zhang, Z., Fu, Y., Zou, Y., et al. (2019). Altered dynamic functional connectivity in weakly-connected state in major depressive disorder. *Clinical Neurophysiology*, 130(11):2096–2104.

Yun, J.-Y. and Kim, Y.-K. (2021). Graph theory approach for the structural-functional brain connectome of depression. *Progress in Neuro-Psychopharmacology and Biological Psychiatry*, 111:110401.

Zalesky, A., Fornito, A., Cocchi, L., Gollo, L. L., and Breakspear, M. (2014). Time-resolved resting-state brain networks. *Proceedings of the National Academy of Sciences*, 111(28):10341–10346.

Zeng, L.-L., Shen, H., Liu, L., Wang, L., Li, B., Fang, P., Zhou, Z., Li, Y., and Hu, D. (2012). Identifying major depression using whole-brain functional connectivity: a multivariate pattern analysis. *Brain*, 135(5):1498–1507.

Zhang, J., Wang, J., Wu, Q., Kuang, W., Huang, X., He, Y., and Gong, Q. (2011). Disrupted brain connectivity networks in drug-naive, first-episode major depressive disorder. *Biological psychiatry*, 70(4):334–342.

Zhao, Z., Zhang, Y., Chen, N., Li, Y., Guo, H., Guo, M., Yao, Z., and Hu, B. (2021). Altered temporal reachability highlights the role of sensory perception systems in major depressive disorder. *Progress in Neuro-Psychopharmacology and Biological Psychiatry*, page 110426.

Zhi, D., Calhoun, V. D., Lv, L., Ma, X., Ke, Q., Fu, Z., Du, Y., Yang, Y., Yang, X., Pan, M., et al. (2018). Aberrant dynamic functional network connectivity and graph properties in major depressive disorder. *Frontiers in psychiatry*, 9:339.

Zhou, G., Zhao, Q., Zhang, Y., Adalı, T., Xie, S., and Cichocki, A. (2016). Linked component analysis from matrices to high-order tensors: Applications to biomedical data. *Proceedings of the IEEE*, 104(2):310–331.

Zhou, T., Kang, J., Cong, F., and Li, X. (2020). Stability-driven non-negative matrix factorization-based approach for extracting dynamic network from resting-state eeg. *Neurocomputing*, 389:123–131.

Zhu, Y., Liu, J., Mathiak, K., Ristaniemi, T., and Cong, F. (2019). Deriving electrophysiological brain network connectivity via tensor component analysis during freely listening to music. *IEEE Transactions on Neural Systems and Rehabilitation Engineering*, 28(2):409–418.

Zhu, Y., Liu, J., Ye, C., Mathiak, K., Astikainen, P., Ristaniemi, T., and Cong, F. (2020a). Discovering dynamic task-modulated functional networks with specific spectral modes using meg. *NeuroImage*, 218:116924.

Zhu, Y., Zhang, C., Poikonen, H., Toiviainen, P., Huotilainen, M., Mathiak, K., Ristaniemi, T., and Cong, F. (2020b). Exploring frequency-dependent brain networks from ongoing eeg using spatial ica during music listening. *Brain topography*, 33(3):289–302.

ORIGINAL PAPERS

PI

FUNCTIONAL CONNECTIVITY OF MAJOR DEPRESSION DISORDER USING ONGOING EEG DURING MUSIC PERCEPTION

by

Wenya Liu, Chi Zhang, Xiaoyu Wang, Jing Xu, Yi Chang, Tapani Ristaniemi, and Fengyu Cong 2020

Clinical Neurophysiology, 131(10), 2413-2422,
https://doi.org/10.1016/j.clinph.2020.06.031

Clinical Neurophysiology 131 (2020) 2413–2422

Contents lists available at ScienceDirect

Clinical Neurophysiology

journal homepage: www.elsevier.com/locate/clinph

Functional connectivity of major depression disorder using ongoing EEG during music perception

Wenya Liu [a,b], Chi Zhang [a], Xiaoyu Wang [a], Jing Xu [c,*], Yi Chang [c,*], Tapani Ristaniemi [b], Fengyu Cong [a,b,d,e,*]

[a] School of Biomedical Engineering, Faculty of Electronic and Electrical Engineering, Dalian University of Technology, 116024 Dalian, China
[b] Faculty of Information Technology, University of Jyväskylä, 40014 Jyväskylä, Finland
[c] Department of Neurology and Psychiatry, First Affiliated Hospital, Dalian Medical University, 116011 Dalian, China
[d] School of Artificial Intelligence, Faculty of Electronic Information and Electrical Engineering, Dalian University of Technology, 116024 Dalian, China
[e] Key Laboratory of Integrated Circuit and Biomedical Electronic System, Liaoning Province. Dalian University of Technology, 116024 Dalian, China

ARTICLE INFO

Article history:
Accepted 29 June 2020
Available online 30 July 2020

Keywords:
Functional connectivity
Ongoing EEG
Major depression disorder
Music perception
Naturalistic stimuli

HIGHLIGHTS

- Major depression causes altered connectivity in delta and beta bands during music perception.
- Beta band connectivity is a promising biomarker for the diagnosis of major depression disorder.
- Naturalistic music stimuli lead to frequency-specific functional connectivity.

ABSTRACT

Objective: The functional connectivity (FC) of major depression disorder (MDD) has not been well studied under naturalistic and continuous stimuli conditions. In this study, we investigated the frequency-specific FC of MDD patients exposed to conditions of music perception using ongoing electroencephalogram (EEG).
Methods: First, we applied the phase lag index (PLI) method to calculate the connectivity matrices and graph theory-based methods to measure the topology of brain networks across different frequency bands. Then, classification methods were adopted to identify the most discriminate frequency band for the diagnosis of MDD.
Results: During music perception, MDD patients exhibited a decreased connectivity pattern in the delta band but an increased connectivity pattern in the beta band. Healthy people showed a left hemisphere-dominant phenomenon, but MDD patients did not show such a lateralized effect. Support vector machine (SVM) achieved the best classification performance in the beta frequency band with an accuracy of 89.7%, sensitivity of 89.4% and specificity of 89.9%.
Conclusions: MDD patients exhibited an altered FC in delta and beta bands, and the beta band showed a superiority in the diagnosis of MDD.
Significance: Our study provided a promising reference for the diagnosis of MDD, and revealed a new perspective for understanding the topology of MDD brain networks during music perception.

1. Introduction

Major depression disorder (MDD) is currently one of the most prevalent psychiatric disorders, and it substantially disrupts patients' lives. MDD patients are usually characterized by deficits of affective and cognitive functions (Kaiser, 2015; Li et al., 2018; Xia et al., 2018). Although many researchers have dedicated themselves to the exploration of the pathophysiology of MDD, the neural mechanisms of its etiology and pathogenesis are still not fully understood. Currently, there are no biomarkers for the clinical diagnosis of MDD (Fingelkurts and Fingelkurts, 2015; Gao et al., 2018; Nugent et al., 2019). Conventionally, the clinical diagnosis of MDD frequently depends on some public criteria, such as Diagnostic and Statistical Manual of Mental Disorders V (DSM-5),

* Corresponding authors at: School of Biomedical Engineering, Faculty of Electronic and Electrical Engineering, Dalian University of Technology, 116024 Dalian, China (F. Cong); Department of Neurology and Psychiatry, First Affiliated Hospital, Dalian Medical University, 116011 Dalian, China (Jing Xu and Yi Chang).
E-mail addresses: xujing_doc@aliyun.com (J. Xu), changee99@gmail.com (Y. Chang), cong@dlut.edu.cn (F. Cong).

https://doi.org/10.1016/j.clinph.2020.06.031
1388-2457/

which makes the diagnosis of MDD very subjective due to human factors and causes faulty diagnostic results (Mumtaz et al., 2015; Nugent et al., 2019). For this reason, noninvasive neuroimaging techniques, such as electroencephalogram (EEG), magnetoencephalography (MEG) and functional magnetic resonance imaging (fMRI), are urgently needed as more effective and intelligent diagnostic tools. EEG is an inexpensive technique that benefits from high temporal resolution. EEG is able to record electrical activity at frequencies related to neuronal activity and to capture the dynamic changes at a millisecond scale. These advantages make EEG a very promising technique for commonly use in the diagnosis of MDD (Baskaran et al., 2012; Mumtaz et al., 2015, 2017).

Many fMRI studies have demonstrated that the pathogenesis of MDD is the abnormality of large-scale brain networks, such as default mode network (DMN) (Zhu et al., 2012; Wu et al., et al., 2013) and affective network (AN) (Avery et al., 2014), or the dysconnectivity of some brain regions, such as corticolimbic pathways (Nugent et al., 2019), rather than the dysfunction of an individual brain region. So, functional connectivity (FC) has proven to be effective to investigate network dysfunction in MDD. FC provides a new line of thought for the diagnosis of MDD patients, and many studies, especially fMRI and EEG studies, have focused on the classification of MDD based on FC analysis (Wang et al., 2017; Gao et al., 2018; Sakai and Yamada, 2019). However, FC analysis and MDD classification always focus on resting-state or highly controlled and repeated stimuli, but the differences in FC under naturalistic and continuous stimuli between healthy people and MDD patients have not been well studied. Compared with resting state, listening to continuous music is more closely related to real-world experience (Wang et al., 2020), and emotional arousal can be induced for affective processing (Mikutta et al., 2012). Music therapy has become an attractive tool for MDD treatment, so understanding the mechanism of the brain response during listening to music is the basis for the diagnosis and treatment of MDD (Michael et al., 2005; Maratos et al., 2008). An increasing amount of literature has demonstrated that human brain networks are different across frequency bands in both resting-state and task conditions, and networks in specific frequency bands may reveal different brain functions (Brookes et al., 2012, 2016; Hillebrand et al., 2012, 2016). Previous studies have demonstrated altered FC in MDD in different frequency bands, so FC analysis across different frequency bands is important to the diagnosis of MDD (Mumtaz et al., 2015; Knott et al., 2001; Whitton et al., 2018). Some studies have found that frequency-specific and large-scale brain networks will emerge during music perception to sustain ongoing cognitive tasks (Alluri et al., 2012; Cong et al., 2013; Wang et al., 2020). A review by Maratos et al., emphasized that music therapy was associated with improvements in mood to treat depression (Maratos et al., 2008). Some researchers have already focused on frequency-specific brain responses to music in depression patients and other psychiatric disorders and have found that music therapy can alter FC and modulate brain responses (Michael et al., 2005; Ramirez et al., 2015; Dharmadhikari et al., 2018). These previous studies support our assumption that altered FC exists in different frequency bands during music perception in MDD patients. However, few studies have investigated the mechanism of dysconnectivity and brain responses of MDD patients during music perception.

For electrophysiological neuroimaging techniques, like EEG, the collected signals from one scalp sensor are actually from the whole brain due to the volume conduction effect (Van Den Broek et al., 1998; Schoffelen and Gross, 2009; Brunner et al., 2016). Brain connectivity in sensor space is usually confounded by volume conduction, and even with the conduction of source reconstruction methods, source leakage still exists due to the ill-posed nature of the inverse problem (O'Neill et al., 2018). An increasing number of studies have demonstrated that the communication of brain regions or neural populations depends on phase interactions (Womelsdorf et al., 2007; Palva and Palva, 2012; He et al., 2019). A zero-lag interaction is considered to be the consequence of volume conduction because signal leakage is instantaneous. Among the phase synchronization methods, phase lag index (PLI) discards the interactions resulting from phase differences of zero, so PLI is not sensitive to the volume conduction effect; thus, it is commonly used in the FC analysis of EEG and MEG studies (Stam et al., 2007; Vinck et al., 2011; Wu et al., 2012). Ruiz-Gómez et al have demonstrated that PLI could reduce the bias introduced by the spurious influence of volume conduction and was superior to the other seven FC synchronization measures (Ruiz-Gómez et al., 2019).

Network analysis methods based on graph theory are widely used to reveal the topology of brain networks (Sporns, 2018; Ren et al., 2019). In EEG sensor space, the brain networks are constituted by nodes representing electrodes and edges representing FC strength between every pair of nodes. The various network properties are efficient measures used to quantify brain functional integration and functional segregation (Rubinov and Sporns, 2010; Liao et al., 2017). Degree, which is a measure of influence, clustering coefficient, which is a measure of functional segregation, and characteristic path length, which is a measure of functional integration, are network properties that are commonly used to quantify the efficiency of information processing (Achard et al., 2006; He et al., 2007; Gong and He, 2015). In this study, we applied degree, clustering coefficient and characteristic path length to quantify the differences between healthy people and MDD patients.

In this study, we collected EEG data from healthy people and MDD patients under conditions of music perception, and used the PLI method to calculate FC across five typically analyzed frequency bands: delta, theta, alpha, beta and gamma bands. After statistical analysis using the network-based-statistic (NBS) method, we compared the two groups through connectivity matrices and graph-theory based network properties in delta and beta frequency bands, which exhibited significant differences. Finally, machine learning methods were used to perform the classification.

2. Methods

2.1. Data acquisition

Nineteen healthy adults (fourteen females and five males) aged 24–65 years in the control (CON) group and twenty adults (fourteen females and six males) with MDD aged 23–58 years in the MDD group were recruited for this experiment. All the patients were from the First Affiliated Hospital of Dalian Medical University in China. This study was approved by the ethics committee of the hospital, and all the participants signed the informed consent before their enrollment. None of the participants reported hearing loss or formal training in music. MDD patients were primarily diagnosed by a clinical expert, and the course of the disease varied from 2 and 36 months. All the participants were tested according to Hamilton Rating Scale for Depression (HRSD), Hamilton Anxiety Rating Scale (HAMA) and Mini-Mental State Examination (MMSE). The means and standard deviations (SD) of age, gender, education and clinical measures for both groups are listed in Table 1. During the experiment, participants were told to sit comfortably in a chair and listen to a piece of music. An 8.5-minute long musical piece of modern tango by Astor Piazzolla was used as the stimulus due to its rich musical structure and high range of variation in musical features, such as dynamics, timbre, tonality and rhythm (Alluri et al., 2012, 2013).

The EEG data were recorded by the Neuroscan Quik-cap device with 64 electrodes arranged according to the international 10–20

Table 1
Means and standard deviations of age, gender, education and clinical measures of the CON group and MDD group.

	CON group		MDD group		Analysis
	Mean	SD(Range)	Mean	SD(Range)	*p*-value
Age	38.4	11.8(24–65)	42.9	11.0(23–58)	>0.05
Education	13.6	3.8(6–20)	12.8	3.4(6–16)	>0.05
HRSD	2.4	1.3(0–4)	23.3	3.6(16–28)	<0.01
HAMA	2.4	1.3(0–5)	19.2	3.0(15–25)	<0.01
MMSE	28.2	0.9(27–30)	28.1	1.1(26–30)	>0.05
Duration	0	0	12.8	8.5(2–36)	–
Gender	14 females, 5 males		14 females, 6 males		–

Abbreviations: CON, control; MDD, major depression disorder; SD, standard deviations; HRSD, Hamilton Rating Scale for Depression; HAMA, Hamilton Anxiety Rating Scale; MMSE, Mini-Mental State Examination.

system. Electrodes placed at the left and right earlobes were used as the references. The data were down-sampled to 256 Hz for further processing and visually checked to remove obvious artifacts from head movements. Eye movements artifacts were rejected by independent component analysis (ICA), and 50-Hz artifacts were removed by short time Fourier transform (STFT). STFT was applied to filter the data into five typically analyzed frequency bands, namely, the delta (0.5–4 Hz), theta (4–8 Hz), alpha (8–13 Hz), beta (13–30 Hz) and gamma (30–80 Hz) bands, for further analysis.

2.2. Phase synchronization

In this study, phase synchronization was measured between all the pairs of channels by the PLI method, which is an asymmetry index that measures the distribution of phase differences (Stam et al., 2007; Vinck et al., 2011). Due to the instantaneous spread of current, the same sources collected by two electrodes are considered to cause a zero-lag phase difference, which is rejected by PLI. Therefore, PLI is less sensitive to the volume conduction effect, and it can reveal the true coupling strength between pairs of channels.

For an EEG signal $x(t), t = 1, 2, 3, \cdots, T$ from one channel, the analytical signal $z(t)$ can be constructed by Hilbert transform,

$$z(t) = x(t) + i\tilde{x}(t) = \frac{1}{\pi} PV \int_{-x}^{\infty} \frac{x(\tau)}{t-\tau} d\tau, \tag{1}$$

where $\tilde{x}(t)$ is the imaginary part, and PV refers to the Cauchy principal value. Then, the instantaneous amplitude$A(t)$ and the instantaneous phase$\varphi(t)$ can be computed as follows:

$$\begin{cases} A(t) = \sqrt{\left[\tilde{x}(t)\right]^2 + [x(t)]^2} \\ \varphi(t) = \arctan\frac{\tilde{x}(t)}{x(t)}. \end{cases} \tag{2}$$

Therefore, the phase difference $\Delta\varphi(t)$ of two signals $x_a(t)$ and $x_b(t)$ at time t can be formulated as:

$$\Delta\varphi(t) = \varphi_a(t) - \varphi_b(t). \tag{3}$$

Then, the PLI index can be defined via

$$PLI = |\langle sign[\Delta\varphi(t)]\rangle|, \quad t = 1 \cdots T. \tag{4}$$

The value of PLI index varies between 0 and 1. A value of 0 indicates no coupling or coupling with a phase difference centered around 0 mod π, and a value of 1 indicates perfect phase synchronization between two signals at a constant lag except 0 or π.

In this study, for the 8.5-minute EEG data with a sampling frequency of 256 Hz, we first removed four unusable electrodes. Then, we removed the first and last 10 seconds of the EEG data to avoid transition effects, and we segmented the EEG data into non-overlapping epochs by a time window of 10 seconds, so there were a total of 49 epochs. Then, an adjacency matrix of 60×60 was calculated by PLI for each epoch and each frequency band.

2.3. Network analysis

Graph theory is normally used after the calculation of the adjacency matrix to quantify the topology of brain networks. In this study, we used three commonly used network measures to quantify influence, functional segregation and functional integration, including degree, clustering coefficient and characteristic path length. All the network measures mentioned above were computed using the Brain Connectivity Toolbox (Rubinov and Sporns, 2010) (http://www.brain-connectivity-toolbox.net).

For an adjacency matrix $\boldsymbol{G}$, with N nodes, w_{ij} represents the connection strength between node i and node j, where $0 \le w_{ij} \le 1$. The diagonal elements mean self-connections of nodes, so $w_{ii} = 0, i = 1, 2, \cdots, N$.

2.3.1. Degree

Degree is considered an important marker of network development and resilience, and for a weighted network, the degree of node i can be defined as follows:

$$k_i = \sum\nolimits_{j \in N} w_{ij} \tag{5}$$

2.3.2. Clustering coefficient

Clustering coefficient is a measure of functional segregation which is a reflection of the local organization of a network by depicting the tendency of a node forming local triangles (Rubinov and Sporns, 2010), and its definition for a weighted network of node i is described as follows:

$$C_i = \frac{2t_i}{k_i(k_i-1)}, \tag{6}$$

where $t_i = \frac{1}{2}\sum_{j,h \in N}\left(w_{ij}w_{ih}w_{jh}\right)^{\frac{1}{3}}$ is the geometric mean of triangles around i. The clustering coefficient for the whole network is defined as the mean of clustering coefficient for all nodes,

$$C = \frac{1}{N}\sum\nolimits_{i \in N} C_i \tag{7}$$

2.3.3. Characteristic path length

Characteristic path length is the average of shortest path length between all pairs of nodes and is commonly used to measure functional integration. Characteristic path length is a reflection of the efficiency of a network (Bullmore and Sporns, 2009). The definition is described as follows:

$$L = \frac{1}{N}\sum\nolimits_{i \in N} \frac{\sum_{j \in N, j \neq i} d_{ij}}{N-1}, \tag{8}$$

where $d_{ij} = \sum_{a_{uv} \in g^{w}_{i \leftrightarrow j}} \frac{1}{w_{uv}}$ is the shortest path length between node i and node j, and $g^{w}_{i \leftrightarrow j}$ is the shortest weighted path between i and j.

2.4. Statistical analysis

To determine in which frequency band a significant difference exists between the CON group and MDD group, Network Based Statistic Toolbox was applied in this study (Zalesky et al., 2010). The NBS method can control the family-wise error when multiple univariate testing is performed at each connection of a network. NBS method is used to identify significant brain network substructures formed by some suprathreshold links but not to identify individual links as being significant. The threshold is used on the test statistic computed for each pairwise connection, and different thresholds can construct different level of sparse graphs. After averaging the adjacency matrices across time windows for each subject, statistical analysis was performed between the CON group and MDD group for each frequency band. A significance level of corrected $P < 0.05$ and a nonparametric permutation test of 5000 permutations were used in this study. T-test was selected for the statistical test, and different test statistic thresholds (t-statistic) were tested to identify the most significant brain network substructures.

2.5. Classification

Considering the limitations of using sliding windows without overlapping, which will lead to the problem that FC topology may not been well described within one fixed time window (Liuzzi et al., 2019), we averaged every six time windows (the connectivity matrices within one minute) to generate one classification sample to highlight the main connectivity patterns during music perception. To improve classification performances, we constructed sparse networks based on the notion of connected graphs to remove redundant information, which can ensure that every node has a connection to another node for a sparse network. The detailed method for threshold selection can be found in reference (Atay and Biyikoğlu, 2005).

In this study, we used the adjacency matrices obtained by PLI to perform classification, and we compared the classification performance using original networks and sparse networks between delta and beta frequency bands and six classifiers, including decision tree (DT), Gaussian mixture model (GMM), k-nearest neighbor (KNN), naïve Bayes (NB), random forest (RF) and support vector machine (SVM). We unfolded the adjacency matrix to a vector as one sample. Because of the symmetry property of the adjacency matrix, we can obtain $N(N-1)/2 = 60(60-1)/2 = 1770$ variables for each sample. Therefore, we can get 152 samples for the CON group and 160 samples for the MDD group. To avoid overfitting, principal component analysis (PCA) was applied for dimension reduction before classification.

To assess the performance of classification, we calculated some statistical evaluation measurements including accuracy, sensitivity, and specificity (Yan et al., 2019), which can be calculated by:

$$\text{accuracy} = \frac{TP + TN}{TP + FP + TN + FN}, \tag{9}$$

$$\text{sensitivity} = \frac{TP}{TP + FN}, \tag{10}$$

$$\text{specificity} = \frac{TN}{TN + FP}, \tag{11}$$

where TP, TN, FP and FN represent true positive, true negative, false positive and false negative, respectively. To obtain a reliable classification result, we shuffled the data order, used 10-fold cross validation, and ran 10 times for each classifier. Then, we averaged the classification results to calculate the final performance for each classifier and each frequency band.

3. Results

3.1. Phase synchronization

After statistical analysis by NBS for each frequency band, a significant difference only existed in two frequency bands: delta and beta bands (delta: $P = 0.0450$, theta: $P = 0.2386$, alpha: $P = 0.3447$, beta: $P = 0.0344$, gamma: $P = 0.0649$). The adjacency matrices for these two frequency bands of the CON group and MDD group are shown in Fig. 1. For the delta frequency band, the connectivity strength increased in the MDD group (delta: mean = 0.0867, SD = 0.0197) compared to the CON group (delta: mean = 0.0853, SD = 0.0178;). However, for the beta frequency band, the connectivity strength of the MDD group (mean = 0.0408, SD = 0.0133) decreased compared with that of the CON group (mean = 0.0485, SD = 0.0143). From Fig. 1, we can see that short-distance synchronization was stronger than long-distance synchronization, and the whole brain connectivity was formed by many small modules.

The significant brain network connections between the CON group and the MDD group in delta and beta frequency bands are shown in Fig. 2. We can see that there were 13 significant connections in the delta band distributed within right central brain areas and between right temporal and left parietal brain regions. While in the beta band, there were 43 significant connections characterized mostly by long-distance edges, which were distributed mostly within frontal brain areas and between frontal and parieta-occipital brain areas. The substructures were considered to be important indicators of the differences between the two groups, which can be promising biomarkers for MDD under conditions of music perception.

3.2. Network analysis

We calculated the degree of each node in delta and beta frequency bands for both groups, as shown in Fig. 3. We obtained the lateralization index (LI) by the formula: $LI = (L - R)/(L + R)$, where L and R represented the degree of left and right hemisphere, respectively (Desmond et al., 1995). Then, we performed t-test for both delta and beta bands, and we obtained $P = 0.0114$ for the delta band and $P < 0.0001$ for the beta band. For the CON group, there was a lateralization effect to the left hemisphere, but for the MDD group, there was no such lateralization effect. From Fig. 3, we can conclude that the degree increased in the delta frequency band for the MDD group (delta: mean = 0.0867, SD = 0.0040;) compared with the CON group (delta: mean = 0.0854, SD = 0.0022), but it decreased in the beta frequency band for the MDD group (mean = 0.0402, SD = 0.0032) compared with the CON group (mean = 0.0480, SD = 0.0031); this finding was consistent with the results from the adjacency matrices as shown in Fig. 1. Fig. 4 shows a boxplot of clustering coefficient and characteristic path length in delta and beta frequency bands of both the CON group and the MDD group. From this finding, we can see that the beta frequency band was the most discriminate for classifying the CON group and the MDD group; therefore, next, we will test the classification performance of each frequency band.

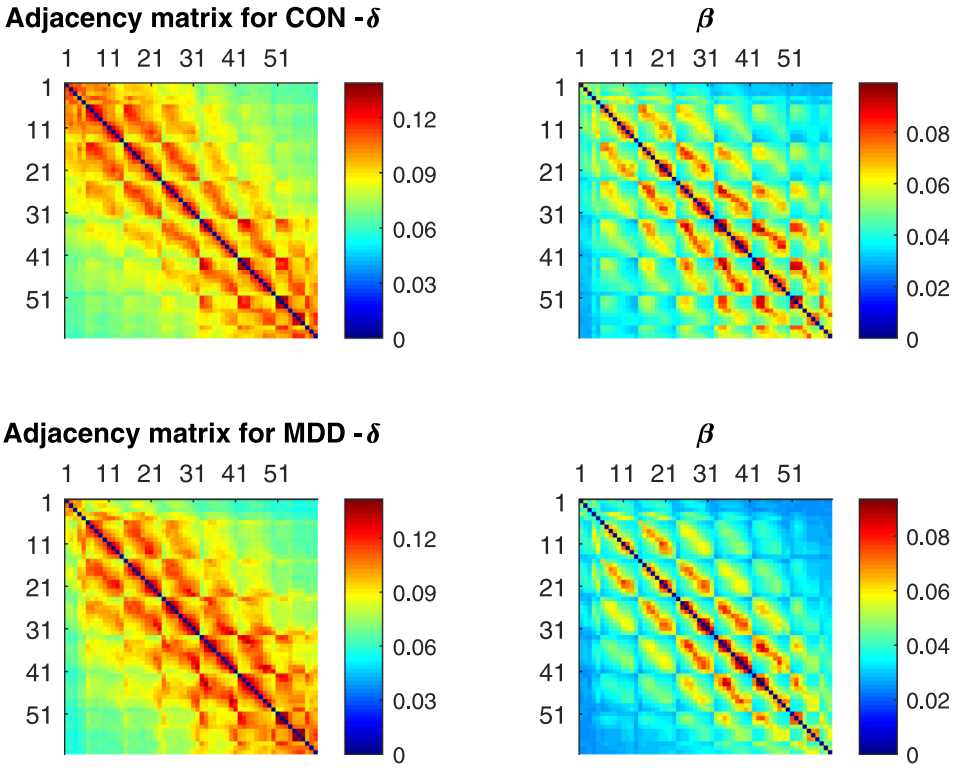

Fig. 1. Averaged adjacency matrices of the CON group and MDD group across time windows for delta and beta frequency bands. Each adjacency matrix is formed by a 60×60 matrix with zero values in the diagonal. CON, control; MDD, major depression disorder.

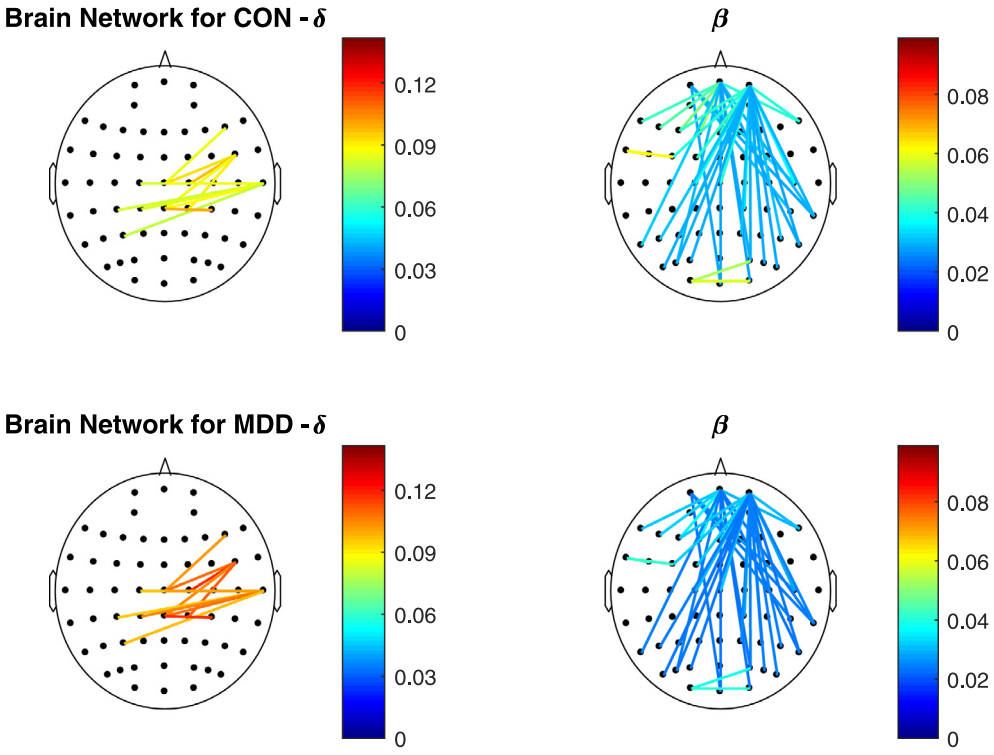

Fig. 2. The significant brain network connections in delta and beta frequency bands of the CON group and MDD group. The results were conducted by the NBS method using 5000 permutations, corrected p value of $p < 0.05$, and maximum component threshold $t > 3.1$ for the delta band and $t > 2.3$ for the beta band. There are 13 significant connections in the delta band and 43 significant connections in the beta band. CON, control; MDD, major depression disorder; NBS, network based statistic.

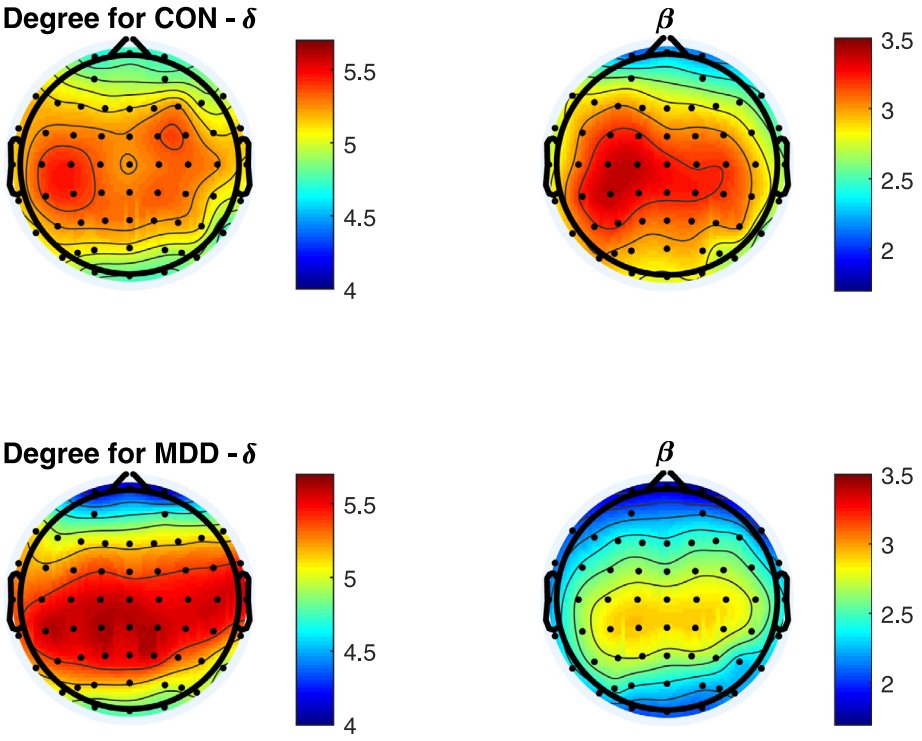

Fig. 3. The degree of each node in delta and beta frequency bands for the CON group and MDD group. CON, control; MDD, major depression disorder.

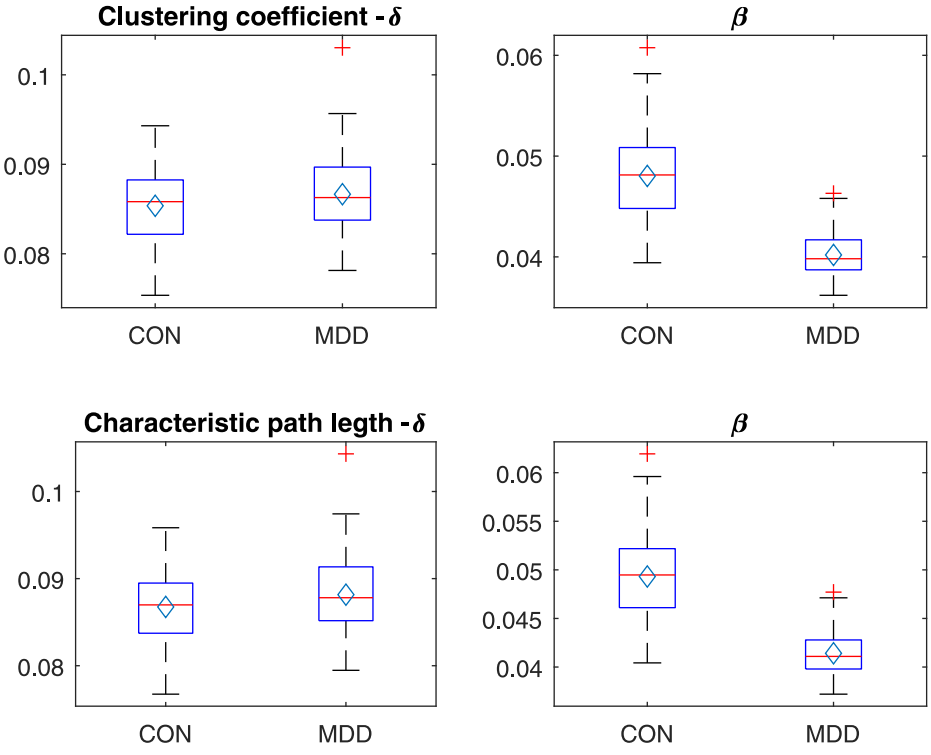

Fig. 4. Boxplot of clustering coefficient and characteristic path length for the CON group and MDD group in delta and beta frequency bands. The upper and lower black lines represent the maximum value and the minimum value, respectively, and the red cross indicates outliers. The bottom and top edges of the blue box indicate the 25th and 75th percentiles, and the red line and rhombus in the box indicate the median value and the mean value, respectively. CON, control; MDD, major depression disorder. (For interpretation of the references to colour in this figure legend, the reader is referred to the web version of this article.)

3.3. Classification results

We tested six classifiers on delta and beta frequency bands, and the classification results are listed in Table 2. The top three classification accuracy results are marked in bold font. From Table 2, we can see that SVM demonstrated the best classification performance, with a classification accuracy of 89.7% among the six classifiers in the beta frequency band using sparse adjacency matrices. Therefore, we can conclude that the beta frequency band was the most discriminate for distinguishing the CON group and MDD group, which was in agreement with the results in Fig. 4. For the best classification performance, we obtained accuracy = 89.7%, sensitivity = 89.4%, and specificity = 89.9%.

The classification performance of sparse networks was better than that of original networks for all the six classifiers and both delta and beta bands. The top three classification performances were all from sparse networks, which meant that adding a threshold to remove some redundant information can efficiently improve the classification performance. In network analysis, it is reasonable to remove weak connections, which are considered to result from the effect of noise and not to represent the true connections between brain regions.

4. Discussion

To the best of our knowledge, this study is the first attempt to investigate the differences in connectivity between healthy people and MDD patients using frequency-specific ongoing EEG FC analysis under conditions of music perception and then to apply classification methods for diagnosis. First, we calculated FC by PLI, which can efficiently decrease the volume conduction effect for each time window and each frequency band. Then, NBS analysis was applied to identify the significant brain network substructures for each frequency band, and we found that significant substructures only existed in delta and beta frequency bands. Then, network properties, including degree, clustering coefficient and characteristic path length, were calculated for delta and beta bands to explore the differences of in the topology between CON and MDD groups. Based on the network analysis, we found that the beta frequency band was the most discriminate for MDD diagnosis. Therefore, we compared the classification performance with six classifiers between those two frequency bands, and the beta band reached the highest classification accuracy through the SVM classifier after constructing sparse networks.

Some previous EEG studies have demonstrated that the perception of music was associated with the synchronization of different frequency bands (Bhattacharya et al., 2001; Ruiz et al., 2009; Wu et al., 2012; Cong et al., 2013). After statistical analysis of connectivity matrices for each frequency band, we found significant brain network connections in delta and beta bands. From the perspective of music, both the delta and beta bands are associated with music perception. An MEG study has demonstrated that beta rhythms coupled with entrained delta-theta oscillations underpin accuracy in musical processing (Doelling and Poeppel, 2015). Arnal et al., also found that delta-beta coupled oscillations were associated with temporal processing (Arnal et al., 2015). Regarding the importance of delta and beta bands during music perception, an altered FC in those two frequency bands may provide an efficient tool for the diagnosis of MDD.

The delta band exhibited increased connectivity in the MDD group with 13 significant connections, and the beta band exhibited decreased connectivity in the MDD group with 43 significant connections, which were mostly constructed by long-distance edges. This contrast between delta and beta bands was also reported in Leuchter's research, which reported that in a resting-state EEG study, the delta band exhibited increased connectivity in the MDD group in fewer highly significant and shorter-distance edges, and the beta band exhibited more significant connections with longer-distance edges (Leuchter et al., 2012). We found that the increased significant connections in the delta band mainly distributed within right central brain areas and between right temporal and left parietal brain regions. The delta band was demonstrated to have a substantial influence on the identification of natural speech fragments in an MEG study (Koskinen et al., 2013). The delta band was already found to be more prominent in the right hemisphere than in the left hemisphere of depressed patients (Kwon et al., 1996), and the delta inter-hemispheric coherence contributed to the classification of MDD patients and healthy controls (Knott et al., 2001). Those findings were consistent with our results that the significant connections in the delta band distributed mostly in the right hemisphere. We also found decreased connectivity distributed mostly within frontal brain areas and between frontal and parietal-occipital brain areas in the beta band in MDD patients. The beta band has been demonstrated to be the predominant frequency band for music perception (Jäncke and Alahmadi, 2016), and Alavash et al., found that networks of the listening brain showed higher segregation of frontal control regions relative to those under task-free resting states, which may support that MDD patients were less involved in listening in our study (Alavash et al., 2019). Many fMRI (Veer et al., 2010; Kaiser et al., 2015) and EEG (Fingelkurts et al., 2007; Fingelkurts and Fingelkurts, 2015) studies have demonstrated that some brain regions and some specific brain networks indicated decreased FC in the MDD group. Olbrich et al., have demonstrated that MDD was characterized by altered EEG FC within frontal brain areas (Olbrich et al., 2014). With hierarchical brain architectures, global integration indicates higher cognition mediated by long-distance connections. Music perception is a high cognition process in the brain, and global integration is needed. Global integration by modulating long-distance connectivity is crucial for task-dependent functions (Markov et al., 2011; Park and Friston, 2013). The decreased long-distance connectivity in the beta band reported in our results, which suggests less communication between remote brain regions, may provide an important biomarker in MDD diagnosis.

The properties based on the graph theory are the quantification of network comparisons. In this study, we compared two network properties, including clustering coefficient and characteristic path length, in delta and beta bands between CON and MDD groups, and those measures have been used in previous studies to identify

Table 2
The classification accuracy of six classifiers in delta and beta frequency bands.

	Network	DT	GMM	KNN	NB	RF	SVM
Delta	Original	54.7%	49.7%	65.7%	61.2%	62.0%	66.9%
	Sparse	60.9%	53.2%	68.7%	62.5%	69.7%	72.9%
Beta	Original	61.4%	49.5%	77.4%	55.2%	70.9%	78.2%
	Sparse	68.5%	54.8%	**85.6%**	56.7%	**82.3%**	**89.7%**

Abbreviations: DT, decision tree; GMM, Gaussian mixture model; KNN, k-nearest neighbor; NB, naïve Bayes; RF, random forest; SVM, support vector machine.

altered network organizations in MDD patients (Ajilore et al., 2014; Ye et al., 2015). From Fig. 4, we can see that more differences appeared in the beta band, which was identical to our results showing that the beta band exhibited more significant connections than the delta band. In the delta band, the MDD group was characterized by higher clustering coefficient and longer characteristic path length, which meant that MDD patients had lower information transfer efficiency and a tendency of regular networks in the delta band. The MDD group showed higher local efficiency in the delta band, and a fMRI study obtained the same findings in MDD patients (Ye et al., 2015). Differently in the beta band, the MDD group presented smaller clustering coefficient and shorter characteristic path length, indicating that the MDD group had a poor local organization ability and a trend toward random networks. Singh et al., also found that depressed patients displayed smaller clustering coefficient in gray matter networks (Singh et al., 2013). Therefore, the topological changes in brain connectome were significant reflections of patients with MDD (Ye et al., 2015).

Music perception has been demonstrated to have a cortical lateralization effect in the human brain, but based on the literature, different sounds appeared about which hemisphere of the brain does music processing more lateralize to (Ohnishi, 2001; Kay et al., 2012). Toiviainen et al., found in a fMRI study that different musical features can cause different hemispheric asymmetry effects (Toiviainen et al., 2014). In the present study, we revealed a left hemispheric lateralization effect in healthy people, and no lateralization effect in MDD patients under naturalistic music listening condition. Alluri et al., demonstrated that left hemispheric primary and supplementary motor areas were more activated than those of the right hemisphere when listening to purely instrumental music (Alluri et al., 2013). The results supported our findings of left hemisphere lateralization in the CON group because we also used a piece of music without lyrics. Furthermore, the left inferior frontal area was reported to be related to the memory of music (Watanabe et al., 2008), which also supported to the reliability of our results. Many studies have reported a lateralized hemispheric dysfunction in major depression (Uytdenhoef et al., 1983; Bench et al., 1993), and this dysfunction was well demonstrated by our results that no hemispheric lateralization effect exists in MDD patients during music perception. Music is capable of inducing emotional arousal (Mikutta et al., 2012), and the left hemisphere predominates during states of low arousal and positive affect (Craig, 2005). EEG studies have found that depressed participants showed a hypoactivation in the left frontal lobe, which was related to the elicitation and recognition of emotions and caused diminished positive affect (Wheeler et al., 1993; Punkanen et al., 2011). This may cause the deficiency of affective processing in depressed patients during music processing.

We tested the classification accuracy of delta and beta bands by six classifiers, and the most commonly used SVM classifier exhibited the best performance in the beta band, which was consistent with the results in Fig. 4. After eliminating weak connections, the classification performance improved for all the classifiers according to Table 2 because applying feature selection to remove redundant information was necessary for classification. An EEG study on male depression by Knott et al., also showed that the beta frequency band was the most discriminate for classification (Knott et al., 2001). Gao et al., conducted a comprehensive review of studies related to the classification of MDD based on magnetic resonance imaging data and compared the methods and classification accuracies of 66 representative studies (Gao et al., 2018). The classification performance in our study was better than that of 76% of the studies mentioned in Gao's work. EEG was more suitable for clinical applications in MDD diagnosis due to its higher temporal resolution and lower cost than fMRI and MEG (Mumtaz et al., 2017). Furthermore, compared with that recorded under resting state conditions, EEG data recorded under naturalistic and continuous stimuli, such as listening to music, is more close to simulate real-world conditions (Wang et al., 2020), and music can induce emotional arousal, which is related to affective processing in MDD patients (Mikutta et al., 2012; Toiviainen et al., 2014). Therefore, music perception tasks may be superior for use in MDD diagnosis. However, it is still a long way to go for the clinical usability, because current studies are mostly based on small datasets (22–90 recordings) acquired under non-naturalistic conditions and highly controlled research settings, and the non-replicability of the research with different methods and experimental conditions also make it challenging for the generalization to clinical diagnosis.

Taken together, when exposed to music listening conditions, both healthy controls and MDD patients exhibited different FC patterns across different frequency bands, and MDD patients were characterized by altered FC in delta and beta bands. Our results, shown above, were well supported by previous studies and can provide a promising perspective for the clinical diagnosis of MDD in the future.

Some important limitations of this study should be declared. First, the analysis was based on the sensor-space level, and the lack of a source reconstruction procedure limited further explanation of the results. Second, the neural correlates and dynamic neural processing of musical emotions are still not well understood (Toiviainen et al., 2014), and the selection of control stimuli, such as music type and duration, still needs further investigation. Furthermore, in the music processing task, how to extract the music-induced activity from ongoing EEG data is quite challenging and still remains an open question (Wang et al., 2020), which is directly related to the reliability of the explanation of the results.

Acknowledgements

This work was supported by National Natural Science Foundation of China (Grant No. 91748105 & Grant No. 81471742 & Grant No. 61703069); National Foundation in China (No. JCKY2019110B009); the Fundamental Research Funds for the Central Universities [DUT2019] in Dalian University of Technology in China; and the scholarships from China Scholarship Council (No. 201706060263).

References

Achard S, Salvador R, Whitcher B, Suckling J, Bullmore E. A resilient, low-frequency, small-world human brain functional network with highly connected association cortical hubs. J Neurosci 2006;26:63–72.
Ajilore O, Lamar M, Leow A, Zhang A, Yang S, Kumar A. Graph theory analysis of cortical-subcortical networks in late-life depression. Am J Geriatr Psychiatry 2014;22:195–206.
Alavash M, Tune S, Obleser J. Modular reconfiguration of an auditory control brain network supports adaptive listening behavior. Proc Natl Acad Sci U S A 2019;116:660–9.
Alluri V, Toiviainen P, Jääskeläinen IP, Glerean E, Sams M, Brattico E. Large-scale brain networks emerge from dynamic processing of musical timbre, key and rhythm. Neuroimage 2012;59:3677–89.
Alluri V, Toiviainen P, Lund TE, Wallentin M, Vuust P, Nandi AK, et al. From vivaldi to beatles and back: Predicting lateralized brain responses to music. Neuroimage 2013;83:627–36.
Arnal LH, Doelling KB, Poeppel D. Delta-beta coupled oscillations underlie temporal prediction accuracy. Cereb Cortex 2015;25:3077–85.
Atay FM, Biyikoğlu T. Graph operations and synchronization of complex networks. Phys Rev E – Stat Nonlinear, Soft Matter Phys 2005;72:016217.
Avery JA, Drevets WC, Moseman SE, Bodurka J, Barcalow JC, Simmons WK. Major depressive disorder is associated with abnormal interoceptive activity and functional connectivity in the insula. Biol Psychiatry 2014;76:258–66.
Baskaran A, Milev R, McIntyre RS. The neurobiology of the EEG biomarker as a predictor of treatment response in depression. Neuropharmacology 2012;63:507–13.
Bench CJ, Friston KJ, Brown RG, Frackowiak RS, Dolan RJ. Regional cerebral blood flow in depression measured by positron emission tomography: The relationship with clinical dimensions. Psychol Med 1993;23:579–90.
Bhattacharya J, Petsche H, Pereda E. Long-range synchrony in the γ band: Role in music perception. J Neurosci 2001;21:6329–37.

Brookes MJ, Liddle EB, Hale JR, Woolrich MW, Luckhoo H, Liddle PF, et al. Task induced modulation of neural oscillations in electrophysiological brain networks. Neuroimage 2012;63:1918–30.
Brookes MJ, Tewarie PK, Hunt BAE, Robson SE, Gascoyne LE, Liddle EB, et al. A multi-layer network approach to MEG connectivity analysis. Neuroimage 2016;132:425–38.
Brunner C, Billinger M, Seeber M, Mullen TR, Makeig S. Volume conduction influences scalp-based connectivity estimates. Front Comput Neurosci 2016;10:1–4.
Bullmore E, Sporns O. Complex brain networks: Graph theoretical analysis of structural and functional systems. Nat Rev Neurosci 2009;10:186–98.
Cong F, Alluri V, Nandi AK, Toiviainen P, Fa R, Abu-Jamous B, et al. Linking brain responses to naturalistic music through analysis of ongoing EEG and stimulus features. IEEE Trans Multimed 2013;15:1060–9.
Craig AD. Forebrain emotional asymmetry: A neuroanatomical basis?. Trends Cogn Sci 2005;9:566–71.
Desmond JE, Sum JM, Wagner AD, Demb JB, Shear PK, Glover GH, et al. Functional MRI measurement of language lateralization in wada-tested patients. Brain 1995;118:1411–9.
Dharmadhikari AS, Tandle AL, Jaiswal SV, Sawant VA, Vahia VN, Jog N. Frontal theta asymmetry as a biomarker of depression. East Asian Arch Psychiatry 2018;28:17–22.
Doelling KB, Poeppel D. Cortical entrainment to music and its modulation by expertise. Proc Natl Acad Sci U S A 2015;112:E6233–42.
Fingelkurts AA, Fingelkurts AA. Altered structure of dynamic electroencephalogram oscillatory pattern in major depression. Biol Psychiatry 2015;77:1050–60.
Fingelkurts AA, Fingelkurts AA, Rytsälä H, Suominen K, Isometsä E, Kähkönen S. Impaired functional connectivity at EEG alpha and theta frequency bands in major depression. Hum Brain Mapp 2007;28:247–61.
Gao S, Calhoun VD, Sui J. Machine learning in major depression: From classification to treatment outcome prediction. CNS Neurosci Ther 2018;24:1037–52.
Gong Q, He Y. Depression, neuroimaging and connectomics: A selective overview. Biol Psychiatry 2015;77:223–35.
He B, Astolfi L, Valdes-Sosa PA, Marinazzo D, Palva SO, Benar CG, et al. Electrophysiological brain connectivity: theory and implementation. IEEE Trans Biomed Eng 2019;66:2115–37.
He Y, Chen ZJ, Evans AC. Small-world anatomical networks in the human brain revealed by cortical thickness from MRI. Cereb Cortex 2007;17:2407–19.
Hillebrand A, Barnes GR, Bosboom JL, Berendse HW, Stam CJ. Frequency-dependent functional connectivity within resting-state networks: An atlas-based MEG beamformer solution. Neuroimage 2012;59:3909–21.
Hillebrand A, Tewarie P, Van Dellen E, Yu M, Carbo EWS, Douw L, et al. Direction of information flow in large-scale resting-state networks is frequency-dependent. Proc Natl Acad Sci U S A 2016;113:3867–72.
Jäncke L, Alahmadi N. Detection of independent functional networks during music listening using electroencephalogram and sLORETA-ICA. Neuroreport 2016;27:455–61.
Kaiser RH, Andrews-Hanna JR, Wager TD, Pizzagalli DA. Large-scale network dysfunction in major depressive disorder. JAMA Psychiatry 2015;72:603–11.
Kay BP, Meng X, DiFrancesco MW, Holland SK, Szaflarski JP. Moderating effects of music on resting state networks. Brain Res 2012;1447:53–64.
Knott V, Mahoney C, Kennedy S, Evans K. EEG power, frequency, asymmetry and coherence in male depression. Psychiatry Res - Neuroimaging 2001;106:123–40.
Koskinen M, Viinikanoja J, Kurimo M, Klami A, Kaski S, Hari R. Identifying fragments of natural speech from the listener's MEG signals. Hum Brain Mapp 2013;34:1477–89.
Kwon JS, Youn T, Jung HY. Right hemisphere abnormalities in major depression: Quantitative electroencephalographic findings before and after treatment. J Affect Disord 1996;40:169–73.
Leuchter AF, Cook IA, Hunter AM, Cai C, Horvath S. Resting-state quantitative electroencephalography reveals increased neurophysiologic connectivity in depression. PLoS One 2012;7:e32508.
Li BJ, Friston K, Mody M, Wang HN, Lu HB, Hu DW. A brain network model for depression: From symptom understanding to disease intervention. CNS Neurosci Ther 2018;24:1004–19.
Liao X, Vasilakos AV, He Y. Small-world human brain networks: Perspectives and challenges. Neurosci Biobehav Rev 2017;77:286–300.
Liuzzi L, Quinn AJ, O'Neill GC, Woolrich MW, Brookes MJ, Hillebrand A, et al. How sensitive are conventional MEG functional connectivity metrics with sliding windows to detect genuine fluctuations in dynamic functional connectivity?. Front Neurosci 2019;13:797.
Maratos AS, Gold C, Wang X, Crawford MJ. Music therapy for depression. Cochrane Database Syst Rev 2008;1:CD004517.
Markov NT, Misery P, Falchier A, Lamy C, Vezoli J, Quilodran R, et al. Weight consistency specifies regularities of macaque cortical networks. Cereb Cortex 2011;21:1254–72.
Michael AJ, Krishnaswamy S, Mohamed J. An open label study of the use of EEG biofeedback using beta training to reduce anxiety for patients with cardiac events. Neuropsychiatr Dis Treat 2005;1:357–63.
Mikutta C, Altorfer A, Strik W, Koenig T. Emotions, arousal, and frontal alpha rhythm asymmetry during beethoven's 5th symphony. Brain Topogr 2012;25:423–30.
Mumtaz W, Malik AS, Yasin MAM, Xia L. Review on EEG and ERP predictive biomarkers for major depressive disorder. Biomed Signal Process Control 2015;22:85–98.
Mumtaz W, Xia L, Ali SSA, Yasin MAM, Hussain M, Malik AS. Electroencephalogram (EEG)-based computer-aided technique to diagnose major depressive disorder (MDD). Biomed Signal Process Control 2017;31:108–15.
Nugent AC, Farmer C, Evans JW, Snider SL, Banerjee D, Zarate CA. Multimodal imaging reveals a complex pattern of dysfunction in corticolimbic pathways in major depressive disorder. Hum Brain Mapp 2019;40:3940–50.
O'Neill GC, Tewarie P, Vidaurre D, Liuzzi L, Woolrich MW, Brookes MJ. Dynamics of large-scale electrophysiological networks: A technical review. Neuroimage 2018;180:559–76.
Ohnishi T. Functional anatomy of musical perception in musicians. Cereb Cortex 2001;11:754–60.
Olbrich S, Tränkner A, Chittka T, Hegerl U, Schönknecht P. Functional connectivity in major depression: Increased phase synchronization between frontal cortical EEG-source estimates. Psychiatry Res – Neuroimaging 2014;222:91–9.
Palva S, Palva JM. Discovering oscillatory interaction networks with M/EEG: Challenges and breakthroughs. Trends Cogn Sci 2012;16:219–30.
Park H-J, Friston K. Structural and functional brain networks: from connections to cognition. Science 2013;342:1238411.
Punkanen M, Eerola T, Erkkilä J. Biased emotional recognition in depression: Perception of emotions in music by depressed patients. J Affect Disord 2011;130:118–26.
Ramirez R, Palencia-Lefler M, Giraldo S, Vamvakousis Z. Musical neurofeedback for treating depression in elderly people. Front Neurosci 2015;9:354.
Ren Y, Cong F, Ristaniemi T, Wang Y, Li X, Zhang R. Transient seizure onset network for localization of epileptogenic zone: effective connectivity and graph theory-based analyses of ECoG data in temporal lobe epilepsy. J Neurol 2019;266:844–59.
Rubinov M, Sporns O. Complex network measures of brain connectivity: Uses and interpretations. Neuroimage 2010;52:1059–69.
Ruiz-Gómez SJ, Hornero R, Poza J, Maturana-Candelas A, Pinto N, Gómez C. Computational modeling of the effects of EEG volume conduction on functional connectivity metrics. Application to Alzheimer's disease continuum. J Neural Eng 2019;16:066019.
Ruiz MH, Koelsch S, Bhattacharya J. Decrease in early right alpha band phase synchronization and late gamma band oscillations in processing syntax in music. Hum Brain Mapp 2009;30:1207–25.
Sakai K, Yamada K. Machine learning studies on major brain diseases: 5-year trends of 2014–2018. Jpn J Radiol 2019;37:34–72.
Schoffelen JM, Gross J. Source connectivity analysis with MEG and EEG. Hum Brain Mapp 2009;30:1857–65.
Singh MK, Kesler SR, Hadi Hosseini SM, Kelley RG, Amatya D, Hamilton JP, et al. Anomalous gray matter structural networks in major depressive disorder. Biol Psychiatry 2013;74:777–85.
Sporns O. Graph theory methods: applications in brain networks. Dialogues Clin Neurosci 2018;20:111–21.
Stam CJ, Nolte G, Daffertshofer A. Phase lag index: Assessment of functional connectivity from multi channel EEG and MEG with diminished bias from common sources. Hum Brain Mapp 2007;28:1178–93.
Toiviainen P, Alluri V, Brattico E, Wallentin M, Vuust P. Capturing the musical brain with Lasso: Dynamic decoding of musical features from fMRI data. Neuroimage 2014;88:170–80.
Uytdenhoef P, Portelange P, Jacquy J, Charles G, Linkowski P, Mendlewicz J. Regional cerebral blood flow and lateralized hemispheric dysfunction in depression. Br J Psychiatry 1983;143:128–32.
Van Den Broek SP, Reinders F, Donderwinkel M, Peters MJ. Volume conduction effects in EEG and MEG. Electroencephalogr Clin Neurophysiol 1998;106:522–34.
Veer IM, Beckmann C, Van Tol M-J, Ferrarini L, Milles J, Veltman D, et al. Whole brain resting-state analysis reveals decreased functional connectivity in major depression. Front Syst Neurosci 2010;4:41.
Vinck M, Oostenveld R, Van Wingerden M, Battaglia F, Pennartz CMA. An improved index of phase-synchronization for electrophysiological data in the presence of volume-conduction, noise and sample-size bias. Neuroimage 2011;55:1548–65.
Wang X, Liu W, Toiviainen P, Ristaniemi T, Cong F. Group analysis of ongoing EEG data based on fast double-coupled nonnegative tensor decomposition. J Neurosci Methods 2020;330:108502.
Wang X, Ren Y, Zhang W. Depression disorder classification of fMRI data using sparse low-rank functional brain network and graph-based features. Comput Math Methods Med 2017;2017:1–11.
Watanabe T, Yagishita S, Kikyo H. Memory of music: Roles of right hippocampus and left inferior frontal gyrus. Neuroimage 2008;39:483–91.
Wheeler RE, Davidson RJ, Tomarken AJ. Frontal brain asymmetry and emotional reactivity: A biological substrate of affective style. Psychophysiology 1993;30:82–9.
Whitton AE, Deccy S, Ironside ML, Kumar P, Beltzer M, Pizzagalli DA. Electroencephalography source functional connectivity reveals abnormal high-frequency communication among large-scale functional networks in depression. Biol Psychiatry Cogn Neurosci Neuroimaging 2018;3:50–8.
Womelsdorf T, Schoffelen JM, Oostenveld R, Singer W, Desimone R, Engel AK, et al. Modulation of neuronal interactions through neuronal synchronization. Science 2007;316:1609–12.
Wu D, Yuan Y, Bai F, You J, Li L, Zhang Z. Abnormal functional connectivity of the default mode network in remitted late-onset depression. J Affect Disord 2013;147:277–87.

Wu J, Zhang J, Liu C, Liu D, Ding X, Zhou C. Graph theoretical analysis of EEG functional connectivity during music perception. Brain Res 2012;1483:71–81.
Xia MR, Si TM, He Y. Imaging connectomics in depression. CNS Neurosci Ther 2018;24:991.
Yan R, Zhang C, Spruyt K, Wei L, Wang Z, Tian L, et al. Multi-modality of polysomnography signals' fusion for automatic sleep scoring. Biomed Signal Process Control 2019;49:14–23.
Ye M, Yang T, Qing P, Lei X, Qiu J, Liu G. Changes of functional brain networks in major depressive disorder: A graph theoretical analysis of resting-state fMRI. PLoS One 2015;10:e0133775.
Zalesky A, Fornito A, Bullmore ET. Network-based statistic: Identifying differences in brain networks. Neuroimage 2010;53:1197–207.
Zhu X, Wang X, Xiao J, Liao J, Zhong M, Wang W, et al. Evidence of a dissociation pattern in resting-state default mode network connectivity in first-episode, treatment-naive major depression patients. Biol Psychiatry 2012;71:611–7.

PII

IDENTIFYING OSCILLATORY HYPERCONNECTIVITY AND HYPOCONNECTIVITY NETWORKS IN MAJOR DEPRESSION USING COUPLED TENSOR DECOMPOSITION

by

Wenya Liu, Xiulin Wang, Jing Xu, Yi Chang, Timo Hämäläinen and Fengyu Cong 2021

IEEE Transactions on Neural Systems & Rehabilitation Engineering, 29, 1895-1904, https://doi.org/10.1109/TNSRE.2021.3111564

Identifying Oscillatory Hyperconnectivity and Hypoconnectivity Networks in Major Depression Using Coupled Tensor Decomposition

Wenya Liu, Xiulin Wang, *Student Member, IEEE*, Jing Xu, Yi Chang, Timo Hämäläinen, *Senior Member, IEEE*, and Fengyu Cong, *Senior Member, IEEE*

***Abstract*— Previous researches demonstrate that major depression disorder (MDD) is associated with widespread network dysconnectivity, and the dynamics of functional connectivity networks are important to delineate the neural mechanisms of MDD. Neural oscillations exert a key role in coordinating the activity of remote brain regions, and various assemblies of oscillations can modulate different networks to support different cognitive tasks. Studies have demonstrated that the dysconnectivity of electroencephalography (EEG) oscillatory networks is related with MDD. In this study, we investigated the oscillatory hyperconnectivity and hypoconnectivity networks in MDD under a naturalistic and continuous stimuli condition of music listening. With the assumption that the healthy group and the MDD group share similar brain topology from the same stimuli and also retain individual brain topology for group differences, we applied the coupled nonnegative tensor decomposition algorithm on two adjacency tensors with the dimension of time × frequency × connectivity × subject, and imposed double-coupled constraints on spatial and spectral modes. The music-induced oscillatory networks were identified by a correlation analysis approach based on the permutation test between extracted temporal factors and musical features. We obtained three hyperconnectivity networks from the individual features of MDD and three hypoconnectivity networks from common features. The results demonstrated that the dysfunction of oscillatory networks could affect the involvement in music perception for MDD patients. Those oscillatory dysconnectivity networks may provide promising references to reveal the pathoconnectomics of MDD and potential biomarkers for the diagnosis of MDD.**

***Index Terms*— Dynamic functional connectivity, coupled tensor decomposition, major depression disorder, naturalistic music stimuli, oscillatory networks.**

Manuscript received January 11, 2021; revised May 19, 2021 and August 5, 2021; accepted September 7, 2021. Date of publication September 9, 2021; date of current version September 17, 2021. This work was supported in part by the National Natural Science Foundation of China under Grant 91748105, in part by the National Foundation in China under Grant JCKY2019110B009 and Grant 2020-JCJQ-JJ-252, in part by the Fundamental Research Funds for the Central Universities in Dalian University of Technology, China, under Grant DUT2019 and Grant DUT20LAB303, and in part by the Scholarships from China Scholarship Council under Grant 201706060263 and Grant 201706060262. *(Corresponding author: Fengyu Cong.)*

This work involved human subjects or animals in its research. Approval of all ethical and experimental procedures and protocols was granted by the First Affiliated Hospital of Dalian Medical University.

Wenya Liu is with the Faculty of Electronic Information and Electrical Engineering, School of Biomedical Engineering, Dalian University of Technology, Dalian 116024, China, and also with the Faculty of Information Technology, University of Jyväskylä, 40014 Jyväskylä, Finland (e-mail: wenyaliu0912@foxmail.com).

Xiulin Wang is with the Department of Radiology, Affiliated Zhongshan Hospital of Dalian University, Dalian 116001, China, and also with the Faculty of Electronic Information and Electrical Engineering, School of Biomedical Engineering, Dalian University of Technology, Dalian 116024, China (e-mail: xiulin.wang@foxmail.com).

Jing Xu and Yi Chang are with the Department of Neurology and Psychiatry, First Affiliated Hospital, Dalian Medical University, Dalian 116011, China (e-mail: xujing.doc@aliyun.com; changee99@gmail.com).

Timo Hämäläinen is with the Faculty of Information Technology, University of Jyväskylä, 40014 Jyväskylä, Finland (e-mail: timo.t.hamalainen@jyu.fi).

Fengyu Cong is with the Faculty of Electronic Information and Electrical Engineering, School of Biomedical Engineering, Dalian University of Technology, Dalian 116024, China, also with the Faculty of Information Technology, University of Jyväskylä, 40014 Jyväskylä, Finland, also with the Faculty of Electronic Information and Electrical Engineering, School of Artificial Intelligence, Dalian University of Technology, Dalian 116024, China, and also with the Key Laboratory of Integrated Circuit and Biomedical Electronic System, Dalian University of Technology, Dalian, Liaoning 116024, China (e-mail: cong@dlut.edu.cn).

Digital Object Identifier 10.1109/TNSRE.2021.3111564

I. Introduction

MAJOR depression disorder (MDD) is a globally common psychiatric disorder characterized by deficits of affective and cognitive functions [1]–[3]. It is almost a consensus to researchers that MDD is accompanied by abnormal functional connectivity (FC) between some brain regions, like cortical regions in the default mode network (DMN), rather than the aberrant response of individual brain regions [3]–[6]. Music therapy is associated with improvements in mood, which has made it an attractive tool for MDD treatment [7]. Previous studies have suggested that the oscillatory asymmetry and dysconnectivity could be the potential biomarkers of MDD during music perception [8]–[10].

An increasing amount of researches have demonstrated that FC presents the potential of temporal variability across different time-scales (from milliseconds to minutes) to support continuous cognitive tasks. This is termed as dynamic functional connectivity (dFC), and it represents the processes by which networks and subnetworks coalesce and dissolve over time, or cross-talk between networks [11]–[13]. Recently, researches have reported abnormal dFC of specific brain regions and

neural networks in MDD using resting-state functional Magnetic Resonance Imaging (RS-fMRI) [3], [5], [13], [14]. For example, Demirtas *et al.* found a decreased variability of FC in the connections between the DMN and the frontoparietal network [5]. Kaiser *et al.* showed that MDD patients presented decreased dFC between medial prefrontal cortical (MPFC) regions and regions of parahippocampal gyrus within the DMN, but increased dFC between MPFC regions and regions of insula. They showed that MDD was related to abnormal patterns of fluctuating communication among brain systems involved in regulating attention and self-referential thinking [13]. The decreased dFC variability was reported between anterior DMN and right central executive network (CEN) in MDD, which indicated a decreased information processing and communication ability [14]. Existing researches about dFC in MDD mostly focus on resting-state conditions. However, little is known about the abnormalities of dFC during music listening conditions.

Benefiting from the high temporal resolution, electroencephalography (EEG) can record electrical brain activity dynamics at a millisecond scale with rich frequency contents. The oscillation acts as a bridge to connect different brain regions with resonant communication, which can regulate changes of neuronal networks and cause qualitative transitions between modes of information processing [15]–[17]. Impaired coordination of brain activity associated with abnormal electrophysiological oscillations contributes to the generation of psychaitric disorders [18]. Numerous studies have investigated EEG oscillatory FC of MDD in resting-state, and dysconnectivity networks are mostly notable in theta, alpha and beta oscillations [16], [19], [20]. However, most previous studies filter EEG signals into a range of frequency bands (e.g., 8-13 Hz for the alpha band), and ignore the exhaustive spectral dynamics in FC [19], [20]. Music perception is a complex cognitive task, which is characterized with dynamics of frequency-specific brain networks for musical features processing [21]–[25]. To the best of our knowledge, the oscillatory dFC in MDD during music perception has not been well investigated yet.

Considering the temporal dynamics and spectral modulations of spatial couplings (e.g., functional connectivity) for multiple participants in a cognitive task, a multi-way dataset structure is naturally formed. This multi-dimensional nature points to the adoption of tensor decomposition models instead of matrix decomposition models, which normally fold some dimensions and ignore the hidden interactions across different modes [24], [26]–[29]. Canonical Polyadic (CP) decomposition is derived in terms of the sum of multiple rank-one tensors, and each rank-one tensor represents the covariation of the corresponding components from each mode [30], [31]. The CP decomposition is well implemented into the extraction of multi-mode EEG features from the multiway dataset (e.g., channel $\times$ frequency $\times$ time $\times$ subject) [31]–[34]. Recently, Zhu *et al.* applied CP decomposition to explore the task-related dFC characterized by spatio-temporal-spectral modes of covariation from the adjacency tensor (connectivity $\times$ time-subject $\times$ frequency) [23], [35]. However, those applications only focus on the decomposition of one single tensor, which are based on the assumption that the underlying spatio-spectral features are consistent among subjects or groups [25], [29]. Coupled tensor decomposition (CTD), the extension of tensor decomposition to multiple block tensors, enables the simultaneous extraction of common features shared among tensors and individual features specified for each tensor. For biomedical data, the coupled matrix, matrix-tensor or tensor decomposition (also known as linked component analysis) are mostly used for data fusion [36]–[38]. However, to the best of our knowledge, no studies have used CTD to investigate the pathologic networks of MDD or other psychiatric disorders.

In our study, we applied a low-rank double-coupled nonnegative tensor decomposition (DC-NTD) model to explore the temporal and spectral dynamics of spatial couplings in MDD during music listening. The proposed analysis pipeline is totally data-driven. We analyzed the whole-brain FC to avoid prior knowledge about regions of interest, and we investigated the exhaustive assemblies of oscillations to avoid the selection of the frequency range. Figure 1 shows the diagram of the analysis pipeline of this study.

In this paper, scalars, vectors, matrices and tensors are denoted by lowercase, boldface lowercase, boldface uppercase and boldface script letters, respectively, e.g., x, $\boldsymbol{x}$, $\boldsymbol{X}$, $\boldsymbol{\mathcal{X}}$. Indices range from 1 to their capital version, e.g., $i = 1, \cdots, I$.

II. Materials and Methods

A. Simulated Data

To validate the feasibility of the proposed method, we firstly applied it on the simulated data. Two tensors with the size of 500 $\times$ 59 $\times$ 2278, representing time $\times$ frequency $\times$ connectivity, were created as follows:

$$\begin{aligned}\boldsymbol{\mathcal{X}}_1 &= \tilde{\boldsymbol{\mathcal{X}}}_1 + \boldsymbol{\mathcal{N}}_1 \\ &= t_1 \circ f_1 \circ c_1 + t_2 \circ f_2 \circ c_2 + t_3 \circ f_3 \circ c_3 + \boldsymbol{\mathcal{N}}_1, \quad (1)\\ \boldsymbol{\mathcal{X}}_2 &= \tilde{\boldsymbol{\mathcal{X}}}_2 + \boldsymbol{\mathcal{N}}_2 \\ &= t_4 \circ f_1 \circ c_1 + t_5 \circ f_2 \circ c_2 + t_6 \circ f_4 \circ c_4 + \boldsymbol{\mathcal{N}}_2, \quad (2)\end{aligned}$$

where $\tilde{\boldsymbol{\mathcal{X}}}_m, m = 1, 2$ represented the ground truth networks, and $\boldsymbol{\mathcal{N}}_n, n = 1, 2$ were the nonnegative noise created by the absolute values of white noise with the size of 500 $\times$ 59 $\times$ 2278. In the time domain, each temporal component $t_i, i = 1, 2, \cdots, 6$ was simulated by the absolute value of white noise to ensure the nonnegativity of the synthetic tensor $\boldsymbol{\mathcal{X}}$, and no coupled temporal component existed between two tensors. In the frequency domain, four spectral components $f_j, j = 1, 2, \cdots, 4$ were constructed by Hanning windows and white noise with bandwidth centered at 5 Hz, 10 Hz, 15 Hz and 20 Hz, and two spectral components were set to be coupled between two tensors. In the adjacency domain, four adjacency components $c_k, k = 1, 2, \cdots, 4$, representing auditory network (AUD), visual network (VIS), salience network (SAN), and dorsal attentional network (DAN), were constructed with the Desikan-Killiany anatomical atlas according to Kabbara's work [39], and two adjacency components were coupled between two tensors. The synthetic data were shown in Figure 2(a).

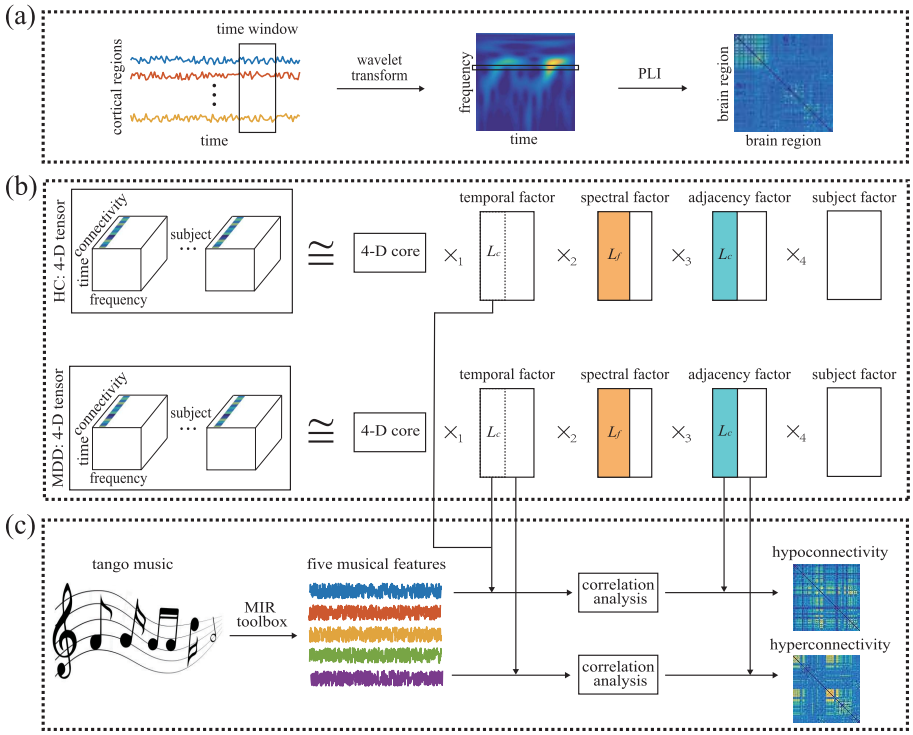

Fig. 1. Diagram of the analysis pipeline. (a) Adjcency matrix construction in each time window and each frequency bin. After source reconstruction, the cortical signals were segmented by overlapping time windows, and wavelet transform was applied for each time course within each time window. Phase lag index was used to obtain the adjacency matrix for each time window and each frequency bin. (b) Adjacency tensor construction and decomposition. A 4-D adjacency tensor was constructed for each group with the dimension of time × frequency × connectivity × subject, and coupled tensor decomposition was implemented with coupled constraints in spectral and adjacency modes. The 4-D core tensor is superdiagonal with values of 1. (c) The identification of hyperconnectivity and hypoconnectivity networks by music modulation. Five musical features were extracted with MIR toolbox from tango music, and correlation analysis was conducted between musical features and decomposed temporal factors to identify music-induced brain networks. Hyperconnectivity and hypoconnectivity networks were summarized from the results of music modulation.

B. EEG Data Description

1) Participants: Twenty MDD patients and nineteen healthy controls (HC) participated in this experiment. All the patients were from the First Affiliated Hospital of Dalian Medical University in China. This study has been approved by the ethics committee of the hospital, and all participants signed the informed consent before their enrollment. None of the participants has reported hearing loss and formal training in music. All the MDD patients were primarily diagnosed by a clinical expert and tested according to Hamilton Rating Scale for Depression (HRSD), Hamilton Anxiety Rating Scale (HAMA) and Mini-Mental State Examination (MMSE). The means and standard deviations (SD) of age, education, clinical measures, duration of illness and gender for both groups were listed in Table I.

2) EEG Data: During the experiment, participants were told to sit comfortably in the chair and listen to a piece of music. A 512-second musical piece of modern tango *Adios Nonino* by Astor Piazzolla was used as the stimulus due to its rich musical structure and high range of variation in musical features such as dynamics, timbre, tonality and rhythm [21], [40]. The EEG data were recorded by the Neuroscan Quik-cap device with 64 electrodes arranged according to the international 10-20 system at the sampling frequency of 1000 Hz. The electrodes placed at the left and right earlobes were used as the references.

TABLE I
MEANS AND STANDARD DEVIATIONS OF AGE, EDUCATION, CLINICAL MEASURES, DURATION OF ILLNESS AND GENDER FOR THE HC GROUP AND THE MDD GROUP

	HC group		MDD group		p-value
	Mean	SD	Mean	SD	
Age	38.4	11.8 (24-65)	42.9	11.0(23-58)	>0.05*
Education	13.6	3.8(6-20)	12.8	3.4(6-16)	>0.05*
HRSD	2.4	1.3(0-4)	23.3	3.6(16-28)	<0.01*
HAMA	2.4	1.3(0-5)	19.2	3.0(15-25)	<0.01*
MMSE	28.2	0.9(27-30)	28.1	1.1(26-30)	>0.05*
Duration	0	0	12.8	8.5(2-36)	-
Gender	14 females, 5 males		14 females, 6 males		>0.05**

Abbreviations: HC, healthy controls; MDD, major depression disorder; SD, standard deviations; HRSD, Hamilton Rating Scale for Depression; HAMA, Hamilton Anxiety Rating Scale; MMSE, Mini-Mental State Examination. The measure unit of duration is month, and the measure unit of age and education is year. *The p-value is calculated by t-test. **The p-value is calculated by chi-squared test.

The data were visually checked to remove obvious artifacts from head movement and down-sampled to $fs = 256$ Hz for further processing. Then 50 Hz notch filter and high-pass and low-pass filters with 1 Hz and 30 Hz cutoff were applied. We interpolated the bad intervals of one channel by

the mean values of their spherical adjacent channels. Eye movements artifacts were rejected by independent component analysis (ICA).

3) Musical Features: In this study, two tonal and three rhythmic features were extracted by a frame-by-frame analysis approach using MIR toolbox [41]. The duration of each frame was 3 seconds, and the overlap between two adjacency frames was 2 seconds. Therefore, we got 510 samples for the time courses of each musical feature at a sampling frequency of 1 Hz. In this study, we only used the first $T = 500$ samples of each musical feature due to the length of recorded EEG data. Tonal features include Mode and Key Clarity, which represent the strength of major of minor mode and the measure of tonal clarity, respectively. Rhythmic features include Fluctuation Centroid, Fluctuation Entropy, and Pulse Clarity. Fluctuation centroid is the geometric mean of the fluctuation spectrum representing the global repartition of rhythm periodicities within the range of 0–10 Hz. Fluctuation Entropy is the Shannon entropy of the fluctuation spectrum representing the global repartition of rhythm periodicities. Pulse Clarity is an estimate of clarity of the pulse.

C. Source Reconstruction

Source reconstruction procedure was performed with open-source Brainstorm software [42]. For forward modeling, we used the symmetric boundary element method (BEM) to compute the volume-conductor model with the MNI-ICBM152 template corresponding to a grid of 15000 cortical sources. For source modeling, minimum norm estimate (MNE) was applied with a measure of the current density map and constrained dipole orientations (normal to cortex). Then, the Desikan-Killiany anatomical atlas was used to parcellate the cortical surface into $C = 68$ regions, and the principal component analysis (PCA) method was performed to construct the time course for each brain region.

D. Dynamic Functional Connectivity

Many studies have reported that the communication of brain regions or neural populations depends on phase interactions for electrophysiological neuroimaging techniques, like EEG [43]. To avoid source leakage, the pairwise synchronization was estimated by PLI to map the whole-brain FC [44]. In this study, to assess the dFC across both time and frequency, we segmented the source-space data into $W = 500$ windows by the sliding window technique with a window length of 3 s and an overlap of 2 s according to the extraction framework of musical features. Then, we computed the time-frequency (TF) decomposition within each time window by the continuous wavelet transform with Morlet wavelets as basis function . We set the frequency bins as 0.5 Hz, and obtained $F = 59$ samples in frequency domain in the range of 1-30 Hz.

For the time window w, we can get the complex TF representation $P_w \in \mathbb{R}^{T_w \times F}$ from wavelet transform, where $T_w = 3fs$, and the time and frequency-dependent phase at time t_w and frequency f can be obtained by

$$\varphi(t_w, f) = \arctan \frac{imag(P_w(t_w, f))}{real(P_w(t_w, f))}, \tag{3}$$

where $imag()$ and $real()$ represent the imaginary part and the real part of a complex value, respectively. For brain regions i and j, PLI can be computed as

$$PLI_{i,j}(w, f) = \frac{1}{T_w} \left| \sum_{t_w=1}^{T_w} sign(\triangle\varphi_{i,j}(t_w, f)) \right|, \tag{4}$$

where $\triangle\varphi_{i,j}(t_w, f)) = \varphi_i(t_w, f) - \varphi_j(t_w, f)$ is the phase difference of brain regions i and j at time t_w and frequency f in time window w. Therefore, for each time window and each frequency point, we can form an adjacency matrix $\boldsymbol{A} \in \mathbb{R}^{C \times C}$, where C means the number of brain regions. Because of the symmetry of FC matrix, we took the upper triangle of $\boldsymbol{A}$ and vectorized it to $\boldsymbol{a} \in \mathbb{R}^{N \times 1}$, where $N = C(C-1)/2 = 2278$ represents the number of unique connections. Then, we can construct two adjacency tensors with the dimension of time $\times$ frequency $\times$ connectivity $\times$ subject, $\boldsymbol{\mathcal{X}}^{\mathrm{HC}} \in \mathbb{R}^{W \times F \times N \times S_{\mathrm{HC}}}$ ($500 \times 59 \times 2278 \times 19$) for the HC group and $\boldsymbol{\mathcal{X}}^{\mathrm{MDD}} \in \mathbb{R}^{W \times F \times N \times S_{\mathrm{MDD}}}$ ($500 \times 59 \times 2278 \times 20$) for the MDD group, where $S_{\mathrm{HC}} = 19$ and $S_{\mathrm{MDD}} = 20$ mean the number of subjects in the HC group and the MDD group, respectively.

E. The Application of Low-Rank Coupled Tensor Decomposition

Considering the high computation load, the nonnegativity of the tensors (constrained to [0,1] due to PLI index) and high correlations in spatial and spectral modes, we applied a low-rank DC-NTD model which was more flexible to add desired constraints.

1) Low-Rank Coupled Tensor Decomposition: With the constructed tensors $\boldsymbol{\mathcal{X}}^{\mathrm{HC}} \in \mathbb{R}^{W \times F \times N \times S_{\mathrm{HC}}}$ and $\boldsymbol{\mathcal{X}}^{\mathrm{MDD}} \in \mathbb{R}^{W \times F \times N \times S_{\mathrm{MDD}}}$, the corresponding CP decomposition can be represented as $\boldsymbol{\mathcal{X}}^{\mathrm{HC}} \simeq \sum_{r=1}^{R_{\mathrm{HC}}} \boldsymbol{u}_r^{(1)} \circ \boldsymbol{u}_r^{(2)} \circ \boldsymbol{u}_r^{(3)} \circ \boldsymbol{u}_r^{(4)} = [\![\boldsymbol{U}^{(1)}, \boldsymbol{U}^{(2)}, \boldsymbol{U}^{(3)}, \boldsymbol{U}^{(4)}]\!]$ and $\boldsymbol{\mathcal{X}}^{\mathrm{MDD}} \simeq \sum_{r=1}^{R_{\mathrm{MDD}}} \boldsymbol{v}_r^{(1)} \circ \boldsymbol{v}_r^{(2)} \circ \boldsymbol{v}_r^{(3)} \circ \boldsymbol{v}_r^{(4)} = [\![\boldsymbol{V}^{(1)}, \boldsymbol{V}^{(2)}, \boldsymbol{V}^{(3)}, \boldsymbol{V}^{(4)}]\!]$, where $\circ$ denotes the vector outer product. $\boldsymbol{u}_r^{(n)}$ and $\boldsymbol{v}_r^{(n)}$ denote the rth component of factor matrices $\boldsymbol{U}^{(n)}$ and $\boldsymbol{V}^{(n)}$, $n = 1, 2, 3, 4$, in the modes of time, frequency, connectivity and subject for two groups. R_{HC} and R_{MDD} are the ranks of $\boldsymbol{\mathcal{X}}^{\mathrm{HC}}$ and $\boldsymbol{\mathcal{X}}^{\mathrm{MDD}}$, respectively. Considering the nonnegativity of constructed tensors and the coupled constraints in spectral and adjacency modes, we formulate it as a double-coupled nonnegative tensor decomposition (DC-NTD) model, where $\boldsymbol{\mathcal{X}}^{\mathrm{HC}}$ and $\boldsymbol{\mathcal{X}}^{\mathrm{MDD}}$ can be jointly analyzed by minimizing the following objective function:

$$\begin{aligned} &\mathcal{J}(\boldsymbol{u}_r^{(n)}, \boldsymbol{v}_r^{(n)}) \\ &= \|\boldsymbol{\mathcal{X}}^{\mathrm{HC}} - \sum_{r=1}^{R_{\mathrm{HC}}} \boldsymbol{u}_r^{(1)} \circ \boldsymbol{u}_r^{(2)} \circ \boldsymbol{u}_r^{(3)} \circ \boldsymbol{u}_r^{(4)}\|_F^2 \\ &\quad + \|\boldsymbol{\mathcal{X}}^{\mathrm{MDD}} - \sum_{r=1}^{R_{\mathrm{MDD}}} \boldsymbol{v}_r^{(1)} \circ \boldsymbol{v}_r^{(2)} \circ \boldsymbol{v}_r^{(3)} \circ \boldsymbol{v}_r^{(4)}\|_F^2 \\ &\quad \text{s.t. } \boldsymbol{u}_r^{(2)} = \boldsymbol{v}_r^{(2)} (r \le L_f),\ \boldsymbol{u}_r^{(3)} = \boldsymbol{v}_r^{(3)} (r \le L_c). \end{aligned} \tag{5}$$

$\|\cdot\|_F$ denotes the Frobenius norm. L_f and L_c denote the number of components coupled in spectral and adjacency modes, and $L_{f,c} \le \min(R_{\mathrm{HC}}, R_{\mathrm{MDD}})$. The fast hierarchical

alternative least squares (FHALS), an accelerated version of the hierarchical alternative least squares (HALS) algorithm, has been effectively applied to a number of (coupled) tensor decomposition problems [25], [45], [46]. In this study, we apply the FHALS algorithm to optimize the DC-NTD problem in (5), and introduce the low-rank approximation to reduce computational complexity [47], [48].

Through the FHALS algorithm, the minimization problem in (5) can be converted into $\max(R_{\mathrm{HC}}, R_{\mathrm{MDD}})$ rank-1 subproblems, which can be solved sequentially and iteratively. We take the rth subproblem as an example:

$$\begin{aligned}\min \mathcal{J}_r = &\|\mathcal{Y}_r^{\mathrm{HC}} - \boldsymbol{u}_r^{(1)} \circ \boldsymbol{u}_r^{(2)} \circ \boldsymbol{u}_r^{(3)} \circ \boldsymbol{u}_r^{(4)}\|_F^2 \\ &+\|\mathcal{Y}_r^{\mathrm{MDD}} - \boldsymbol{v}_r^{(1)} \circ \boldsymbol{v}_r^{(2)} \circ \boldsymbol{v}_r^{(3)} \circ \boldsymbol{v}_r^{(4)}\|_F^2, \quad (6)\end{aligned}$$

where $\mathcal{Y}_r^{\mathrm{HC}} \doteq \mathcal{X}^{\mathrm{HC}} - \sum_{k\neq r}^{R_{\mathrm{HC}}} \boldsymbol{u}_k^{(1)} \circ \boldsymbol{u}_k^{(2)} \circ \boldsymbol{u}_k^{(3)} \circ \boldsymbol{u}_k^{(4)}$ and $\mathcal{Y}_r^{\mathrm{MDD}} \doteq \mathcal{X}^{\mathrm{MDD}} - \sum_{k\neq r}^{R_{\mathrm{MDD}}} \boldsymbol{v}_k^{(1)} \circ \boldsymbol{v}_k^{(2)} \circ \boldsymbol{v}_k^{(3)} \circ \boldsymbol{v}_k^{(4)}$. When calculating one of the variables, we need to fix the other variables and let the corresponding derivative be zero. For example, to determine $\boldsymbol{u}_r^{(n)}$, we let $\partial \mathcal{J}_r / \partial \boldsymbol{u}_r^{(n)}$ be zero, and then we can obtain the following solution:

$$\boldsymbol{u}_r^{(n)} = \boldsymbol{Y}_{r,(n)}^{\mathrm{HC}} \left[\boldsymbol{u}_r\right]^{\odot -n} / \left[\boldsymbol{u}_r{}^T \boldsymbol{u}_r\right]^{\circledast -n}, \quad (7)$$

where $\boldsymbol{Y}_{r,(n)}^{\mathrm{HC}}$ is the mode-n matricization of $\mathcal{Y}_r^{\mathrm{HC}}$. $\odot$ and $\circledast$ denote the Khatri-Rao product and Hadamard (element-wise) product. $\left[\boldsymbol{u}_r\right]^{\odot -n} = \boldsymbol{u}_r^{(4)} \odot \cdots \odot \boldsymbol{u}_r^{(n+1)}) \odot \boldsymbol{u}_r^{(n-1)}) \odot \cdots \odot \boldsymbol{u}_r^{(1)}$ and $\left[\boldsymbol{u}_r{}^T \boldsymbol{u}_r\right]^{\circledast -n} = \left([\boldsymbol{u}_r]^{\odot -n}\right)^T [\boldsymbol{u}_r]^{\odot -n}$. Taking $\boldsymbol{Y}_{r,(n)}^{\mathrm{HC}} = \boldsymbol{X}_{(n)}^{\mathrm{HC}} - \boldsymbol{U}^{(n)}[\boldsymbol{U}^{\odot -n}]^T + \boldsymbol{u}_r^{(n)}[\boldsymbol{u}_r^{\odot -n}]^T$ into (7), we can get

$$\boldsymbol{u}_r^{(n)} = \boldsymbol{u}_r^{(n)} + \left[\boldsymbol{X}_{(n)}^{\mathrm{HC}} \boldsymbol{u}_r^{\odot -n} - \boldsymbol{U}^{(n)} \boldsymbol{\Gamma}_r^{(n)}\right] / \boldsymbol{\Gamma}_{(r,r)}^{(n)}, \quad (8)$$

where $\boldsymbol{X}_{(n)}^{\mathrm{HC}}$ is the mode-n matricization of $\mathcal{X}^{\mathrm{HC}}$ and $\boldsymbol{\Gamma}^{(n)} = \left[\boldsymbol{U}^T \boldsymbol{U}\right]^{\circledast -n}$. Suppose that the rank-$\tilde{R}_{\mathrm{HC}}$ approximation of $\mathcal{X}^{\mathrm{HC}}$ obtained by unconstrained tensor factorization is expressed as $[\![\tilde{\boldsymbol{U}}^{(1)}, \tilde{\boldsymbol{U}}^{(2)}, \tilde{\boldsymbol{U}}^{(3)}, \tilde{\boldsymbol{U}}^{(4)}]\!]$, $\tilde{R}_{\mathrm{HC}} \leq R_{\mathrm{HC}}$, thus the mode-$n$ unfolding of $\mathcal{X}^{\mathrm{HC}}$ can be written as $\boldsymbol{X}_{(n)}^{\mathrm{HC}} = \tilde{\boldsymbol{U}}^{(n)} \left[\tilde{\boldsymbol{U}}^{\odot -n}\right]^T$. Therefore, the learning rule of $\boldsymbol{u}_r^{(n)}$ can be reformulated as follows:

$$\boldsymbol{u}_r^{(n)} = \boldsymbol{u}_r^{(n)} + \left[\tilde{\boldsymbol{U}}^{(n)} \tilde{\boldsymbol{\Gamma}}_r^{(n)} - \boldsymbol{U}^{(n)} \boldsymbol{\Gamma}_r^{(n)}\right] / \boldsymbol{\Gamma}_{(r,r)}, \quad (9)$$

where $\tilde{\boldsymbol{\Gamma}}^{(n)} = [\tilde{\boldsymbol{U}}^T \boldsymbol{U}]^{\circledast -n}$. Analogously, we can obtain the learning rule of $\boldsymbol{v}_r^{(n)}$ as follows:

$$\boldsymbol{v}_r^{(n)} = \boldsymbol{v}_r^{(n)} + \left[\tilde{\boldsymbol{V}}^{(n)} \tilde{\boldsymbol{\Lambda}}_r^{(n)} - \boldsymbol{V}^{(n)} \boldsymbol{\Lambda}_r^{(n)}\right] / \boldsymbol{\Lambda}_{(r,r)}^{(n)}, \quad (10)$$

where $\boldsymbol{\Lambda}^{(n)} = \left[\boldsymbol{V}^T \boldsymbol{V}\right]^{\circledast -n}$ and $\tilde{\boldsymbol{\Lambda}}^{(n)} = [\tilde{\boldsymbol{V}}^T \boldsymbol{V}]^{\circledast -n}$. The rank-$\tilde{R}_{\mathrm{MDD}}$ approximation of $\mathcal{X}^{\mathrm{MDD}}$ is expressed as $[\![\tilde{\boldsymbol{V}}^{(1)}, \tilde{\boldsymbol{V}}^{(2)}, \tilde{\boldsymbol{V}}^{(3)}, \tilde{\boldsymbol{V}}^{(4)}]\!]$, $\tilde{R}_{\mathrm{MDD}} \leq R_{\mathrm{MDD}}$. Specially, if $r \leq L_f$, $\boldsymbol{u}_r^{(2)} = \boldsymbol{v}_r^{(2)}$ and if $r \leq L_c$, $\boldsymbol{u}_r^{(3)} = \boldsymbol{v}_r^{(3)}$, thus their solutions should be calculated as:

$$\begin{aligned}\boldsymbol{u}_r^{(2)} &= \boldsymbol{v}_r^{(2)} \\ &= \boldsymbol{u}_r^{(2)} + \left[\tilde{\boldsymbol{U}}^{(2)} \tilde{\boldsymbol{\Gamma}}_r^{(2)} - \boldsymbol{U}^{(2)} \boldsymbol{\Gamma}_r^{(2)} + \tilde{\boldsymbol{V}}^{(2)} \tilde{\boldsymbol{\Lambda}}_r^{(2)} - \boldsymbol{V}^{(2)} \boldsymbol{\Lambda}_r^{(2)}\right] \\ &\quad / \left[\boldsymbol{\Gamma}_{(r,r)}^{(2)} + \boldsymbol{\Lambda}_{(r,r)}^{(2)}\right], \quad (11)\end{aligned}$$

and

$$\begin{aligned}\boldsymbol{u}_r^{(3)} &= \boldsymbol{v}_r^{(3)} \\ &= \boldsymbol{u}_r^{(3)} + \left[\tilde{\boldsymbol{U}}^{(3)} \tilde{\boldsymbol{\Gamma}}_r^{(3)} - \boldsymbol{U}^{(3)} \boldsymbol{\Gamma}_r^{(3)} + \tilde{\boldsymbol{V}}^{(3)} \tilde{\boldsymbol{\Lambda}}_r^{(3)} - \boldsymbol{V}^{(3)} \boldsymbol{\Lambda}_r^{(3)}\right] \\ &\quad / \left[\boldsymbol{\Gamma}_{(r,r)}^{(3)} + \boldsymbol{\Lambda}_{(r,r)}^{(3)}\right], \quad (12)\end{aligned}$$

In order to obtain the nonnegative components, a simple "half-rectifying" nonlinear projection is applied. We update $\boldsymbol{u}_r^{(n)}$ and $\boldsymbol{v}_r^{(n)}$ successively in each subproblem, and the $\max(R_{\mathrm{HC}}, R_{\mathrm{MDD}})$ subproblems are optimized alternatively one after another until convergence. In this study, we adopt alternating least squares (ALS, [49]) algorithm to perform low-rank approximation. The FHALS-based DC-NTD algorithm is summarized in **Algorithm** 1.

Algorithm 1 DC-NTD-FHALS Algorithm

Input: $\mathcal{X}^{\mathrm{HC}}$, $\mathcal{X}^{\mathrm{MDD}}$, L_f, L_c, R_{HC}, R_{MDD}, $\tilde{R}_{\mathrm{HC}}$, $\tilde{R}_{\mathrm{MDD}}$
Initialization: $\boldsymbol{U}^{(n)}$, $\boldsymbol{V}^{(n)}$, $n = 1, 2, 3, 4$
Calculate $\tilde{\boldsymbol{U}}^{(n)}$, $\tilde{\boldsymbol{V}}^{(n)}$, $n = 1, 2, 3, 4$ via unconstrained ALS
while *unconvergence* **do**
  for $n = 1, 2, \cdots, 4$ **do**
    for $r = 1, 2, \cdots max(R_{HC}, R_{MDD})$ **do**
      Update $\boldsymbol{u}_r^{(n)}$, $\boldsymbol{u}_r^{(n)}$ via (9), (10), (11) and (12)
    end
  end
end
Output: $\boldsymbol{U}^{(n)}$, $\boldsymbol{V}^{(n)}$, $n = 1, 2, 3, 4$

2) Selection of Components: In this section, we will describe how to determine the number of totally extracted components R_{HC} and R_{MDD}, which refers to the hidden information in low-dimensional space for each block data, and the number of coupled components L_f and L_c, which reveal the common features between two-block data. For the selection of R_{HC} and R_{MDD}, we performed PCA on the matricization data $\mathcal{X}_{(3)} \in \mathbb{R}^{F \times WNS}$ unfolded along frequency mode for each block data, and kept the number of components with 95% explained variance. The selection of the number of coupled components is a key issue for the conduction of the DC-NTD-FHALS algorithm and the explanation of results, and it always becomes an open issue depending on practical applications. In this study, we performed the fourth-order CP tensor decomposition based on the FHALS algorithm on two-block data separately, and calculated the correlation maps of extracted components between two-block data in spectral and adjacency modes, respectively. According to the correlation maps, we will select the number of highly correlated (coupled) components. The detailed implication procedure will be described in the results section.

F. Identification of Music-Induced Hyperconnectivity and Hypoconnectivity Networks

After the conduction of the low-rank DC-NTD-FHALS algorithm, we need to identify the music-induced oscillatory

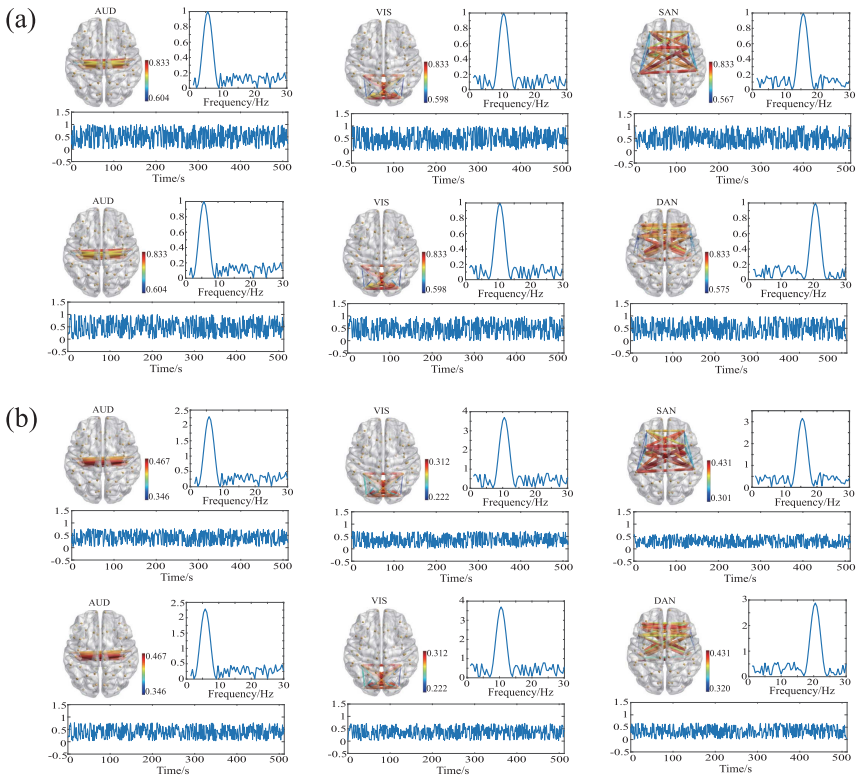

Fig. 2. Simulation illustration. (a) Three spatio-temporal-spectral patterns were simulated for two groups, and the first two patterns were identical in adjacency and spectral modes. (b) The reconstructed spatio-temporal-spectral patterns.

networks that are abnormal involved in the MDD group. We conducted a correlation analysis approach between temporal factors and five musical features with Pearson correlation based on the permutation test method. To ensure the statistical significance of the correlation and consider the problem of multiple comparison, the Monte Carlo method and permutation test were applied to compute a significant threshold of correlation for each musical feature [21]–[23], [25]. For the time course of each musical feature, we kept the real part and replaced the imaginary part with random uniformly distributed phases, and performed Pearson correlation with the time courses of the extracted temporal components. Then, we repeated this procedure 100000 times, and obtained the threshold for each musical feature at a significant level of $p_{corrected} < 0.05$.

The coupled spectral and adjacency components are common features between CON and MDD groups, and the remaining components are individual features of each group. The oscillatory networks among common features that are involved in music perception in the HC group but not in the MDD group are identified as hypoconnectivity networks, and the oscillatory networks among individual features that are involved in music perception in the MDD group are identified as hyperconnectivity.

III. Results

A. Results of Simulated Data

We implemented the low-rank DC-NTD-FHALS algorithm on the synthetic data, and we set $SNR = 15$, $L_f = L_c = 2$, and $R_{\text{HC}} = R_{\text{MDD}} = 3$. The extracted temporal, spectral and adjacency factors were shown in Figure 2(b). We ran 10 times of the low-rank DC-NTD-FHALS algorithm, and we obtained stable decomposition results with an averaged tensor fit of 0.864 and an averaged running time of 113.27 seconds.

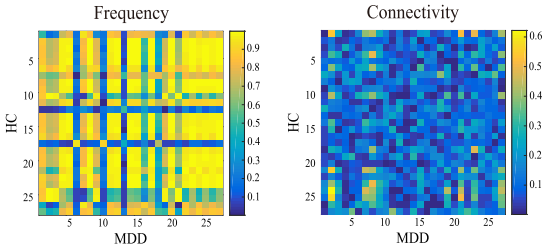

Fig. 3. Correlation analysis of the spectral factor and the adjacency factor extracted from the 4-D tensor decomposition for each block data.

B. Results of EEG Data

Through PCA analysis on the unfolded data along the spectral mode for two-block data, we extracted $R_{HC} = R_{MDD} = 27$ components for both HC group and MDD group. Then we performed the fourth-order CP tensor decomposition on each block data, and computed the correlation maps of spectral and adjacency factors between two groups, as shown in Figure 3. According to the correlation maps, we set the number of coupled components in the spectral mode $L_f = 25$ and the number of coupled components in the adjacency mode $L_c = 7$. We ran 20 times of the low-rank DC-NTF-FHALS algorithm,

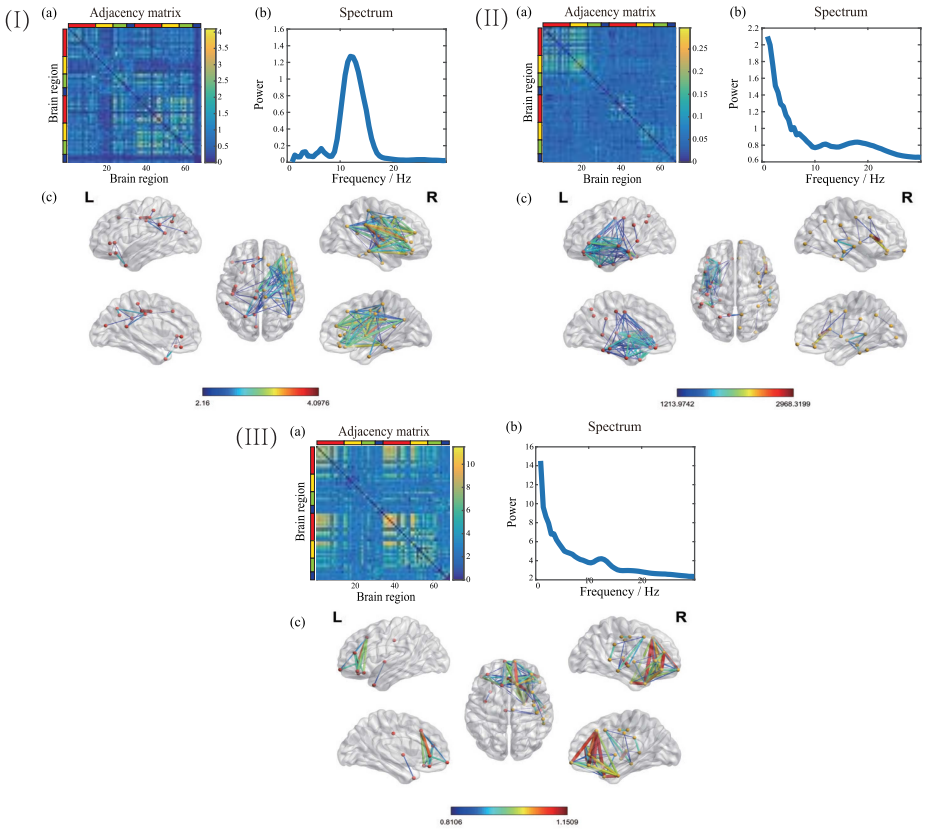

Fig. 4. Three oscillatory hyperconnectivity networks. (a) Adjacency matrix representation of the network. The 68 brain regions are ordered from the left hemisphere to the right hemisphere. Within each hemisphere, the brain regions are arranged in the order of frontal lobe, temporal lobe, parietal lobe, and occipital lobe, as indicated in red, yellow, green, and blue color, respectively. Within each lobe, the brain regions are ordered according to their y-location from anterior regions to posterior regions. (b) The spectral component of the network. (c) Cortical space representation of the network in Lateral, medial and dorsal view. The networks I, II, and III are related to the musical features of Fluctuation Centroid, Fluctuation Centroid, and Key Clarity, respectively.

and the averaged running time was 12616 seconds. The running time was 63819 seconds by one implementation of the DC-NTF-FHALS algorithm without the low-rank approximation, which indicated that the low-rank approximation could greatly reduce the computational load.

After applying the low-rank DC-NTF-FHALS algorithm and correlation analysis with musical features, we summarized the results of 20 times of implementation and obtained three oscillatory hyperconnectivity networks, as shown in Figure 4, and three oscillatory hypoconnectivity networks, as shown in Figure 5. For hyperconnectivity networks, Figure 4I shows a right hemisphere dominated network modulated by oscillations of alpha and beta (10-16 Hz) bands and the musical feature of Fluctuation Centroid. The strong connections of this network connect the core regions of DMN, including medial prefrontal cortex (mPFC), precuneus cortex, and posterior cingulate cortex (PCC). Figure 4II indicates a left auditory-related network modulated by delta oscillations and the Fluctuation Centroid feature. An aberrant delta-specific prefrontal network is identified, which is related to the musical feature of Key Clarity, as shown in Figure 4III. For hypoconnectivity networks, Figure 5I and Figure 5II exhibit fronto-parietal networks which are mainly related to attention control. The fronto-parietal networks are modulated by oscillations of 8-14 Hz and 10-19 Hz and musical features of Mode and Fluctuation Entropy, respectively. Figure 5III shows a low-frequency (delta oscillations) modulated prefrontal network which is significantly related to the musical feature of Mode, and this network is implicated in complex cognitive functions.

IV. Discussion

As far as we know, this study is the first attempt to investigate the aberrant dFC across temporal evolution and spectral modulation in MDD during music listening based on a coupled tensor decomposition approach. This study proposed a comprehensive framework to extract the FC networks characterized by spatio-temporal-spectral modes of covariation. We summarized three overactive oscillatory networks and three underactive oscillatory networks according to the analysis of musical modulations.

MDD is characterized with imbalanced communications among large-scale functional networks, including hyperconnectivity and hypoconnectivity within specific brain networks or between distinct brain networks during resting-state, see a meta-analysis in study [6]. In our study, we also found hyperconnectivity and hypoconnectivity functional networks in naturalistic music perception. We identified a right hemisphere dominated hyperconnectivity network which involved the essential regions of DMN, including mPFC, PCC and precuneus cortex, as shown in Figure 4I.

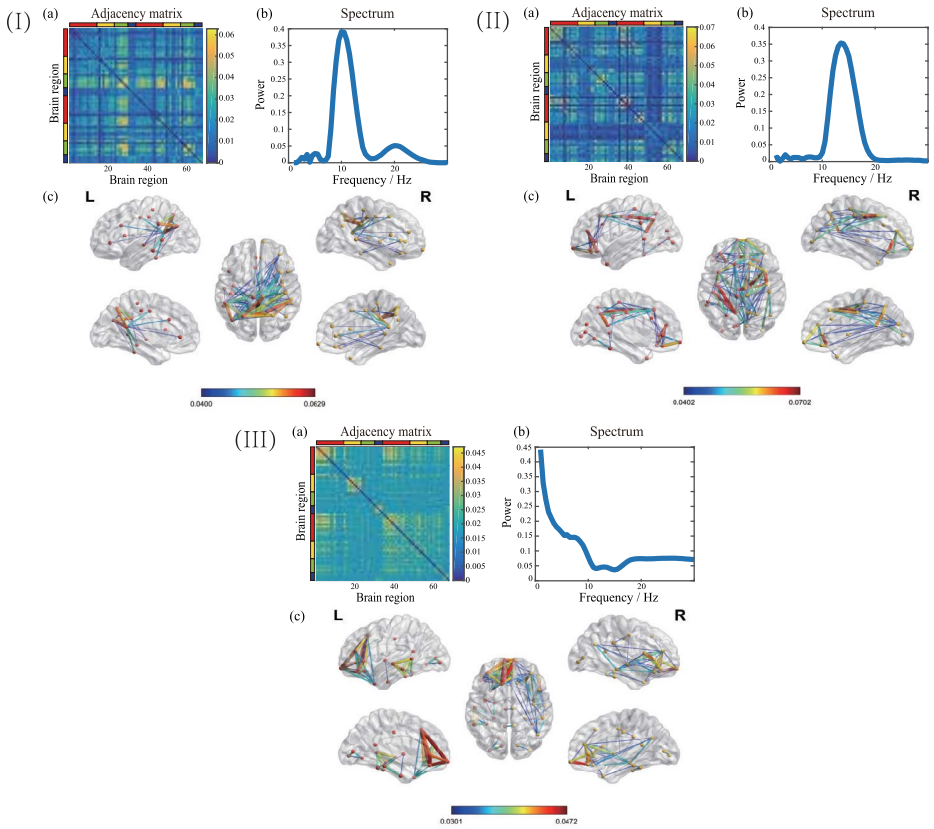

Fig. 5. Three oscillatory hypoconnectivity networks. (a) Adjacency matrix representation of the network. The 68 brain regions are ordered from left hemisphere to right hemisphere. Within each hemisphere, the brain regions are arranged in the order of frontal lobe, temporal lobe, parietal lobe, and occipital lobe, as indicated in red, yellow, green, and blue color, respectively. Within each lobe, the brain regions are ordered according to their y-location from anterior regions to posterior regions. (b) The spectral component of the network. (c) Cortical space representation of the network in Lateral, medial and dorsal view. The networks I, II, and III are related to the musical features of Mode, Fluctuation Entropy, and Fluctuation Entropy, respectively.

The hyperconnectivity in DMN are often considered as reflecting rumination, where MDD patients perseverate on negative, self-referential thoughts [50], [51]. Many researches have reported the hyperconnectivity within DMN in MDD, which supports that within-DMN hyperconnectivity is related to enhanced the positive connectivity in MDD [6], [51]. Figure 4II shows a delta band-modulated and left auditory-related network, which is activated by a rhythmic feature of Fluctuation Centroid. The delta band was demonstrated to have a substantial influence on the identification of natural speech fragments in a MEG study [52], and the decoding of rhythmic features was found to be significantly correlated with the auditory cortex during music perception [21], [53]. The abnormal delta band-modulated and left auditory-related network identified in our study might indicate that MDD patients were less involved in music perception. We identified two delta band modulated prefrontal networks, both of which were related to tonal features, Key Clarity and Mode, as shown in Figure 4III and Figure 5III. However, the prefrontal network in Figure 4III was hyperactive and right hemisphere lateralized, and the prefrontal network in Figure 5III was hypoactive and left hemisphere lateralized. The prefrontal cortex has been implicated in planning complex cognitive behavior, decision making and working memory. There are numerous lines of evidence demonstrating that prefrontal cortex is dysregulated in depression, and both increased and decreased functional connections in the prefrontal network may lead to the failure of inhibitory control in depression [54]–[57]. Those two prefrontal networks also have abnormal connections with temporal poles, which may indicate the dysfunction in semantic integration during music listening [58], [59]. Our findings are well supported by those literatures that the dysconnectivity in the prefrontal network can influence the high-order cognitive functions and information integration during music perception in MDD. Figure 5I and Figure 5II indicate hypoconnectivity fronto-parietal networks modulated by different oscillations and musical features. The abnormal development of the fronto-parietal network is a common feature across many psychiatric disorders with the deficit in cognitive control. Previous studies have demonstrated that MDD is characterized by hypoconnectivity within the frontoparietal network, which is involved in the top-down modulation of attention and emotion [6], [19], [60].

In our study, the key issue of applying coupled tensor decomposition is the selection of the number of all the extracted components and the number of coupled components. There are several methods for the selection of the number of extracted components in tensor/matrix decomposition, such as

PCA, the difference of fit (DIFFIT), model order selection, and so on [31]. In our study, due to that the spectral mode retains the minimum samples compared with temporal and adjacency modes, we applied PCA on the unfolded data along the spectral mode to determine the number of extracted components. We believe this unfolding format can help to approach the true underlying low-dimensional space. However, the selection of the number of coupled components and the coupled modes mainly relys on the data characteristics. Refer to our previous study, we use a correlation analysis in the spectral and adjacency modes in our study [25].

The scales of the reconstructed spatial, temporal and spectral factors are different from those in the synthetic data, see Figure 2. The scale indeterminacy will not change the topology of networks, the evolution of time courses and the modulation of oscillations. However, the addition of the constraints on scales will increase the model complexity and computational cost. In the present study, we only consider the group differences between HC and MDD groups by extracting the common features and individual features. Subject differences are omitted and covered in the residuals of the coupled tensor decomposition, and we assume that the extracted components are shared by all the subjects within each group. The problem of subject differences may bring more challenges, but it is also a crucial and realistic issue, especially in clinical applications.

We clarify two important limitations in this study. First, we do not have the anatomical images from the individual participant, and we use the MNI-ICBM152 template in forwarding modeling. Using the same anatomical MRI will influence the accuracy of source reconstruction. Second, the results have limited explanations due to the music type we selected. Further studies should investigate different music types, and we also need to consider the music preferences of participants.

V. Conclusion

In this study, we investigated the oscillatory hyperconnectivity and hypoconnectivity networks elicited by musical stimuli in MDD. Considering the high-dimensional structure of the datasets and group differences between HC and MDD groups, a comprehensive framework was proposed based on coupled tensor decomposition, and six abnormal connectivity networks with spatio-temporal-spectral modes of covariation were identified in MDD during music listening. Our findings are well supported and verified by previous literatures. Our research may serve as a signature of the brain's functional topography characterizing MDD, and provide novel biomarkers for the clinical diagnosis and treatment in MDD. The spectral profiles and spatial networks are usually characterized with sparsity, and the sparse regularization will be considered in the coupled tensor decomposition model in the future work. The neural correlates and dynamic neural processing of musical emotions have not been well studied, and the future work will also focus on the selection of control stimuli.

Acknowledgment

This study is to memorize Prof. Tapani Ristaniemi for his great help to the authors Fengyu Cong, Wenya Liu, and Xiulin Wang.

References

[1] I. H. Gotlib and J. Joormann, "Cognition and depression: Current status and future directions," *Annu. Rev. Clin. Psychol.*, vol. 6, no. 1, pp. 285–312, Mar. 2010.

[2] P. C. Mulders, P. F. van Eijndhoven, A. H. Schene, C. F. Beckmann, and I. Tendolkar, "Resting-state functional connectivity in major depressive disorder: A review," *Neurosci. Biobehav. Rev.*, vol. 56, pp. 330–344, Sep. 2015.

[3] G. Li *et al.*, "Large-scale dynamic causal modeling of major depressive disorder based on resting-state functional magnetic resonance imaging," *Hum. Brain Mapping*, vol. 41, no. 4, pp. 865–881, 2020.

[4] Y. I. Sheline, J. L. Price, Z. Yan, and M. A. Mintun, "Resting-state functional MRI in depression unmasks increased connectivity between networks via the dorsal nexus," *Proc. Nat. Acad. Sci. USA*, vol. 107, no. 24, pp. 11020–11025, 2010.

[5] M. Demirtaş *et al.*, "Dynamic functional connectivity reveals altered variability in functional connectivity among patients with major depressive disorder," *Hum. Brain Mapping*, vol. 37, no. 8, pp. 2918–2930, Aug. 2016.

[6] R. H. Kaiser, J. R. Andrews-Hanna, T. D. Wager, and D. A. Pizzagalli, "Large-scale network dysfunction in major depressive disorder: A meta-analysis of resting-state functional connectivity," *JAMA Psychiatry*, vol. 72, no. 6, pp. 603–611, 2015.

[7] A. Maratos, C. Gold, X. Wang, and M. Crawford, "Music therapy for depression," *Cochrane Database Systematic Rev.*, vol. 1, 2008.

[8] R. Ramirez, M. Palencia-Lefler, S. Giraldo, and Z. Vamvakousis, "Musical neurofeedback for treating depression in elderly people," *Frontiers Neurosci.*, vol. 9, p. 354, Oct. 2015.

[9] A. Dharmadhikari *et al.*, "Frontal theta asymmetry as a biomarker of depression," *East Asian Arch. Psychiatry*, vol. 28, no. 1, p. 17, 2018.

[10] W. Liu *et al.*, "Functional connectivity of major depression disorder using ongoing EEG during music perception," *Clin. Neurophysiol.*, vol. 131, no. 10, pp. 2413–2422, Oct. 2020.

[11] C. Chang and G. H. Glover, "Time–frequency dynamics of resting-state brain connectivity measured with fMRI," *NeuroImage*, vol. 50, no. 1, pp. 81–98, 2010.

[12] E. A. Allen, E. Damaraju, S. M. Plis, E. B. Erhardt, T. Eichele, and V. D. Calhoun, "Tracking whole-brain connectivity dynamics in the resting state," *Cerebral Cortex*, vol. 24, no. 3, pp. 663–676, 2014.

[13] R. H. Kaiser *et al.*, "Dynamic resting-state functional connectivity in major depression," *Neuropsychopharmacology*, vol. 41, no. 7, pp. 1822–1830, 2016.

[14] J. Wang *et al.*, "Abnormal dynamic functional network connectivity in unmedicated bipolar and major depressive disorders based on the triple-network model," *Psychol. Med.*, vol. 50, no. 3, pp. 465–474, Feb. 2020.

[15] G. Buzsaki, *Rhythms of the Brain*. London, U.K.: Oxford Univ. Press, 2006.

[16] A. A. Fingelkurts and A. A. Fingelkurts, "Altered structure of dynamic electroencephalogram oscillatory pattern in major depression," *Biol. Psychiatry*, vol. 77, no. 12, pp. 1050–1060, Jun. 2015.

[17] Y. Yan *et al.*, "Human cortical networking by probabilistic and frequency-specific coupling," *NeuroImage*, vol. 207, Feb. 2020, Art. no. 116363.

[18] L. E. Gascoyne *et al.*, "Motor-related oscillatory activity in schizophrenia according to phase of illness and clinical symptom severity," *NeuroImage, Clin.*, vol. 29, Jan. 2021, Art. no. 102524.

[19] A. E. Whitton, S. Deccy, M. L. Ironside, P. Kumar, M. Beltzer, and D. A. Pizzagalli, "Electroencephalography source functional connectivity reveals abnormal high-frequency communication among large-scale functional networks in depression," *Biol. Psychiatry, Cognit. Neurosci. Neuroimag.*, vol. 3, no. 1, pp. 50–58, Jan. 2018.

[20] A. A. Fingelkurts, A. A. Fingelkurts, H. Rytsälä, K. Suominen, E. Isometsä, and S. Kähkönen, "Impaired functional connectivity at EEG alpha and theta frequency bands in major depression," *Hum. Brain Mapping*, vol. 28, no. 3, pp. 247–261, 2007.

[21] V. Alluri, P. Toiviainen, I. P. Jääskeläinen, E. Glerean, M. Sams, and E. Brattico, "Large-scale brain networks emerge from dynamic processing of musical timbre, key and rhythm," *NeuroImage*, vol. 59, no. 4, pp. 3677–3689, 2012.

[22] F. Cong *et al.*, "Linking brain responses to naturalistic music through analysis of ongoing EEG and stimulus features," *IEEE Trans. Multimedia*, vol. 15, no. 5, pp. 1060–1069, Aug. 2013.

[23] Y. Zhu, J. Liu, K. Mathiak, T. Ristaniemi, and F. Cong, "Deriving electrophysiological brain network connectivity via tensor component analysis during freely listening to music," *IEEE Trans. Neural Syst. Rehabil. Eng.*, vol. 28, no. 2, pp. 409–418, Feb. 2020.

[24] Y. Zhu *et al.*, "Exploring frequency-dependent brain networks from ongoing eeg using spatial ICA during music listening," *Brain Topography*, vol. 33, no. 3, pp. 289–302, 2020.

[25] X. Wang, W. Liu, P. Toiviainen, T. Ristaniemi, and F. Cong, "Group analysis of ongoing EEG data based on fast double-coupled nonnegative tensor decomposition," *J. Neurosci. Methods*, vol. 330, Jan. 2020, Art. no. 108502.

[26] N. Leonardi *et al.*, "Principal components of functional connectivity: A new approach to study dynamic brain connectivity during rest," *Neuroimage*, vol. 83, pp. 937–950, Dec. 2013.

[27] G. C. O'Neill *et al.*, "Measurement of dynamic task related functional networks using MEG," *NeuroImage*, vol. 146, pp. 667–678, Feb. 2017.

[28] C. Chatzichristos, E. Kofidis, L. De Lathauwer, S. Theodoridis, and S. Van Huffel, "Early soft and flexible fusion of EEG and fMRI via tensor decompositions," 2020, *arXiv:2005.07134*. [Online]. Available: http://arxiv.org/abs/2005.07134

[29] A. Cichocki, "Tensor decompositions: A new concept in brain data analysis?" 2013, *arXiv:1305.0395*. [Online]. Available: http://arxiv.org/abs/1305.0395

[30] T. G. Kolda and B. W. Bader, "Tensor decompositions and applications," *SIAM Rev.*, vol. 51, no. 3, pp. 455–500, 2009.

[31] F. Cong, Q.-H. Lin, L.-D. Kuang, X.-F. Gong, P. Astikainen, and T. Ristaniemi, "Tensor decomposition of EEG signals: A brief review," *J. Neurosci. Methods*, vol. 248, pp. 59–69, Jun. 2015.

[32] D. Wang, Y. Zhu, T. Ristaniemi, and F. Cong, "Extracting multimode ERP features using fifth-order nonnegative tensor decomposition," *J. Neurosci. Methods*, vol. 308, pp. 240–247, Oct. 2018.

[33] F. Miwakeichi, E. Martínez-Montes, P. A. Valdés-Sosa, N. Nishiyama, H. Mizuhara, and Y. Yamaguchi, "Decomposing EEG data into space–time–frequency components using parallel factor analysis," *NeuroImage*, vol. 22, no. 3, pp. 1035–1045, 2004.

[34] M. Mørup, L. K. Hansen, C. S. Herrmann, J. Parnas, and S. M. Arnfred, "Parallel factor analysis as an exploratory tool for wavelet transformed event-related EEG," *NeuroImage*, vol. 29, no. 3, pp. 938–947, 2006.

[35] Y. Zhu *et al.*, "Discovering dynamic task-modulated functional networks with specific spectral modes using MEG," *NeuroImage*, vol. 218, Sep. 2020, Art. no. 116924.

[36] G. Zhou *et al.*, "Linked component analysis from matrices to high-order tensors: Applications to biomedical data," *Proc. IEEE*, vol. 104, no. 2, pp. 310–331, Feb. 2016.

[37] Y. Jonmohamadi, S. Muthukumaraswamy, J. Chen, J. Roberts, R. Crawford, and A. Pandey, "Extraction of common task features in EEG-fMRI data using coupled tensor-tensor decomposition," *Brain Topography*, vol. 33, no. 5, pp. 636–650, Sep. 2020.

[38] B. Rivet, M. Duda, A. Guerin-Dugue, C. Jutten, and P. Comon, "Multimodal approach to estimate the ocular movements during EEG recordings: A coupled tensor factorization method," in *Proc. 37th Annu. Int. Conf. IEEE Eng. Med. Biol. Soc. (EMBC)*, Aug. 2015, pp. 6983–6986.

[39] A. Kabbara, W. EL Falou, M. Khalil, F. Wendling, and M. Hassan, "The dynamic functional core network of the human brain at rest," *Sci. Rep.*, vol. 7, no. 1, pp. 1–16, Dec. 2017.

[40] V. Alluri *et al.*, "From vivaldi to beatles and back: Predicting lateralized brain responses to music," *NeuroImage*, vol. 83, pp. 627–636, Dec. 2013.

[41] O. Lartillot and P. Toiviainen, "MIR in MATLAB (II): A toolbox for musical feature extraction form audio," in *Proc. 7th Int. Conf. Music Inf. Retr. (ISMIR)*, 2002, pp. 287–288.

[42] F. Tadel, S. Baillet, J. C. Mosher, D. Pantazis, and R. M. Leahy, "Brainstorm: A user-friendly application for MEG/EEG analysis," *Comput. Intell. Neurosci.*, vol. 2011, pp. 1–13, Oct. 2011.

[43] T. Womelsdorf *et al.*, "Modulation of neuronal interactions through neuronal synchronization," *Science*, vol. 316, no. 5831, pp. 1609–1612, 2007.

[44] C. J. Stam, G. Nolte, and A. Daffertshofer, "Phase lag index: Assessment of functional connectivity from multi channel EEG and MEG with diminished bias from common sources," *Hum. Brain Mapping*, vol. 28, no. 11, pp. 1178–1193, Nov. 2007.

[45] A. Cichocki, R. Zdunek, and S.-I. Amari, "Hierarchical ALS algorithms for nonnegative matrix and 3D tensor factorization," in *Proc. Int. Conf. Independ. Compon. Anal. Signal Separat.* Berlin, Germany: Springer, 2007, pp. 169–176.

[46] A. Cichocki and A.-H. Phan, "Fast local algorithms for large scale nonnegative matrix and tensor factorizations," *IEICE Trans. Fundam. Electron., Commun. Comput. Sci.*, vol. 92, no. 3, pp. 708–721, 2009.

[47] G. Zhou, A. Cichocki, and S. Xie, "Fast nonnegative matrix/tensor factorization based on low-rank approximation," *IEEE Trans. Signal Process.*, vol. 60, no. 6, pp. 2928–2940, Jun. 2012.

[48] X. Wang, "Coupled nonnegative matrix/tensor factorization in brain imaging data," JYU dissertations, Dept. Inf. Technol., Univ. Jyväskylä, Jyväskylä, Finland, 2020.

[49] A. Cichocki, R. Zdunek, A. H. Phan, and S.-I. Amari, *Nonnegative Matrix and Tensor Factorizations: Applications to Exploratory Multi-Way Data Analysis and Blind Source Separation*. Hoboken, NJ, USA: Wiley, 2009.

[50] Y. I. Sheline *et al.*, "The default mode network and self-referential processes in depression," *Proc. Nat. Acad. Sci. USA*, vol. 106, no. 6, pp. 1942–1947, 2009.

[51] M. G. Berman, S. Peltier, D. E. Nee, E. Kross, P. J. Deldin, and J. Jonides, "Depression, rumination and the default network," *Social Cognit. Affect. Neurosci.*, vol. 6, no. 5, pp. 548–555, Oct. 2011.

[52] M. Koskinen, J. Viinikanoja, M. Kurimo, A. Klami, S. Kaski, and R. Hari, "Identifying fragments of natural speech from the listener's MEG signals," *Hum. Brain Mapping*, vol. 34, no. 6, pp. 1477–1489, Jun. 2013.

[53] P. Toiviainen, V. Alluri, E. Brattico, M. Wallentin, and P. Vuust, "Capturing the musical brain with lasso: Dynamic decoding of musical features from fMRI data," *NeuroImage*, vol. 88, pp. 170–180, Mar. 2014.

[54] B. D. Hare and R. S. Duman, "Prefrontal cortex circuits in depression and anxiety: Contribution of discrete neuronal populations and target regions," *Mol. Psychiatry*, vol. 25, no. 1, pp. 2742–2758, 2020.

[55] M. S. George, T. A. Ketter, and R. M. Post, "Prefrontal cortex dysfunction in clinical depression," *Depression*, vol. 2, no. 2, pp. 59–72, 1994.

[56] S. F. Taylor and I. Liberzon, "Neural correlates of emotion regulation in psychopathology," *Trends Cognit. Sci.*, vol. 11, no. 10, pp. 413–418, Oct. 2007.

[57] M. R. Bennett, "The prefrontal–limbic network in depression: A core pathology of synapse regression," *Prog. Neurobiol.*, vol. 93, no. 4, pp. 457–467, Apr. 2011.

[58] M. P. van den Heuvel, R. C. W. Mandl, C. J. Stam, R. S. Kahn, and H. E. H. Pol, "Aberrant frontal and temporal complex network structure in schizophrenia: A graph theoretical analysis," *J. Neurosci.*, vol. 30, no. 47, pp. 15915–15926, Nov. 2010.

[59] K. Tsapkini, C. E. Frangakis, and A. E. Hillis, "The function of the left anterior temporal pole: Evidence from acute stroke and infarct volume," *Brain*, vol. 134, no. 10, pp. 3094–3105, Oct. 2011.

[60] J. L. Vincent, I. Kahn, A. Z. Snyder, M. E. Raichle, and R. L. Buckner, "Evidence for a frontoparietal control system revealed by intrinsic functional connectivity," *J. Neurophysiol.*, vol. 100, no. 6, pp. 3328–3342, Dec. 2008.

PIII

ALPHA BAND DYSCONNECTIVITY NETWORKS IN MAJOR DEPRESSION DURING RESTING STATE

by

Wenya Liu, Xiulin Wang, Fengyu Cong and Timo Hämäläinen 2021

29th European Signal Processing Conference (EUSIPCO 2021), Dublin, Ireland,

Accepted

Request a copy from the author.

PIV

EXPLORING OSCILLATORY DYSCONNECTIVITY NETWORKS IN MAJOR DEPRESSION DURING RESTING STATE USING COUPLED TENSOR DECOMPOSITION

by

Wenya Liu, Xiulin Wang, Timo Hämäläinen and Fengyu Cong 2021

submitted to IEEE Transactions on Biomedical Engineering

Request a copy from the author.